Mode-Coupling Theory: Generalizations, High Dimensions and Microscopic Dynamics

Dissertation
zur Erlangung des Grades
„Doktor der Naturwissenschaften“

am Fachbereich Physik, Mathematik und Informatik
der Johannes Gutenberg-Universität
in Mainz

vorgelegt von
Bernhard Schmid
geboren in München

Mainz im August 2011

1. Berichterstatter:
2. Berichterstatter:

Tag der mündlichen Prüfung: 14. September 2011

D77

Parts of this work have been published previously in:

- B. Schmid and R. Schilling
  Glass transition of hard spheres in high dimensions
  Phys. Rev. E **81**, 041502 (2010)

- R. Schilling and B. Schmid
  Comment on "Mode-Coupling Theory as a Mean-Field Description of the Glass Transition"
  Phys. Rev. Lett. **106**, 049601 (2011)

- W. Schirmacher, B. Schmid and H. Sinn
  Theory of collective excitations in simple liquids
  Eur. Phys. J. Special Topics **196**, 3 (2011)

- B. Schmid and W. Schirmacher
  Modified mode-coupling theory for the collective dynamics of simple liquids
  J. Phys.: Condens. Matter **23**, 254211 (2011)

Abstract

This work contains several applications of the mode-coupling theory (MCT) [1] and is separated into three parts. In the first part we investigate the liquid-glass transition of hard spheres for dimensions $d \to \infty$ analytically and numerically up to $d = 800$ in the framework of MCT. We find that the critical packing fraction $\varphi_c(d)$ scales as $d^2 2^{-d}$, which is larger than the Kauzmann packing fraction $\varphi_K(d)$ found by a small-cage expansion by Parisi and Zamponi [2]. The scaling of the critical packing fraction is different from the relation $\varphi_c(d) \sim d2^{-d}$ found earlier by Kirkpatrick and Wolynes [3]. This is due to the fact that the k dependence of the critical collective and self nonergodicity parameters $f_k^c(d)$ and $f_k^{c,(s)}(d)$ was assumed to be Gaussian in the previous theories [2, 3]. We show that in MCT this is not the case. Instead $f_k^c(d)$ and $f_k^{c,(s)}(d)$, which become identical in the limit $d \to \infty$, converge to a non-Gaussian master function on the scale $k \sim d^{3/2}$. We find that the numerically determined value for the exponent parameter λ and therefore also the critical exponents a and b depend on the dimension d, even at the largest evaluated dimension $d = 800$.

In the second part we compare the results of a molecular-dynamics simulation of liquid Lennard-Jones argon far away from the glass transition [4] with MCT. We show that the agreement between theory and computer simulation can be improved by taking binary collisions into account [5]. We find that an empiric prefactor of the memory function of the original MCT equations leads to similar results.

In the third part we derive the equations for a mode-coupling theory for the spherical components of the stress tensor. Unfortunately it turns out that they are too complex to be solved numerically.

Zusammenfassung

Diese Arbeit beinhaltet mehrere Anwendungen der Modenkopplungstheorie (MCT) [1] und ist in drei Teile gegliedert. Im ersten Teil wird der Glasübergang von harten Kugeln im Grenzfall der Dimension $d \to \infty$ analytisch und numerisch bis zu $d = 800$ im Formalismus der MCT untersucht. Wir stellen fest, dass die kritische Packungsdichte $\varphi_c(d)$ mit $d^2 2^{-d}$ skaliert, was größer ist als die Kauzmann-Packungsdichte $\varphi_K(d)$, die durch eine small-cage-Entwicklung von Parisi und Zamponi bestimmt worden ist [2]. Die d-Abhängigkeit der kritischen Packungsdichte unterscheidet sich auch von der Relation $\varphi_c(d) \sim d 2^{-d}$, die von Kirkpatrick und Wolynes festgestellt worden ist [3]. Dies liegt daran, dass in den bisherigen Theorien angenommen wurde, dass die k-Abhängigkeit der kritischen kollektiven und selbst-Nichtergodizitätsparameterparameter $f_k^c(d)$ und $f_k^{c,(s)}(d)$ Gaußförmig ist [2, 3]. Wir zeigen, dass dies in der MCT nicht der Fall ist. Stattdessen werden $f_k^c(d)$ und $f_k^{c,(s)}(d)$ im Limes $d \to \infty$ identisch und konvergieren auf einer Skala $k \sim d^{3/2}$ gegen eine nicht-Gaußsche Masterfunktion. Wir erhalten, dass der numerisch bestimmte Wert des Exponenten-Parameters λ und deshalb auch die kritischen Exponenten a und b sogar bei der höchsten untersuchten Dimension $d = 800$ von der Dimension abhängen.

Im zweiten Teil der Arbeit werden die Ergebnisse einer Molekular-Dynamik-Simulation von flüssigem Lennard-Jones-Argon weit vom Glasübergang entfernt [4] mit der Modenkopplungstheorie verglichen. Wir zeigen, dass sich die Übereinstimmung zwischen Theorie und Computersimulation dabei verbessern lässt, indem paarweise Stöße der Teilchen berücksichtigt werden [5]. Wir stellen auch fest, dass ein empirischer Vorfaktor der ursprünglichen MCT-Gleichungen zu ähnlichen Ergebnissen führt.

Im dritten Teil wird eine Modenkopplungstheorie für die sphärischen Komponenten von Stress-Tensoren hergeleitet. Leider stellt es sich dabei heraus, dass die sich ergebenden Gleichungen zu kompliziert sind, um numerisch gelöst zu werden.

Contents

1 Introduction

A glass is an amorphous material that does not have the long-range translational periodicity of a crystal, but behaves mechanically like a solid. This means that static properties of a glass, such as the equilibrium structure, are indistinguishable from liquids. However, its dynamic properties are different from liquids. The glass is usually created from a supercooled liquid when crystallization is suppressed. The relaxation times slow down near the glass transition in a small temperature range over several orders of magnitude. This slowing-down shows up in the low frequency spectra of the glass-forming liquid. This also has an influence on related quantities, such that liquids and glasses can also be distinguished for example by their viscosity. The liquid has a finite viscosity and no shear stiffness, while the ideal glass has a divergent viscosity and a finite shear stiffness. Because a divergent viscosity cannot be measured, the experimentalist defines everything with a viscosity lower than $10^{12} Pa \cdot s$ as a liquid and materials with a higher viscosity as a glass. The glass transition temperature T_g, defined in such a way, is quite arbitrary, because one could also take a different viscosity to distinguish between the glass and the liquid.

The mode-coupling theory (MCT), published in 1984 by Bengtzelius, Götze and Sjölander [6] was the first microscopic theory to predict the features of the dynamics of simple liquids near the glass transition. Since then its properties have been studied in great detail [1, 7–9]. It predicts a transition from a liquid to a glass with a discontinuous jump of the long-time limit of the density autocorrelation function, generally under an increase of density or a decrease of temperature. This may not be true for some systems such as an attractive square-well system, where some reentrant behaviour may occur, as studied by Dawson et al. [10]. Its only input is the static structure factor, which changes continuously at the glass transition. The relaxation times and viscosities are predicted to follow a relation $\propto (T - T_c)^{-\gamma}$, allowing to define a critical temperature T_c, not as arbitrary as the glass transition temperature T_g.

One can also use MCT to find a microscopic description of the glass transition of network glasses, such as silica glass, where covalent bonds play a crucial role. The only problem is then, that one also has to insert the direct three-point correlation function,

which is usually neglected in MCT due to the convolution approximation, to find an appropriate description of the system, as was found by Kob and Sciortino [11]. In order to avoid such difficulties one usually applies MCT to simpler model systems such as simple liquids where the interaction between the single particles may be described by a spherically symmetric pair potential, although MCT has also been applied to molecular liquids consisting of linear molecules by Schilling and Scheidsteger [12]. The simplest pair potential is the one of hard spheres. The application of MCT to a system of hard spheres in three dimensions has been studied in great detail by Franosch et al. [13]. The hard spheres may resemble a system of colloids. If all the particles have the same diameter, the system usually crystallizes, before the glass transition takes place, which is a problem when one wants to compare the predictions of MCT with experiments. One possibility to prevent crystallization is to use multicomponent systems. Applying MCT, such systems have been studied by Barrat & Latz [14] and Götze & Voigtmann [15] in three dimensions.

The real world has three spatial dimensions. However, it may be useful to study the MCT equations in spaces with dimensions different from three. For example it is easier to do experiments or computer simulations, where the particles are confined in one direction. The particles may either be confined between two walls, such that their movement is limited between the walls, which has been studied by Lang et al. [16]. The other possibility is that they may not move in one direction at all, which means that the system may be described as a two-dimensional system. That is why the mode-coupling equations have been derived for arbitrary dimensions by Bayer et al. [17] and have also been studied for two-dimensional hard disks [17]. Again, this has been generalized for a system of hard spheres with two different diameters by Hajnal et al. [18].

Besides the interest to find out whether there is a qualitative difference in the glass transition, one of the main reasons why one applies the theories for the glass transition to two-dimensional systems is, that it is easier to evaluate experiments and computer simulations in such systems. However, one may also apply these theories to d-dimensional systems, with d larger than 3. The disadvantage is, that computer simulations may become much more difficult and real experiments may become impossible. But the big advantage can be, that analytical theories may simplify drastically. For example it was shown for a system of hard spheres that in the virial expansion of the equation of state the third and higher virial term vanishes exponentially, if 2^d times the packing fraction does not increase exponentially with d [19, 20]. As we will see, also the direct correlation function for a system of hard spheres becomes exceptionally

simple in the limit of high dimensions. It has also been argued that even if all the spheres have the same diameter, crystallization may be suppressed in the limit of high dimensions, because the densest packed system may not be crystalline in such a case [21].

Instead of interpreting the glass transition as a dynamic transition, there have also been attempts to describe it as a static transition. This can be done in the framework of *replica theory* (see the work of Parisi and Zamponi [22] and references therein). In replica theory, one considers a number of copies (or *replicas*, therefore the name) of the system, where the particles of the replicas are forced into the same state by a small inter-replica coupling force, which may be switched off at the end of the calculations.

One may then consider the *static* correlations between different replicas of the system, which is equivalent to investigating the long-time limit of the correlation functions, as it is done in MCT. Thus the dynamic problem has been converted into a simpler equilibrium problem. A crucial quantity in relation with the glass transition, which can be evaluated within replica theory, is the *configurational entropy*, also known as *complexity* [22]. This is the difference between the total entropy and the vibrational entropy of the system.

There are two different temperatures (or in the case of hard spheres packing fractions, i.e. the volume filled by the spheres divided by the total volume of the system), which play a role for the glass transition. The first one is the temperature T_d (or φ_d respectively for hard spheres), where there is a transition from the liquid state to an exponential number (i.e. the number of particles appears in the exponent) of metastable states. Since the ergodic liquid is only counted as a single configuration, the configurational entropy jumps at this temperature (or packing fraction respectively) from zero to a finite value. It has been argued that this temperature (or packing fraction) is equivalent to the critical MCT temperature (or packing fraction) [23]. The second temperature is the Kauzmann temperature $T_K < T_d$ (or Kauzmann packing fraction $\varphi_K > \varphi_d$), where the number of states changes from an exponential to an algebraic number. This means that the configurational entropy vanishes at this state.

One may also compare the dimension dependence of the critical packing fraction of MCT with the Kauzmann packing fraction, which has been evaluated by Parisi and Zamponi to scale for $d \to \infty$ as $2^{-d} d \ln d$ [2, 22]. From such a comparison one may learn more than from the simple comparison of both theories for a three-dimensional system, where there will always be deviations in the numerical value of the critical packing fraction, which may always be explained by the uncontrolled approximations of MCT.

Another advantage of MCT compared to replica theory is the fact, that it can be used to evaluate the dynamics of the system, which is not possible for replica theory for the reasons mentioned above. This may also be possible in the liquid phase, far away from the glass transition. It has the advantage of being the only simple microscopic theory which explains the structure of the memory function with two different relaxation times [24]. However, the MCT approximations are constructed in such a way, that they are justified near the liquid-glass transition, where a strong separation of time scales takes place. The good agreement between experimental and simulational data away from the glass transition may then be an unexpected finding [24, 25].

Another property of MCT, which may be seen as advantage or disadvantage is the fact, that the only input needed is the static structure factor. The disadvantage may be, that systems, which have very similar static pair correlation functions, may still have a different dynamics in reality, as was argued by Berthier and Tarjus [26]. If this is not just caused by not taking the direct three-point correlation function into account or by the slight difference in the static two-point correlation function, which may be important near to the glass transition, this may indicate a problem of MCT. This problem of MCT becomes more obvious due to the fact, that it cannot describe the dynamics of systems where the static correlations are known to be not existent, but which are reportedly known to exhibit a glass transition, as was shown by Schilling and Szamel [27, 28]. It may therefore be desirable to have a theory, which is similar to MCT, but which still contains the pair potential of the particles in the liquid glass former as an input. This may be a modified MCT which takes some corrections due to the projection onto pairs of density modes into account [1, 5], or which uses correlation functions of stress tensors instead of densities.

This work consists of four parts. In chapter 2 we will first summarize the physical definitions and the results of MCT which are already well known. In chapter 3 we will apply the MCT equations to a system of hard spheres in high dimensions. In chapter 4 we will apply MCT to a Lennard-Jones liquid away from the glass transition and compare it to a computer simulation by Levesque et al. [4]. Based on these results we also propose a modified version of MCT, motivated by a theory of Sjögren et al. [5]. In chapter 5 we work out a mode-coupling theory for stress tensors, where it turns out that these equations are too complex to be solved numerically.

2 Description of the system and derivation of the mode-coupling equations

This chapter contains a summary of the physical definitions and the properties of the mode-coupling equations, which will be needed in the following chapters. First we want to give an overview over the basic equations used to describe the physical systems, which will be investigated later. Afterwards we want to give a short introduction into the Mori-Zwanzig formalism, which is required to derive the mode-coupling equations. Finally we want to show which approximations are needed to derive the mode-coupling equations and which properties the solutions of these equations have.

2.1 Basic definitions

The systems we want to describe are known as *simple liquids*. For more details we refer to the book of Hansen and McDonald [29], from which also most of the following definitions are taken. We consider a d-dimensional system of N particles with mass m in a volume V interacting with a pair potential $u(r)$. $\vec{r}^n(t)$ and $\vec{p}^n(t)$ are the positions and momenta of a particle n at time t. The state of the system is described by the *configuration*

$$\vec{\Gamma} = \left(\vec{r}^1, ..., \vec{r}^N, \vec{p}^1, ...\vec{p}^N\right)^T \tag{2.1}$$

which contains all the positions and momenta of the particles. The classical Hamiltonian for this system can then be written as

$$H(\vec{\Gamma}) = \sum_{n=1}^{N} \frac{\left(\vec{p}^n\right)^2}{2m} + U\left(\vec{r}^1, ..., \vec{r}^N\right) \tag{2.2}$$

with the potential energy

$$U\left(\vec{r}^{1},...,\vec{r}^{N}\right)=\frac{1}{2}\sum_{\substack{n,m=1\\ n\neq m}}^{N}u\left(\vec{r}^{n}-\vec{r}^{m}\right). \tag{2.3}$$

The *canonical average* of any observable quantity A can then be written as

$$\langle A\rangle=\frac{\int \mathrm{d}^{2Nd}\Gamma e^{-\beta H\left(\vec{\Gamma}\right)}A\left(\vec{\Gamma}\right)}{\int \mathrm{d}^{2Nd}\Gamma e^{-\beta H\left(\vec{\Gamma}\right)}} \tag{2.4}$$

with $\beta=1/k_BT$. With this we can now define a *scalar product*

$$\begin{aligned}\langle A|B\rangle &:= \langle\delta A^{*}\delta B\rangle\\ &= \langle\left(A-\langle A\rangle\right)^{*}\left(B-\langle B\rangle\right)\rangle\\ &= \left(\langle A^{*}B\rangle-\langle A\rangle^{*}\langle B\rangle\right)\end{aligned} \tag{2.5}$$

which has all the mathematical properties of a scalar product [1]. Hamilton's equations of motion can then be written as

$$\dot{\vec{r}}^{n} = \frac{\partial H}{\partial\vec{p}^{n}}=\frac{\vec{p}^{n}}{m} \tag{2.6a}$$

$$\dot{\vec{p}}^{n} = -\frac{\partial H}{\partial\vec{r}^{n}} \tag{2.6b}$$

which means that any time derivative of a quantity A can be written as

$$\begin{aligned}\dot{A} &= \sum_{n=1}^{N}\left(\frac{\partial A}{\partial\vec{r}^{n}}\dot{\vec{r}}^{n}+\frac{\partial A}{\partial\vec{p}}\dot{\vec{p}}^{n}\right)\\ &= \sum_{n=1}^{N}\left(\frac{\partial A}{\partial\vec{r}^{n}}\frac{\partial H}{\partial\vec{p}^{n}}-\frac{\partial A}{\partial\vec{p}^{n}}\frac{\partial H}{\partial\vec{r}^{n}}\right)\\ &= -\left\{H,A\right\}\\ &\equiv i\mathcal{L}A.\end{aligned} \tag{2.7}$$

In the last line of Eq. (2.7) we have defined the *Liouville operator* $\mathcal{L}$. By integrating Eq. (2.7) we obtain

$$A\left(t\right)=e^{i\mathcal{L}t}A. \tag{2.8}$$

To simplify notations we note that any time-dependent quantity, where the time is omitted, shall be equivalent to this quantity at $t = 0$. It shall also be noted that it can be proven easily for time-independent systems (i.e. the Hamiltonian does not depend explicitly on the time t) that $\mathcal{L}$ is Hermitian with respect to the scalar product defined in Eq. (2.5), i.e.

$$\langle A|\mathcal{L}B\rangle = \langle \mathcal{L}A|B\rangle \tag{2.9}$$

and $e^{i\mathcal{L}t}$ is unitary, i.e.

$$\left\langle A|e^{i\mathcal{L}t}B\right\rangle = \left\langle e^{-i\mathcal{L}t}A|B\right\rangle . \tag{2.10}$$

We can now define *correlation functions*

$$C_{\mu\nu}(t) = \langle A_\mu(t)\,|A_\nu\rangle \tag{2.11}$$

where it can be proven that these correlation functions are Hermitian for systems which are invariant under time-inversion, i.e.

$$C_{\mu\nu}(t) = C^*_{\nu\mu}(t) . \tag{2.12}$$

The quantities in which we are interested the most are the *microscopic density*

$$\rho(\vec{r},t) = \sum_{n=1}^{N} \delta(\vec{r} - \vec{r}_n(t)) \tag{2.13}$$

and its Fourier transform

$$\begin{aligned} \rho_{\vec{k}}(t) &= \int \mathrm{d}^d r\; e^{-i\vec{k}\cdot\vec{r}}\rho(\vec{r},t) \\ &= \sum_{n=1}^{N} e^{-i\vec{k}\vec{r}^n(t)} \end{aligned} \tag{2.14}$$

because they become slow variables near the glass transition. Their correlation functions are known as *van Hove function* $G(\vec{r},t)$

$$G(\vec{r},t) = \frac{1}{n}\left\langle \rho(\vec{r}+\vec{r}_0, t+t_0)\,\rho(\vec{r}_0,t_0)\right\rangle \tag{2.15}$$

where n is the *particle density* of the system

$$n = N/V. \tag{2.16}$$

The *intermediate scattering function* is defined as

$$F\left(\vec{k},t\right)=\frac{1}{N}\left\langle \rho_{\vec{k}}\left(t\right)|\rho_{\vec{k}}\right\rangle . \tag{2.17}$$

The value of $F\left(\vec{k},t\right)$ at $t=0$ is known as *static structure factor*

$$S\left(\vec{k}\right)=F\left(\vec{k},0\right). \tag{2.18}$$

The static structure factor is related to the *radial distribution function*

$$g\left(\vec{r}\right)=\frac{1}{Nn}\left\langle \sum_{n=1}^{N}\sum_{m=1,m\neq n}^{N}\delta\left(\vec{r}-\vec{r}^{n}+\vec{r}^{m}\right)\right\rangle \tag{2.19}$$

via

$$S\left(\vec{k}\right)=1+n\int \mathrm{d}^{3}r\; e^{i\vec{k}\vec{r}}\left(g\left(\vec{r}\right)-1\right). \tag{2.20}$$

The temporal Fourier transform of the intermediate scattering function is known as *dynamic structure factor*

$$S\left(\vec{k},\omega\right)=\frac{1}{2\pi}\int_{-\infty}^{\infty}\mathrm{d}t\; F\left(\vec{k},t\right)e^{i\omega t}, \tag{2.21}$$

which can be also determined experimentally. Another important quantity is the *microscopic current*. It is related to the microscopic densities via the *continuity equation*

$$\vec{\nabla}\cdot\vec{j}\left(\vec{r},t\right)+\dot{\rho}\left(\vec{r},t\right)=0, \tag{2.22}$$

which can be written in Fourier space as

$$\dot{\rho}_{\vec{k}}\left(t\right)=-i\vec{k}\cdot\vec{j}_{\vec{k}}\left(t\right). \tag{2.23}$$

From this we find that the microscopic current can be defined as

$$\vec{j}_{\vec{k}}\left(t\right)=\sum_{n=1}^{N}\frac{\vec{p}^{n}(t)}{m}e^{-i\vec{k}\vec{r}^{n}(t)}. \tag{2.24}$$

The microscopic current can be split up into a longitudinal and a transverse part, where the longitudinal part is

$$j_{\vec{k}}^{L}\left(t\right)=\frac{\vec{k}}{k}\cdot\vec{j}_{\vec{k}}\left(t\right). \tag{2.25}$$

2.2 Mori-Zwanzig formalism

In order to understand the results of the mode coupling theory, we give a short summary of the Mori-Zwanzig projector technique [1, 30]. This technique considers the Laplace transform of the correlation function

$$\begin{aligned} C_{\mu\nu}(z) &= i\int_0^\infty \mathrm{d}t e^{izt} C_{\mu\nu}(t), \qquad \mathrm{Im}(z) > 0 \\ &= i\int_0^\infty \mathrm{d}t e^{izt} \langle A_\mu | e^{-i\mathcal{L}t} | A_\nu \rangle \\ &= -\left\langle A_\mu \right| (z-\mathcal{L})^{-1} \left| A_\nu \right\rangle . \end{aligned} \tag{2.26}$$

We now introduce the projection operator P with

$$P = \sum_{\alpha,\beta} |A_\alpha\rangle \langle A|A\rangle^{-1}_{\alpha\beta} \langle A_\beta| \tag{2.27}$$

and the corresponding orthogonal operator Q

$$Q = 1 - P$$

where $(\langle A|A\rangle^{-1}_{\alpha\beta})$ is the inverse of $(\langle A_\alpha|A_\beta\rangle)$, i.e. $\sum_\beta \langle A|A\rangle^{-1}_{\alpha\beta} \langle A_\beta|A_\gamma\rangle = \delta_{\alpha\gamma}$. This normalization is needed to fulfill the general property required for any projection operator $P^2 = P$ and $Q^2 = Q$. The result of the Mori-Zwanzig projector formalism is then [1, 30]

$$C_{\mu\nu}(z) = -\sum_\beta \left(z\cdot I - \Omega + M(z)\right)^{-1}_{\mu\beta} C_{\beta\nu}(0) \tag{2.28}$$

with

$$i\Omega_{\mu\nu} = \sum_\alpha \left\langle A_\mu | \dot{A}_\alpha \right\rangle \langle A|A\rangle^{-1}_{\alpha\nu} \tag{2.29}$$

and the memory function

$$M_{\mu\nu}(z) = -\sum_\alpha \left\langle \dot{A}_\mu \right| Q \left(z - Q\mathcal{L}Q\right)^{-1} Q \left| \dot{A}_\alpha \right\rangle \langle A|A\rangle^{-1}_{\alpha\nu} . \tag{2.30}$$

This can be written in time space as

$$\dot{C}_{\mu\nu}(t) + i\sum_\alpha \Omega_{\mu\alpha} C_{\alpha\nu}(t) + \int_0^t dt' \sum_\alpha M_{\mu\alpha}(t-t') C_{\alpha\nu}(t') = 0 \tag{2.31}$$

with

$$M_{\mu\nu}(t) = \left\langle \dot{A}_\mu \right| Q e^{-iQ\mathcal{L}Qt} Q \left| \dot{A}_\alpha \right\rangle \langle A|A\rangle^{-1}_{\alpha\nu} . \tag{2.32}$$

With this formalism the mode-coupling equations can be derived.

2.3 Mode-coupling equations

In this section we want to show how the mode-coupling equations can be derived. For details we refer to the book of Wolfgang Götze [1]. There are in fact two possibilities to derive the mode-coupling equations from the Mori-Zwanzig formalism. The first one is to apply the Mori-Zwanzig formalism to the two dynamic variables

$$\begin{aligned} A_0 &= \rho_{\vec{k}} \\ A_1 &= j^L_{\vec{k}}. \end{aligned} \tag{2.33}$$

The transverse currents do not couple to these two variables, because the correlation functions between these two variables and the transverse current are zero due to symmetry reasons. The other possibility is to use the Mori-Zwanzig formalism with only $A_0 = \rho_{\vec{k}}$ as dynamic variable and $P_0 = |A_0\rangle \langle A_0|A_0\rangle^{-1} \langle A_0|$ as projector. We now realize, that if we set $\left|\tilde{A}\right\rangle = Q_0 \left|\dot{A}_0\right\rangle$ and $\tilde{\mathcal{L}} = Q_0 \mathcal{L} Q_0$, the memory function in Eq. (2.30) becomes very similar to the correlation function in Eq. (2.26). This means that we can again apply the Mori- Zwanzig formalism to this memory function. The result can then be written for

$$\begin{aligned} \phi_k(t) &= \frac{\left\langle \rho_{\vec{k}}(t) \left| \rho_{\vec{k}} \right\rangle \right.}{\left\langle \rho_{\vec{k}} | \rho_{\vec{k}} \right\rangle} \\ &= F\left(\vec{k}, t\right) / S\left(\vec{k}\right) \end{aligned} \tag{2.34}$$

as a two-step continued fraction

$$\phi_k(z) = \frac{-1}{z - \frac{\Omega_0^2(k)}{z + M_k(z)}} \tag{2.35}$$

or in time space

$$\ddot{\phi}_k(t) + \Omega_0^2(k)\phi_k(t) + \int_0^t dt' M_k(t-t')\dot{\phi}_k(t') = 0 \tag{2.36}$$

with the microscopic frequencies

$$\Omega_0^2(k) = \frac{k_B T}{m} k^2 / S(k) \tag{2.37}$$

and the memory function

$$M_k(t) = \left\langle F_{\vec{k}}^L \right| e^{-iQ\mathcal{L}Qt} \left| F_{\vec{k}}^L \right\rangle \tag{2.38}$$

with the "forces"

$$\left| F_{\vec{k}}^L \right\rangle = \sqrt{\frac{m}{N k_B T}} Q\mathcal{L} \left| j_{\vec{k}}^L \right\rangle \tag{2.39}$$

and the projector

$$P = \frac{\left|\rho_{\vec{k}}\right\rangle \left\langle\rho_{\vec{k}}\right|}{\left\langle\rho_{\vec{k}}|\rho_{\vec{k}}\right\rangle} + \frac{\left|j_{\vec{k}}^L\right\rangle \left\langle j_{\vec{k}}^L\right|}{\left\langle j_{\vec{k}}^L | j_{\vec{k}}^L\right\rangle} \tag{2.40}$$

and $Q = 1 - P$. The initial conditions are $\phi_k(t=0) = 1$ and $\dot{\phi}_k(t=0) = 0$. Until now the derivation is still exact. It does not seem that we have simplified the problem, we have only shifted the difficulties in the evaluation of $\phi_k(t)$ to the evaluation of $M_k(t)$. To really find some solvable equations we have to apply the mode-coupling approximations. These approximations shall be valid for long times. This is not meant in a mathematical sense, e.g. as an expansion with the inverse time as a small parameter. It is rather motivated by physical intuition, leading to a separation between "slow" variables and "fast" variables. The first approximation of the slow part of the memory function consists of a projection onto pairs of density modes, i.e.

$$M_k(t) \tilde{=} \left\langle F_{\vec{k}}^L \right| P_2 e^{-iQ\mathcal{L}Qt} P_2 \left| F_{\vec{k}}^L \right\rangle \tag{2.41}$$

with

$$P_2 \equiv \sum_{\vec{p},\vec{q},\vec{p}',\vec{q}'}{}' \left|\rho_{\vec{p}}\rho_{\vec{q}}\right\rangle g_{\vec{p},\vec{q},\vec{p}',\vec{q}'} \left\langle\rho_{\vec{p}'}\rho_{\vec{q}'}\right| \tag{2.42}$$

where the prime in $\sum'$ indicates an ordering $\vec{p} < \vec{q}$ to prevent double counting and $g_{\vec{p},\vec{q},\vec{p}',\vec{q}'}$ can be determined from $(P_2)^2 = P_2$. This approximation is motivated by the fact, that $\mathcal{L} j_{\vec{k}}^L$, which appears in $F_{\vec{k}}^L$ (Eq. (2.39)) can be written as

$$\mathcal{L} j_{\vec{k}}^L = -\frac{1}{Vm} \sum_{\vec{q}} \frac{\vec{k}\cdot\vec{q}}{k} u(\vec{q}) \left(\rho_{\vec{k}-\vec{q}}\rho_{\vec{q}}\right) - \frac{1}{m^2} \sum_n \frac{\left(\vec{k}\cdot\vec{p}^n\right)^2}{k} e^{-i\vec{k}\vec{r}^n} \tag{2.43}$$

i.e. the first term in Eq. (2.43) consists of a pair of density modes. Additionally, this is in fact the simplest choice for a projection onto a slow variable because through the factor Q in $F_{\vec{k}}^L$ (Eq. (2.39)) the single densities and currents are already projected out. The second approximation consists of a factorization of the kind

$$\left\langle \rho_{\vec{p}}\rho_{\vec{q}}\right| e^{-iQ\mathcal{L}Qt}\left|\rho_{\vec{p}'}\rho_{\vec{q}'}\right\rangle \cong \left\langle \rho_{\vec{p}}\right| e^{-i\mathcal{L}t}\left|\rho_{\vec{p}'}\right\rangle \left\langle \rho_{\vec{q}}\right| e^{-i\mathcal{L}t}\left|\rho_{\vec{q}'}\right\rangle . \tag{2.44}$$

This reminds of a mean-field approximation $\langle AB\rangle \cong \langle A\rangle \langle B\rangle$. It shall be noted, that such a kind of approximation is only valid, because on the left side of Eq. (2.44) a *reduced dynamics* $Q\mathcal{L}Q$ is applied, which means that single-mode contributions are projected out. If this would not be the case, one would also expect contributions of the kind $\left\langle \rho_{\vec{p}}\rho_{\vec{q}}\right| Pe^{-i\mathcal{L}t}P\left|\rho_{\vec{p}'}\rho_{\vec{q}'}\right\rangle$ which contain terms proportional to $\left\langle \rho_{\vec{k}}\right| e^{-i\mathcal{L}t}\left|\rho_{\vec{k}}\right\rangle$, i.e. single-mode contributions. With this approximation also $g_{\vec{p},\vec{q},\vec{p}',\vec{q}'}$ in Eq. (2.42) can be evaluated to be

$$g_{\vec{p},\vec{q},\vec{p}',\vec{q}'} = \frac{\delta_{\vec{p},\vec{p}'}\delta_{\vec{q},\vec{q}'}}{S_p S_q}.$$

A third approximation is applied, which is in fact not crucial for MCT, it only reduces the amount of static input required to solve the mode-coupling equations. $P_2\left|F_{\vec{k}}^L\right\rangle$ contains terms of the kind $S(\vec{k})$, but also $S^{(3)}(\vec{k},\vec{k}') = \frac{1}{N}\langle\rho(\vec{k}+\vec{k}')^*\rho(\vec{k}')\rho(\vec{k})\rangle$ which can be described by the Ornstein-Zernike equation for three-particle correlation functions [31]

$$S^{(3)}\left(\vec{k},\vec{k}'\right) = S\left(k\right)S\left(k'\right)S(|\vec{k}+\vec{k}'|)\left(1+n^2c^{(3)}(\vec{k},\vec{k}')\right). \tag{2.45}$$

In the convolution approximation $n^2c^{(3)}(\vec{k},\vec{k}')$ is neglected compared to 1. It is shown in section 3.5.7, that this approximation is legitimate in the limit $d\to\infty$ at the critical MCT packing fraction. We now introduce a normalized memory function $m_k\left(t\right)$, which consists of the slow part of the original memory function, Eq. (2.38), where the microscopic frequencies, Eq. (2.37), i.e. the explicit temperature dependence is factored out. The fast part of the memory function (cf. section 4.2) is approximated by a $\delta-$function in time with the prefactor ν_k , i.e.

$$M_k(t) = \nu_k\delta\left(t\right) + \Omega_0^2(k)m_k\left(t\right). \tag{2.46}$$

The result of the mode-coupling approximations is then that $m_k\left(t\right)$ can be written as a functional of the time-dependent density correlation functions

$$m_k(t) = \mathcal{F}_k\left[\phi_q(t)\right] \tag{2.47}$$

with

$$\mathcal{F}_k\left[\phi_q(t)\right] = \int \frac{\mathrm{d}^d p}{(2\pi)^d} \tilde{V}\left(\vec{k}, \vec{p}, \vec{k}-\vec{p}\right) \phi_p(t)\, \phi_{|\vec{k}-\vec{p}|}(t) \tag{2.48}$$

and

$$\tilde{V}\left(\vec{k}, \vec{p}, \vec{q}\right) = \frac{n}{2} \frac{S(k)\, S(p)\, S(q)}{k^4} \left(\vec{k} \cdot \left(\vec{p} c(p) + \vec{q} c(q)\right)\right)^2 . \tag{2.49}$$

Equations (2.36), (2.46), (2.47), (2.48) and (2.49) represent a set of equations, which can be solved self consistently for the density correlation functions $\phi_k(t)$ with only static quantities, i.e. the static structure factor or direct correlation function, required as input.

2.4 Solution of the mode-coupling equations

Now we have all the equations needed to investigate the glass transition as described by mode-coupling theory. In order to understand what we are looking for, we first want to give an overview about the general properties of the mode-coupling equations. For details we again refer to the book of Wolfgang Götze [1].
The nonergodicity parameter for the collective correlator is the long-time limit of the normalized intermediate scattering function (provided this long-time limit exists), i.e.

$$f_k(P) = \lim_{t\to\infty} \phi_k(t; P) = -\lim_{z\to 0} z\phi_k(z; P) \tag{2.50}$$

and similarly for the self correlator

$$f_k^{(s)}(P) = \lim_{t\to\infty} \phi_k^{(s)}(t; P) = -\lim_{z\to 0} z\phi_k^{(s)}(z; P), \tag{2.51}$$

where the control parameters, which can be more than one, are written here in the short form P. This can be for example the packing fraction φ, in the case of hard spheres, and the spatial dimension d. They are the order parameters for the liquid-glass transition, i.e.

$$f_k(P) = \begin{cases} 0 & , \text{ liquid} \\ > 0 & , \text{ glass.} \end{cases} \tag{2.52}$$

From Eq. (2.35) or (2.36) one obtains

$$f_k(P) / \left[1 - f_k(P)\right] = \mathcal{F}_k\left[f_q(P); P\right]. \tag{2.53}$$

$f_k(P)$ as defined in Eq. (2.50) is a solution of Eq. (2.53), but Eq. (2.53) also has other solutions. For example $f_k(P) \equiv 0$ is always a solution of Eq. (2.53) when $\mathcal{F}_k[f_q(P)]$ has a structure as defined in Eq. (2.48). The properties of $f_k(P)$ as defined in Eq. (2.50) are [7]:

$$\bullet f_k(P) \text{ is real (same as } \phi_k(t;P)) \tag{2.54a}$$

$$\bullet 0 \le f_k(P) \le 1 \text{ for all } k \tag{2.54b}$$

$$\bullet f_k(P) \text{ is the largest solution of Eq. (2.53) compatible with Eq. (2.54b)} \tag{2.54c}$$

It can be shown [1] that the true solution can be found by iterating the equation

$$f_k^{(i+1)}(P) = \frac{\mathcal{F}_k\left[f_q^{(i)}(P);P\right]}{\mathcal{F}_k\left[f_q^{(i)}(P);P\right]+1} \tag{2.55}$$

with the initial value

$$f_k^{(0)}(P) \equiv 1. \tag{2.56}$$

In order to understand the implication of Eq. (2.53) we want to keep in mind that the schematic model, which can be motivated from Eq. (2.53) by only taking into account a single wavevector k_0 [6], i.e.

$$f(v)/[1-f(v)] = \mathcal{F}[f(v);v] \tag{2.57}$$

with the functional

$$\mathcal{F}[f;v] = vf^2, \tag{2.58}$$

where v is the only external parameter, has the three solutions (which may be complex for certain v):

$$\begin{aligned} \hat{f}_{(1)}(v) &= 0 \\ \hat{f}_{(2)}(v) &= \frac{1}{2}\left(1+\sqrt{1-\frac{4}{v}}\right) \\ \hat{f}_{(3)}(v) &= \frac{1}{2}\left(1-\sqrt{1-\frac{4}{v}}\right). \end{aligned} \tag{2.59}$$

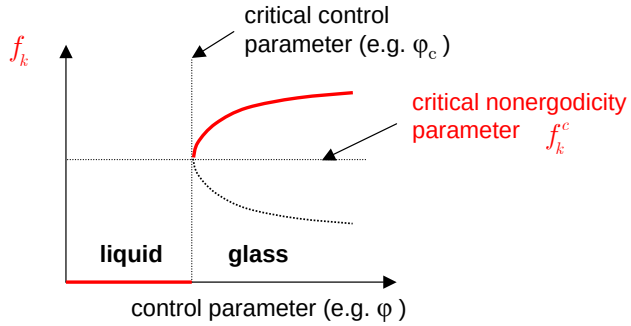

Figure 2.1: Schematic illustration of the dependence of the nonergodicity parameter on an external control parameter.

From Eqs. (2.54) we find the physical solution to be

$$f(v) = \begin{cases} 0 & v < 4 \\ \frac{1}{2}\left(1 + \sqrt{1 - \frac{4}{v}}\right) & v \geq 4 \end{cases} . \tag{2.60}$$

So there is a jump in $f(v)$ at $v^c = 4$ from $f(v) = 0$ to $f^c \equiv f(v^c) = \frac{1}{2}$. This means that even when the static quantities depend smoothly on the control parameters, there can be a jump in the dynamic quantities. This is also known as dynamic glass transition. In the k-dependent theory the result is basically quite similar to the schematic model. But in general this set of equations cannot be solved analytically any more. However, the solution for the nonergodicity parameters may still show the same jump as in the schematic model (cf. Fig. 2.1). If there are two control parameters (e.g. packing fraction φ and spatial dimension d, if we assume d to be a continuous variable, as will be done in section 3.4.2), the solutions $\hat{f}_k(P)$ of Eq. (2.53) can be interpreted as surfaces in this two-dimensional parameter space. The two generic singularities for such surfaces are known as *folds* (or A_2 singularities) and *cusps* (or A_3 singularities) [32]. They are shown schematically in Fig. 2.2. From this it becomes clear, that the endpoint of an A_2 singularity is an A_3 singularity. In order to characterize the glass transition at A_2 singularities, Eq. (2.53) can be expanded to lowest order around the state P^c, where the glass transition occurs [1]. In this expansion there appears the *stability matrix* A_{kp} which can be written at the critical point as

$$A^c_{kp} = (1 - f^c_k) \frac{\partial \mathcal{F}_k\left[f^c_q; P^c\right]}{\partial f^c_p} \left(1 - f^c_p\right) . \tag{2.61}$$

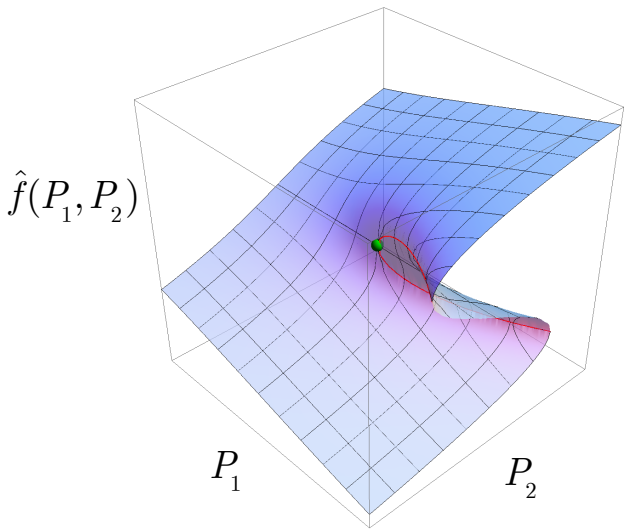

Figure 2.2: Schematic illustration of a cusp (green) and fold singularity (red).

It is here $f_k^c = f_k(P^c)$. From the implicit function theorem it can be shown that a fold bifurcation in $f_k(P)$ can only occur, when one of the eigenvalues of the stability matrix approaches unity. So it can be shown that at the glass transition the stability matrix has a maximum eigenvalue 1, which is generically non-degenerate [1]. The left and right eigenvectors of the stability matrix to the eigenvalue 1 shall be denoted by $\hat{a}_k$ and a_k respectively, i.e.

$$\begin{aligned} \int \mathrm{d}k\ \hat{a}_k A^c_{kp} &= \hat{a}_p \\ \int \mathrm{d}p\ A^c_{kp} a_p &= a_k \end{aligned} \tag{2.62}$$

with $\hat{a}_k > 0$ and $a_k > 0$ for all k [1], where the integrals may be replaced by the appropriate Riemann sums. They may be normalized as

$$\begin{aligned} \int \mathrm{d}k\ \hat{a}_k a_k &= 1 \\ \int \mathrm{d}k\ \hat{a}_k a_k a_k &= 1. \end{aligned} \tag{2.63}$$

We can now expand Eq. (2.53) around P^c in lowest order, where we assume $(P-P^c) \ll P^c$ and $f_k - f_k^c \ll 1$. The result reads

$$f_k(P) \cong f_k^c + h_k \sqrt{\sigma(P)/(1-\lambda)} \tag{2.64}$$

where the *critical amplitude* h_k is defined as

$$h_k = (1 - f_k^c)\, a_k \tag{2.65}$$

and the *separation parameter*, which describes the distance of the state from glass transition, can be written as

$$\sigma(P) = \int \mathrm{d}k\ \hat{a}_k \left(\mathcal{F}_k \left[f_q^c; P \right] - \mathcal{F}_k \left[f_q^c; P^c \right] \right) \tag{2.66}$$

with

$$\sigma(P) \begin{cases} < 0: & \text{liquid} \\ \geq 0: & \text{glass} \end{cases} . \tag{2.67}$$

The *exponent parameter* is given as

$$\lambda = \int \mathrm{d}k \int \mathrm{d}p \int \mathrm{d}q\ \hat{a}_k A_{kpq} a_p a_q \tag{2.68}$$

with

$$A_{kpq} = \frac{1}{2}(1 - f_k^c) \frac{\partial^2 \mathcal{F}_k \left[f_q^c; P \right]}{\partial f_p^c \partial f_p^c} \left(1 - f_p^c\right) \left(1 - f_q^c\right). \tag{2.69}$$

The reason why λ is also known as exponent parameter will become clear when we investigate the time dependence of the correlators $\phi_k(t)$ described by the mode-coupling equations. Eq. (2.35), with (2.46) and $\nu_k = 0$ inserted, becomes for sufficiently long times, i.e. small frequencies

$$\frac{z\phi_k(z)}{1 + z\phi_k(z)} = z m_k(z) \tag{2.70}$$

It is quite remarkable, that this equation does not contain any microscopic frequencies and thus no explicit temperature dependence. If we now expand Eq. (2.70) in a similar way as Eq. (2.53) we obtain :

$$\phi_k(t) = f_k^c + h_k G(t) \tag{2.71}$$

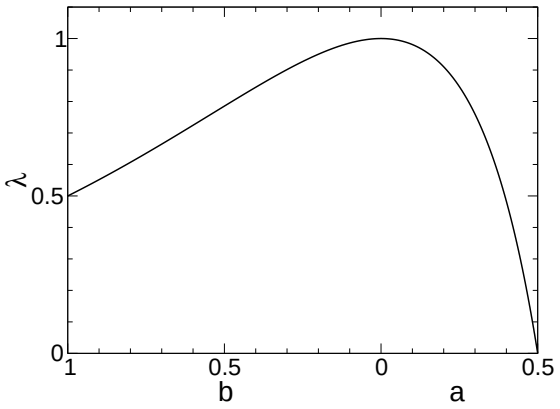

Figure 2.3: Relation between the exponent parameter λ and the critical exponents a and b.

where $G(t)$ fulfills the equation

$$\sigma + \lambda \left(-zLT\left[G(t)^2\right](z)\right) - \left(-zG(z)\right)^2 = 0 \tag{2.72}$$

The first remarkable result of Eqs. (2.71) and (2.72) is that the k and t dependence factorize. For $\sigma = 0$ one obtains the critical law

$$G(t) = \left(\frac{t_0}{t}\right)^a \tag{2.73}$$

where a is the solution of (cf. Fig. 2.3)

$$\lambda = \frac{\left(\Gamma(1-a)\right)^2}{\Gamma(1-2a)} \tag{2.74}$$

with

$$0 < a < \frac{1}{2}. \tag{2.75}$$

For $\sigma > 0$ (i.e. in the glassy state) one obtains

$$G(t) = \sqrt{\frac{\sigma}{1-\lambda}} + \sqrt{\sigma}\left(\frac{t_\sigma}{t}\right)^a \tag{2.76}$$

with the time scale

$$t_\sigma = \frac{t_0}{|\sigma|^{1/2a}}. \tag{2.77}$$

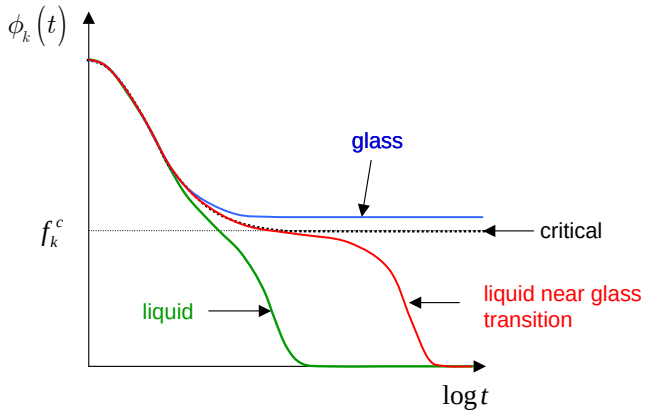

Figure 2.4: Schematic illustration of the time dependence of a correlation function as described by MCT.

For $\sigma < 0$ (i.e. in the liquid state) one obtains for $t \ll t_\sigma$

$$G(t) = \sqrt{|\sigma|}\left(\frac{t_\sigma}{t}\right)^a. \tag{2.78}$$

In the liquid state $\phi_k(t)$ finally relaxes to zero. So there is a second time scale, which describes the initial decay from the plateau. This relation, which is also known as von Schweidler law, can be written as

$$G(t) \propto -\left(\frac{t}{\tau}\right)^b \tag{2.79}$$

where b is the solution of (cf. Fig. 2.3)

$$\lambda = \frac{(\Gamma(1+b))^2}{\Gamma(1+2b)} \tag{2.80}$$

with $b > 0$ and with the time scale

$$\tau = \frac{t_0}{|\sigma|^\gamma} \text{ with } \gamma = \frac{1}{2a} + \frac{1}{2b}. \tag{2.81}$$

The time dependence of the correlators and their relation to the critical exponents is shown schematically in Figs. 2.4 and 2.5. These two time scales can be understood physically by the cage effect [1] as shown in Fig. 2.6.

The red sphere is caught in a cage built by the green spheres. The first time scale

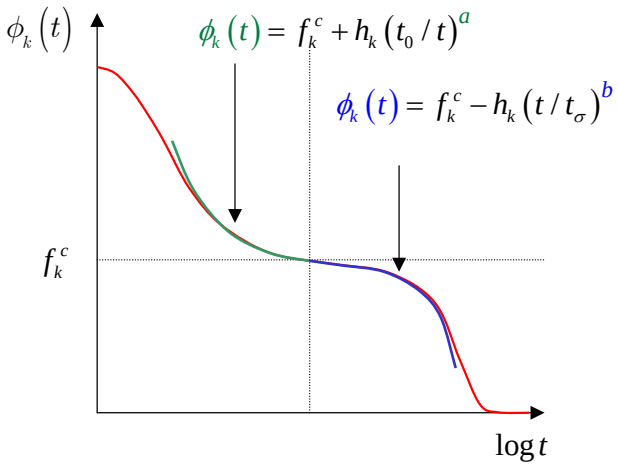

Figure 2.5: Critical exponents a and b as they appear in the time dependence of a correlation function.

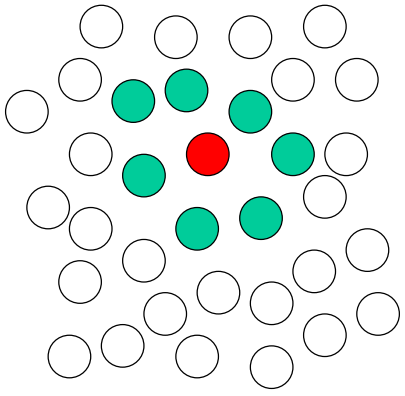

Figure 2.6: Illustration of the cage effect. The red sphere is caught in a cage consisting of the green spheres.

is the one that describes the oscillations of the red sphere inside the cage. This time scale is only weakly density dependent. The second time scale is determined by the time needed for the red particle to escape from the cage. This is only possible when the green particles move in such a way, that the cage opens. This time scale can be much longer than the first time scale. Additionally it is strongly density dependent. There may be a critical density, such that if the density of the system gets close to this critical density, the time needed for one particle to escape from the cage diverges as in Eq. (2.81). If the density of the system is larger than this critical density, the particle cannot escape from the cage any more. Because this is true for all the particles in the system, the system becomes nonergodic, i.e. it becomes a glass. For other systems, which do not consist of hard particles, one may use the temperature instead of the density as control parameter.

In real glass formers the transition from a glass to a liquid is not as sharp as described by MCT. The relaxation time only follows the relation given in Eq. (2.81) for a limited temperature range, but it does not diverge at a critical temperature. This is shown in Fig. 2.7. This may be explained by some additional hopping processes [33], through which the system may still stay ergodic. One may use the experimentally determined relaxation times to define a *glass transition temperature* T_g. At the glass transition temperature the relaxation time has a value of 100s, which is in fact quite an arbitrary definition. From Fig. 2.7 it can be seen that we have in general $T_c > T_g$.

Another temperature which is often used to characterize the glass transition is the Kauzmann temperature [34]. The Kauzmann temperature is the temperature, at which the linearly extrapolated entropy of the supercooled phase becomes equal to the entropy of the crystal phase. This is illustrated in Fig. 2.8. From this it can be seen that $T_K < T_g$, i.e.

$$T_K < T_c \tag{2.82}$$

or equivalently

$$\varphi_K > \varphi_c. \tag{2.83}$$

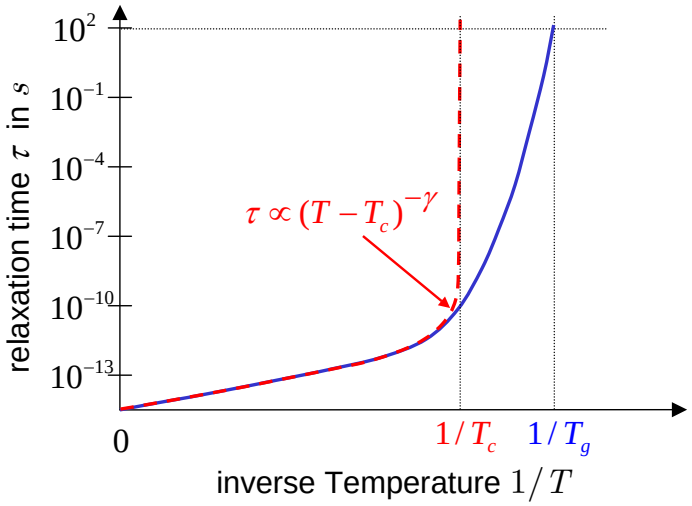

Figure 2.7: Relaxation time as described by MCT (red dashed line) and of real glass formers (blue solid line) [35].

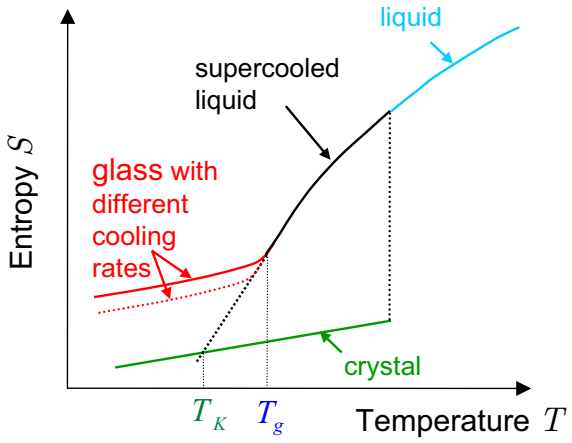

Figure 2.8: Illustration of the Kauzmann temperature T_K and the glass-transition temperature T_g, which depends on the cooling rate.

3 Mode-coupling theory in high dimensions

It is well known that some physical problems can be simplified drastically in the limit of the dimension d going to infinity. This is the case for equilibrium phase transitions (e.g. the Ising model) where above an upper critical dimension the critical exponents of the system become the same as in the corresponding mean-field theory. As was already mentioned in relation with Eq. (2.44), the factorization approximation may be interpreted as a mean-field theory with the two-point density correlator as an order parameter, as it was done by Biroli and Bouchaud [36]. The mean-field approximation then consists of neglecting the fluctuations between two of these density correlation functions, while in the full theory these fluctuations still have to be taken into account. It was argued, that the upper critical dimension, i.e. the dimension where these fluctuations do not influence the critical behaviour, is $d_c = 8$ for systems with [37] and $d_c = 6$ for systems without conserved quantities [36]. The critical exponents $a(d)$ and $b(d)$ may nevertheless depend on the spatial dimension d because the required static input, i.e. the static structure factor at the glass transition singularity, is also dimension dependent.

Additionally, it was shown that the equation of state for the fluid phase of a hard sphere system can be evaluated by a virial expansion, where only the first two virial coefficients are nonvanishing if 2^d times the packing fraction does not increase exponentially or stronger with d [19, 20]. This also simplifies the evaluation of the direct correlation function, needed as input for MCT, where the expansion in Mayer functions is dominated by a single term in the limit $d \to \infty$ (see section 3.3.1).

This motivates the investigation of the solution of the mode-coupling equations in high dimensions. This has already been done in a model which has not been solved with the full k dependence, but where a Gaussian ansatz has been used for the nonergodicity parameter [3] (see also section 3.5.6). In contrast to this, we want to solve the mode-coupling equation for a system of hard spheres with full k dependence in arbitrary dimensions. Besides the usual solution in $d = 3$ this has already been done for $d = 2$

[17, 18] and $d = 4$ [38]. It was claimed that the agreement of MCT with a computer simulation improves in $d = 4$ compared to $d = 3$ [38], which may lead to the assumption that the accuracy of the predictions of MCT may improve for high dimensions and MCT may eventually become exact in the limit $d \to \infty$. This is another motivation for the investigation of the MCT equations in high dimensions. This includes the question, whether the A_2 singularity of the mode-coupling equations still exists in the limit $d \to \infty$. Another interesting aspect is whether the collective and self nonergodicity parameters become equal and Gaussian in the limit of high dimensions, as was assumed in a previous investigation [3].

In order to do so, we first want to summarize some mathematical relations needed later in the discussion of the MCT equations in arbitrary dimensions. Then we want to show how the mode-coupling equations can be derived in arbitrary dimensions, which has already been done previously by Bayer et al. [17]. Afterward we want to discuss the static quantities needed as input for the MCT equations. With this we can then examine the numerical and analytical solution of the MCT equations.

3.1 Mathematical preliminaries

3.1.1 d-dimensional polar coordinates

We start with the introduction of d-dimensional polar coordinates. With these polar coordinates, the Cartesian coordinates $x_1, x_2, ..., x_d$ of any vector $\vec{r} = (x_1, x_2, ..., x_d)^T$ can be written as

$$\begin{aligned} x_1 &= r \cos\varphi \prod_{j=1}^{d-2} \sin\theta_j \\ x_2 &= r \sin\varphi \prod_{j=1}^{d-2} \sin\theta_j \\ x_n &= r \cos\theta_{n-2} \prod_{j=n-1}^{d-2} \sin\theta_j, \qquad 3 \leq n \leq d-1 \\ x_d &= r \cos\theta_{d-2} \end{aligned} \tag{3.1}$$

with the radius r with

$$0 \leq r = |\vec{r}| \tag{3.2}$$

and the angles φ and $\theta_1, ..., \theta_n$ with

$$\begin{aligned} &0 \leq \varphi \leq 2\pi \\ &0 \leq \theta_n \leq \pi, \quad n = 1, .., d-2. \end{aligned} \tag{3.3}$$

For arbitrary dimensions, the volume element $\mathrm{d}^d r$ can be written as

$$\mathrm{d}^d r = r^{d-1} \mathrm{d}r \ \mathrm{d}\Omega_d \tag{3.4}$$

with the solid angle $\mathrm{d}\Omega_d$. This can also be written equivalently as

$$\mathrm{d}^d r = (r \sin\theta_{d-2})^{d-2} \, \mathrm{d}\Omega_{d-1} \ r \ \mathrm{d}r \ \mathrm{d}\theta_{d-2} \tag{3.5}$$

with the solid angle $\mathrm{d}\Omega_{d-1}$ of a system with $d-1$-dimensional polar coordinates. With $\mathrm{d}\Omega_2 = d\varphi$ one then obtains with complete induction

$$\mathrm{d}^d r = r^{d-1} \mathrm{d}r \ \mathrm{d}\varphi \prod_{n=1}^{d-2} (\sin\theta_n)^n \, \mathrm{d}\theta_n. \tag{3.6}$$

3.1.2 Surface and Volume of the d-dimensional sphere

We now want to derive a formula for the surface Ω_d of the d-dimensional unit sphere. To do so, we make use of the fact, that there are two different ways to solve the integral $\int \mathrm{d}^d r e^{-r^2}$. The first one is

$$\int \mathrm{d}^d r e^{-r^2} = \left(\int_{-\infty}^{\infty} e^{-x^2} dx \right)^d = \sqrt{\pi}^d. \tag{3.7}$$

This integral can also be solved in Cartesian coordinates

$$\begin{aligned} \int \mathrm{d}^d r e^{-r^2} &= \int_0^\infty \mathrm{d}r \int \mathrm{d}\Omega_d e^{-r^2} r^{d-1} \\ &= \Omega_d \int_0^\infty \mathrm{d}r \ e^{-r^2} r^{d-1} \\ &= \Omega_d \frac{1}{2} \int_0^\infty \mathrm{d}t \ e^{-t} t^{\frac{d}{2}-1} \\ &= \Omega_d \frac{1}{2} \Gamma\left(\frac{d}{2}\right) \end{aligned} \tag{3.8}$$

with the Γ function

$$\Gamma(x) = \int_0^\infty \mathrm{d}t\ e^{-t} t^{x-1}. \tag{3.9}$$

Comparison of (3.7) with (3.8) leads to the result

$$\Omega_d = \frac{2\pi^{\frac{d}{2}}}{\Gamma\left(\frac{d}{2}\right)}. \tag{3.10}$$

The surface of a d-dimensional sphere with radius R can then be written as

$$\Omega_d(R) = \frac{2\pi^{\frac{d}{2}}}{\Gamma\left(\frac{d}{2}\right)} R^{d-1}. \tag{3.11}$$

The volume of the d-dimensional sphere with radius R is then

$$\begin{aligned} V_d(R) &= \int_0^R \mathrm{d}r\ \Omega_d(r) \\ &= \frac{\pi^{\frac{d}{2}}}{\Gamma\left(\frac{d}{2}+1\right)} R^d. \end{aligned} \tag{3.12}$$

3.1.3 d-dimensional bipolar coordinates

For solving the MCT equations we do not need d-dimensional polar coordinates, but d-dimensional bipolar coordinates. To understand this, we remind of the fact, that polar coordinates are especially useful for spherically symmetric functions, which means that the value of the function only depends on the distance from the origin, i.e. if $f(\vec{r}) = f(r)$. If the function depends on the distance from the origin and on the distance from the point $\vec{r}'$, i.e.

$$f(\vec{r}) = f(r, s) \tag{3.13}$$

with

$$\begin{aligned} r &= |\vec{r}| \\ s &= |\vec{r} - \vec{r}'|, \end{aligned} \tag{3.14}$$

then bipolar coordinates are more useful. Without loss of generality we set

$$|\vec{r}'| = r_0 \tag{3.15}$$

and

$$\vec{r}' || \vec{e}_d \tag{3.16}$$

i.e. with $\vec{r}' = (x'_1, x'_2, ..., x'_d)^T$

$$\begin{aligned} x'_d &= r_0 \\ x'_n &= 0 \quad \text{for } n < d. \end{aligned} \tag{3.17}$$

From (3.1), (3.14) and (3.17) we then obtain

$$s = \sqrt{r^2 + r_0^2 - 2rr_0 \cos\theta_{d-2}} \tag{3.18}$$

which also means that[1]

$$f(r, s) = f(r, \theta_{d-2}). \tag{3.19}$$

So after transformation into d-dimensional polar coordinates we obtain

$$\begin{aligned} \int \mathrm{d}^d r \; f(\vec{r}) &= \int_0^\infty \mathrm{d}r \int \mathrm{d}\Omega_d \; r^{d-1} f(r, \theta_{d-2}) \\ &= \underbrace{\int \mathrm{d}\Omega_{d-1}}_{\Omega_{d-1}} \int_0^\infty \mathrm{d}r \int_0^\pi \mathrm{d}\theta_{d-2} \left(r \sin\theta_{d-2}\right)^{d-2} \; r \; f(r, \theta_{d-2}) \end{aligned} \tag{3.20}$$

where Eq. (3.5) has been used. We can now apply the transformation

$$(r, \theta_{d-2}) \to (r, s) \tag{3.21}$$

with

$$\begin{aligned} s &= |\vec{r} - \vec{r}_0| = \sqrt{r^2 + r_0^2 - 2rr_0 \cos\theta_{d-2}} \\ \mathrm{d}\theta_{d-2} &= \frac{s}{rr_0 \sin\theta_{d-2}} \mathrm{d}s \end{aligned} \tag{3.22}$$

[1] As a general remark, we note here, that functions, that have the same name, but different arguments, are treated as different functions. This means that for example $f(r)$ and and $f(k)$ are not the same functions, if r has the unit of a length and k has the unit of an inverse length. This is known in programming as *overloading* of functions. Additionally, a fourier transform may be implied as $f\left(\vec{k}\right) = \int \mathrm{d}^3 r \; e^{-i\vec{k}\vec{r}} f(\vec{r})$. We may also sometimes use the implicit definition $r = |\vec{r}|$.

and

$$\begin{aligned}\sin\theta_{d-2} &= \sqrt{1-\cos\theta_{d-2}^2} = \sqrt{1-\left(\frac{r^2+r_0^2-s^2}{2rr_0}\right)^2} \\ &= \frac{1}{2rr_0}\sqrt{4r^2r_0^2-\left(r^2+r_0^2-s^2\right)^2}. \end{aligned} \tag{3.23}$$

This leads to the final result for the integration in bipolar coordinates

$$\int \mathrm{d}^d r\ f\left(\vec{r}\right) = \Omega_{d-1}\int_0^\infty \mathrm{d}r \int_{|r_0-r|}^{r_0+r} \mathrm{d}s\ 2^{3-d} r\ s\ r_0^{2-d}\left(4r^2r_0^2-\left(r^2+r_0^2-s^2\right)^2\right)^{\frac{d-3}{2}} f\left(r,s\right) \tag{3.24}$$

where the integrational borders are given by the triangle inequalities

$$\int_0^\infty dr \int_0^\infty ds\ \theta\left(r_0-r+s\right)\theta\left(r_0+r-s\right)\theta\left(-r_0+r+s\right)\cdots = \int_0^\infty dr \int_{|r_0-r|}^{r_0+r} ds \cdots . \tag{3.25}$$

3.1.4 d-dimensional Fourier transform

We now want to derive a general equation for the d-dimensional Fourier transform for spherically symmetric functions. With Eq. (3.5) this Fourier transform can be written as

$$\begin{aligned} f\left(k\right) &= \int \mathrm{d}^d r e^{i\vec{k}\vec{r}} f\left(r\right) \\ &= \Omega_{d-1}\int_0^\infty \mathrm{d}r\ r^{d-1} f\left(r\right)\int_0^\pi \mathrm{d}\theta_{d-2}\ \left(\sin\theta_{d-2}\right)^{d-2} e^{ikr\cos\theta_{d-2}} \\ &= \Omega_{d-1}\int_0^\infty \mathrm{d}r\ r^{d-1} f\left(r\right)\int_{-1}^1 \mathrm{d}t\ \sqrt{1-t^2}^{d-3} e^{ikrt} \end{aligned} \tag{3.26}$$

where we have set without loss of generality

$$\vec{k}||\vec{e}_d. \tag{3.27}$$

With (cf. [39], Eq. (8.411))

$$\int_{-1}^1 \mathrm{d}t\ \sqrt{1-t^2}^{d-3} e^{ikrt} = \sqrt{\pi}\left(\frac{kr}{2}\right)^{1-\frac{d}{2}} J_{\frac{d}{2}-1}\left(kr\right)\Gamma\left(\frac{d-1}{2}\right), \tag{3.28}$$

where $J_n(x)$ is the Bessel function, one obtains

$$f(k) = \sqrt{\pi}\Omega_{d-1}\Gamma\left(\frac{d-1}{2}\right)\left(\frac{2}{k}\right)^{\frac{d}{2}-1}\int_0^\infty dr\; r^{\frac{d}{2}} f(r)\, J_{\frac{d}{2}-1}(kr)\,. \tag{3.29}$$

With Eq. (3.10) the final result reads

$$f(k) = (2\pi)^{\frac{d}{2}}\left(\frac{1}{k}\right)^{\frac{d}{2}-1}\int_0^\infty \mathrm{d}r\; r^{\frac{d}{2}} f(r)\, J_{\frac{d}{2}-1}(kr)\,. \tag{3.30}$$

The inverse transformation is then equivalently

$$\begin{aligned} f(r) &= \frac{1}{(2\pi)^d}\int \mathrm{d}^d k e^{-i\vec{k}\vec{r}} f(k) \\ &= (2\pi)^{-\frac{d}{2}}\left(\frac{1}{r}\right)^{\frac{d}{2}-1}\int_0^\infty \mathrm{d}k\; k^{\frac{d}{2}} f(k)\, J_{\frac{d}{2}-1}(kr)\,. \end{aligned} \tag{3.31}$$

3.2 Mode-coupling equations in high dimensions

We now want to use the results of the previous section to simplify the memory function (2.48) and (2.49) of the mode-coupling equations. After transformation into bipolar coordinates (cf. Eq. (3.24)) and with

$$|\vec{k}-\vec{p}|^2 = k^2 - 2\vec{k}\cdot\vec{p} + p^2 \tag{3.32}$$

which means that

$$\vec{k}\cdot\vec{p} = \frac{1}{2}\left(k^2 + p^2 - |\vec{k}-\vec{p}|^2\right) \tag{3.33}$$

and

$$\delta\left(\vec{k}-\vec{p}-\vec{q}\right) V\left(\vec{k},\vec{p},\vec{q}\right) = \tag{3.34}$$

$$= \delta\left(\vec{k}-\vec{p}-\vec{q}\right)\frac{n}{8}\frac{S(k)\,S(p)\,S(q)}{k^4}\left(\left(k^2+p^2-q^2\right)c(p) + \left(k^2+q^2-p^2\right)c(q)\right)^2$$

we obtain the following result for the functional of the memory function in arbitrary dimensions

$$\begin{aligned}
&\mathcal{F}_k\left[\phi_q(t)\right] = \\
= \;& n\frac{\Omega_{d-1}}{(4\pi)^d}\frac{S(k)}{k^{d+2}}\int_0^\infty \mathrm{d}p \int_{|k-p|}^{k+p} \mathrm{d}q\; p\; q\; S(p)\, S(q)\left(4k^2p^2 - \left(k^2+p^2-q^2\right)^2\right)^{\frac{d-3}{2}} \\
& \cdot \left(\left(k^2+p^2-q^2\right)c(p) + \left(k^2+q^2-p^2\right)c(q)\right)^2 \phi_p(t)\,\phi_q(t)\,. \qquad (3.35)
\end{aligned}$$

This can also be written as

$$\mathcal{F}_k\left[\phi_q(t)\right] = \frac{\Omega_{d-1}}{(4\pi)^d}\int_0^\infty \mathrm{d}p \int_{|k-p|}^{k+p} \mathrm{d}q\; V(k,p,q)\,\phi_p(t)\,\phi_q(t) \qquad (3.36)$$

with

$$\begin{aligned}
V(k,p,q) \;=\; & n\frac{p\;q}{k^{d+2}} S(k)\, S(p)\, S(q)\left(4k^2p^2 - \left(k^2+p^2-q^2\right)^2\right)^{\frac{d-3}{2}} \\
& \cdot \left(\left(k^2+p^2-q^2\right)c(p) + \left(k^2+q^2-p^2\right)c(q)\right)^2 . \qquad (3.37)
\end{aligned}$$

For completeness we note here that for the self correlation function

$$\phi_k^{(s)}(t) = \left\langle e^{i\vec{k}(\vec{r}^n(t)-\vec{r}^n(0))}\right\rangle$$

where n is an arbitrary particle, one can derive with similar steps

$$\ddot{\phi}_k^{(s)}(t) + \left(\Omega_0^{(s)}(k)\right)^2 \phi_k^{(s)}(t) + \left(\Omega_0^{(s)}(k)\right)^2 \int_0^t dt' m_k^{(s)}(t-t')\dot{\phi}_k^{(s)}(t') = 0 \qquad (3.38)$$

with

$$\left(\Omega_0^{(s)}(k)\right)^2 = \frac{k_B T}{m}k^2 \qquad (3.39)$$

and with the memory function

$$m_k^{(s)}(t) = \mathcal{F}_k^{(s)}\left[\phi_q(t), \phi_q^{(s)}(t)\right] \qquad (3.40)$$

with

$$\mathcal{F}_k^{(s)}\left[\phi_q(t), \phi_q^{(s)}(t)\right] = \frac{\Omega_{d-1}}{(4\pi)^d}\int_0^\infty \mathrm{d}p \int_{|k-p|}^{k+p} \mathrm{d}q\; V^{(s)}(k,p,q)\,\phi_p^{(s)}(t)\,\phi_q(t) \qquad (3.41)$$

and

$$V^{(s)}(k,p,q) = n\frac{p\ q}{k^{d+2}}S\left(p\right)\left(4k^2p^2-\left(k^2+p^2-q^2\right)^2\right)^{\frac{d-3}{2}} \cdot\left(\left(k^2+p^2-q^2\right)c\left(p\right)\right)^2. \tag{3.42}$$

3.3 Static input

3.3.1 Direct correlation function

The equilibrium statistical properties of hard sphere systems in d dimensions become exceptionally simple for $d \to \infty$ in a certain density range. For example it has been shown for a system of hard spheres that in the virial expansion of the equation of state the third and higher virial term vanishes exponentially, if 2^d times the packing fraction does not increase exponentially with d [19, 20]. In order to solve the MCT equations we only need the direct correlation function $c\left(k\right)$ as input, the static structure factor can then be obtained via the Ornstein-Zernike relation. Generally the direct correlation function $c\left(|\vec{r}-\vec{r}\,'|\right) \equiv c^{(2)}(\vec{r},\vec{r}\,')$ can be expanded in Mayer functions, which can be written for a system of hard spheres with diameter σ

$$f\left(r\right) = e^{-\beta v(r)} - 1 = -\theta\left(\sigma - r\right) \tag{3.43}$$

(cf. [29], Eq. (3.8.7)). This diagrammatic expansion can be seen in Fig. 3.1. The lines are Mayer functions, the circles represent particle coordinates. The white circles are the positions $\vec{r}$ and $\vec{r}\,'$ in the function $c^{(2)}(\vec{r},\vec{r}\,')$. Over the black circles one has to integrate with a single particle density as a prefactor. The expansion consists of all

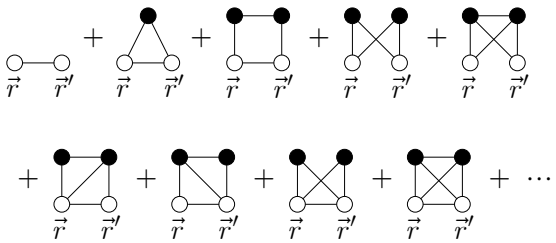

Figure 3.1: Diagrammatic expansion of the direct correlation function $c^{(2)}(\vec{r},\vec{r}\,')$ in Mayer functions [29].

diagrams which are free of connecting circles, i.e. circles whose removal would lead to a disconnected diagram. For example the first term can be written as

$$c_0^{(2)}(\vec{r},\vec{r}') = -\theta\left(\sigma - |\vec{r}-\vec{r}'|\right), \tag{3.44}$$

the second term in Fig. 3.1 is then

$$c_1^{(2)}(\vec{r},\vec{r}') = -\theta\left(\sigma - |\vec{r}-\vec{r}'|\right) n \int \mathrm{d}^d r_1 \theta\left(\sigma - |\vec{r}-\vec{r}_1|\right)\theta\left(\sigma - |\vec{r}'-\vec{r}_1|\right). \tag{3.45}$$

If $n\int d^d r_1 \theta\left(\sigma - |\vec{r}-\vec{r}_1|\right)\theta\left(\sigma - |\vec{r}'-\vec{r}_1|\right)$ becomes much smaller than 1 in the limit $d \to \infty$, then $c_1^{(2)}(\vec{r},\vec{r}')$ can be neglected compared to $c_0^{(2)}(\vec{r},\vec{r}')$. We now want to understand, why this is the case for a certain density range. The integrational volume contributing to $\int d^d r_1 \theta\left(\sigma - |\vec{r}-\vec{r}_1|\right)\theta\left(\sigma - |\vec{r}'-\vec{r}_1|\right)$ lies within a sphere with center at $\left(\vec{r}+\vec{r}'\right)/2$ and radius

$$R = \sqrt{\sigma^2 - \left(\frac{\vec{r}-\vec{r}'}{2}\right)^2} \tag{3.46}$$

with

$$R < \sigma \tag{3.47}$$

in the relevant case $0 < |\vec{r}-\vec{r}'| < \sigma$, because $c_1^{(2)}(\vec{r},\vec{r}')$ is equal to zero for $|\vec{r}-\vec{r}'| > \sigma$. This means that

$$n\int \mathrm{d}^d r_1 \theta\left(\sigma - |\vec{r}-\vec{r}_1|\right)\theta\left(\sigma - |\vec{r}'-\vec{r}_1|\right) < nV_d\left(R\right) \tag{3.48}$$

where $V_d\left(R\right)$ is the volume of a d-dimensional sphere with radius R (cf. Eq. (3.12)). If we now introduce the packing fraction φ, i.e. the ratio of the volume filled by the spheres to the total volume of the system

$$\varphi = nV_d\left(\frac{\sigma}{2}\right) = 2^{-d} nV_d\left(\sigma\right) \tag{3.49}$$

we obtain together with Eq. (3.12)

$$nV_d\left(R\right) = 2^d \varphi \left(\frac{R}{\sigma}\right)^d \tag{3.50}$$

i.e. we obtain for all packing fractions, where $2^d\varphi$ does not increase exponentially or faster with d, also $nV_d\left(R\right)$ becomes exponentially small with increasing d because $R/\sigma < 1$ (cf. Eq. (3.47)). It will be shown later, that this is the case for the critical

MCT packing fraction. From Eqs. (3.45), (3.48) and (3.50) we obtain that in this case $c_1^{(2)}(\vec{r},\vec{r}')$ can be neglected for $d \to \infty$. From a similar argument it can be seen that this is also the case for the other diagrams in the expansion of $c\,(r)$.

So for $d \to \infty$ we have

$$c\,(r) = f\,(r) = -\theta\,(\sigma - r) \tag{3.51}$$

from which we obtain together with Eq. (3.29)

$$c\,(k;d) = -\sqrt{\pi}\Omega_{d-1}\Gamma\left(\frac{d-1}{2}\right)\left(\frac{2}{k}\right)^{\frac{d}{2}-1}\int_0^\sigma \mathrm{d}r\; r^{\frac{d}{2}} J_{\frac{d}{2}-1}\,(kr)\,. \tag{3.52}$$

With

$$\int_0^1 \mathrm{d}x\; x^{\nu+1} J_\nu\,(ax) = a^{-1} J_{\nu+1}\,(a) \tag{3.53}$$

(cf. [39], Eq. (6.561.5)) or respectively

$$\int_0^\sigma \mathrm{d}r\; r^{\frac{d}{2}} J_{\frac{d}{2}-1}\,(kr) = \frac{\sigma^{\frac{d}{2}}}{k} J_{\frac{d}{2}}\,(k\sigma) \tag{3.54}$$

we obtain

$$c\,(k;d) = -\frac{1}{2}\sqrt{\pi}\Omega_{d-1}\Gamma\left(\frac{d-1}{2}\right)\left(\frac{2\sigma}{k}\right)^{\frac{d}{2}} J_{\frac{d}{2}}\,(k\sigma)\,. \tag{3.55}$$

With

$$\Omega_{d-1} = \frac{2\pi^{\frac{d-1}{2}}}{\Gamma\left(\frac{d-1}{2}\right)} \tag{3.56}$$

(cf. Eq. (3.10)) this yields the following

$$c\,(k;d) = -\,(2\pi)^{\frac{d}{2}}\,\sigma^d \frac{1}{(\sigma k)^{\frac{d}{2}}} J_{\frac{d}{2}}\,(k\sigma)\,. \tag{3.57}$$

From a series expansion of $J_{\frac{d}{2}}\,(k\sigma)$ we obtain for $d \to \infty$ on a scale $k\sigma/\sqrt{d} = \bar{k} = O(1)$

$$c\left(\bar{k}\sqrt{d}/\sigma;d\right) \cong -\sigma^d \frac{\pi^{\frac{d}{2}}}{\Gamma\left(\frac{d}{2}+1\right)} \exp\left(-\frac{1}{2}\bar{k}^2\right). \tag{3.58}$$

The converging of the direct correlation function to this master function on the scale $\bar{k}$ can be seen in Fig. 3.2. On a scale $k\sigma/d = \tilde{k} = O(1)$ we obtain from an asymptotic

expansion of $J_{\frac{d}{2}}(k\sigma)$ for $\tilde{k} < 1/2$ (cf. [40], Eq. (9.3.7))

$$\begin{aligned} & c\left(\tilde{k}d/\sigma; d\right) = \\ = & -\left(\frac{2\pi}{\tilde{k}d}\right)^{\frac{d}{2}} \sigma^d \frac{1}{\sqrt{\pi d}} \left(1 - 4\tilde{k}^2\right)^{-1/4} \exp\left[-\frac{d}{2}\operatorname{arctan\,h}\sqrt{1-4\tilde{k}^2} + \frac{d}{2}\sqrt{4\tilde{k}^2-1}\right] \\ & \cdot (1 + O(1/d)) \end{aligned} \tag{3.59}$$

and for $\tilde{k} > 1/2$ (cf. [40], Eq. (9.3.3))

$$\begin{aligned} & c\left(\tilde{k}d/\sigma; d\right) = \\ = & -2\left(\frac{2\pi}{\tilde{k}d}\right)^{\frac{d}{2}} \sigma^d \frac{1}{\sqrt{\pi d}} \left(4\tilde{k}^2 - 1\right)^{-1/4} \\ & \cdot \left(\cos\left[\frac{d}{2}\sqrt{4\tilde{k}^2-1} - \frac{d}{2}\arctan\sqrt{4\tilde{k}^2-1} - \frac{\pi}{4}\right] + O(1/d)\right). \end{aligned} \tag{3.60}$$

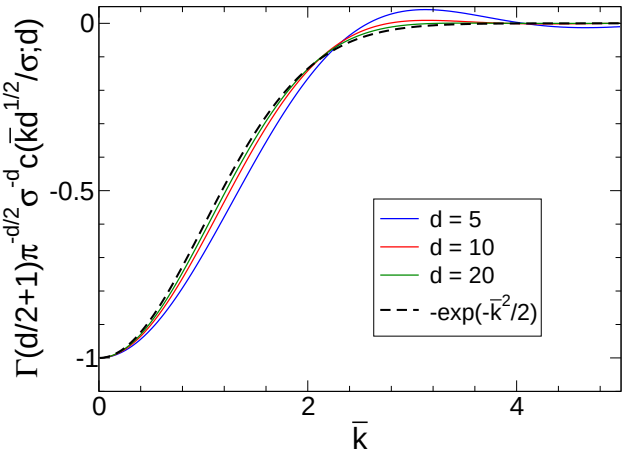

Figure 3.2: Illustration of the convergence of the direct correlation function $c(k; d)$ to the master function given in Eq. 3.58 on a scale $\bar{k} = k\sigma/\sqrt{d}$.

3.3.2 Static structure factor

We now want to take a closer look at the properties of the static structure factor, which can be determined via the Ornstein-Zernike equation [29]

$$S(k) = \frac{1}{1 - nc(k)}. \tag{3.61}$$

With the packing fraction φ

$$\begin{aligned} \varphi &= nV_d(\sigma/2) \\ &= n\frac{\pi^{\frac{d}{2}}}{\Gamma\left(\frac{d}{2}+1\right)}\left(\frac{\sigma}{2}\right)^d \end{aligned} \tag{3.62}$$

or respectively the density n

$$n = \varphi\frac{\Gamma\left(\frac{d}{2}+1\right)}{\pi^{\frac{d}{2}}}\left(\frac{2}{\sigma}\right)^d \tag{3.63}$$

we obtain from Eq. (3.58) for the static structure factor

$$S(k;d,\varphi) \cong \frac{1}{1 + 2^d\varphi\exp\left(-\frac{1}{2}\frac{(k\sigma)^2}{d}\right)}. \tag{3.64}$$

For $\varphi = 2^{-d}\bar{\varphi}$ this yields on a scale $k\sigma/\sqrt{d} = \bar{k} = O(1)$

$$\begin{aligned} S\left(\bar{k}\sqrt{d}/\sigma;d,2^{-d}\bar{\varphi}\right) &\cong \frac{1}{1+\bar{\varphi}\exp\left(-\frac{1}{2}\bar{k}^2\right)} \\ &\equiv \bar{S}\left(\bar{k};\bar{\varphi}\right). \end{aligned} \tag{3.65}$$

The converging of the direct correlation function to this master function on the scale $\bar{k}$ can be seen in Fig. 3.3. It can be seen, that $\bar{S}\left(\bar{k};\bar{\varphi}\right)$ increases monotonically from $1/(1+\bar{\varphi})$ to 1 for $\bar{k} \to \infty$ without showing any peaks.

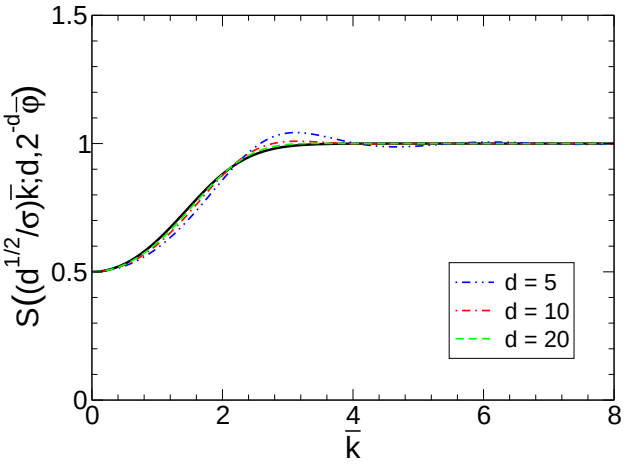

Figure 3.3: Static structure factor $S\left(k; d, 2^{-d}\bar{\varphi}\right)$ on the scale $\bar{k} = k\sigma/\sqrt{d}$ for $\bar{\varphi} = 1$ and $d = 5$, 10, 20. The bold black line is $\bar{S}\left(\bar{k}; 1\right)$ (cf. Eq. (3.65)).

3.3.3 Critical packing fraction for diverging static structure factor

We now want to take a closer look, at what packing fraction the static structure factor diverges. The static structure factor has to diverge at a certain packing fraction, because the direct correlation function is non-negative in some range in k space, caused by the oscillations of the Bessel function (cf. Eq. (3.57)). If we increase the packing fraction, until $nc\left(k\right) = 1$ somewhere, then the denominator in Eq. (3.61) can become zero and the static structure factor diverges. In order to find the packing fraction $\varphi_*\left(d\right)$ at which this happens the first time, we have to determine the position $k_*\left(d\right)$ of the maximum of $\left(\frac{1}{k}\right)^{\frac{d}{2}} J_{\frac{d}{2}}\left(k\right)$, which describes the k dependence of the direct correlation function (Eq. (3.57)):

$$0 = \frac{\partial}{\partial k}\left[\left(\frac{1}{k\sigma}\right)^{\frac{d}{2}} J_{\frac{d}{2}}\left(k\sigma\right)\right]_{k=k_*(d)} = -\left(\frac{1}{k\sigma}\right)^{\frac{d}{2}} J_{\frac{d}{2}+1}\left(k\sigma\right)\Big|_{k=k_*(d)} \tag{3.66}$$

i.e.

$$J_{\frac{d}{2}+1}\left(k_*\left(d\right)\sigma\right) \stackrel{!}{=} 0. \tag{3.67}$$

From the asymptotic expansion of the first zero of the Bessel function (cf. [40], Eq. (9.5.14)) we then find

$$\begin{aligned} k_* (d)\, \sigma &= \left(\frac{d}{2}+1\right) + a \cdot \left(\frac{d}{2}+1\right)^{\frac{1}{3}} \\ a &\cong 1.8557571 \end{aligned} \tag{3.68}$$

From Eqs. (3.57),(3.61) and (3.63) we then obtain

$$\varphi_* (d) = \left[-\Gamma\left(\frac{d}{2}+1\right) 2^{3d/2} (k\sigma)^{-\frac{d}{2}} J_{\frac{d}{2}} (k\sigma) \Big|_{k=k_*(d)} \right]^{-1}. \tag{3.69}$$

We can now expand all the terms appearing in Eq. (3.69) in the limit $d \to \infty$. The asymptotic expansion of the Gamma function is given by the Sterling formula

$$\Gamma (x) \cong \sqrt{\frac{2\pi}{x}} \left(\frac{x}{e}\right)^x \tag{3.70}$$

i.e.

$$\Gamma\left(\frac{d}{2}+1\right) \cong \sqrt{d\pi} \left(\frac{d}{2}\right)^{\frac{d}{2}} e^{-\frac{d}{2}}. \tag{3.71}$$

$(k_* (d)\, \sigma)^{-\frac{d}{2}}$ can be expanded as

$$(k_* (d)\, \sigma)^{-\frac{d}{2}} \cong \left(\frac{d}{2}\right)^{-\frac{d}{2}} \exp\left(-1 - a\left(\frac{d}{2}\right)^{\frac{1}{3}}\right), \tag{3.72}$$

the expansion of $J_{d/2} (k_* (d)\, \sigma)$ is given as (cf. [40], Eq. (9.5.18))

$$\begin{aligned} J_{d/2} (k_* (d)\, \sigma) &= J'_{d/2+1} (k_* (d)\, \sigma) \cong -b_0 \cdot (d/2+1)^{-2/3}, \\ b_0 &\cong 1.1131028 \end{aligned} \tag{3.73}$$

Altogether we obtain

$$\varphi_* (d) \cong c_0 \cdot d^{1/6} \exp\left(a_0 (d/2)^{1/3}\right) \left(\sqrt{8/e}\right)^{-d}, \tag{3.74}$$

$$c_0 = b_0^{-1} \pi^{-1/2} 2^{-2/3} e \cong 0.867956, \tag{3.75}$$

i.e. the leading d dependence of $\varphi_* (d)$ is the exponential factor $(\sqrt{8/e})^{-d} \cong (1.7155)^{-d}$. The result (3.74) for $\varphi_* (d)$ has already been obtained earlier [41–43], however, with

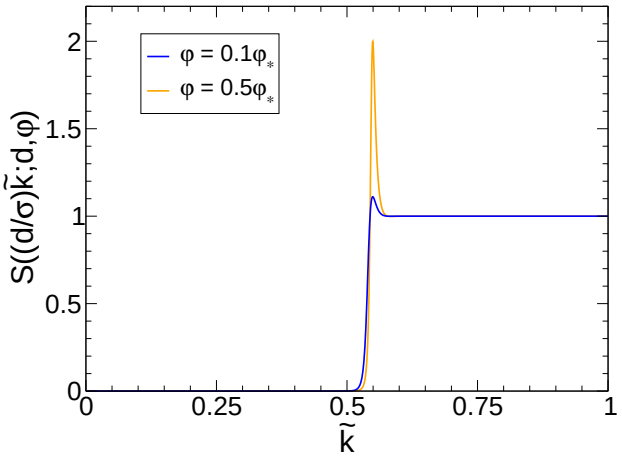

Figure 3.4: $S\left(k;d,\varphi\right)$ on the scale $\tilde{k}=k\sigma/d$ for $d=200$ and $\varphi=0.1\varphi_*$, $\varphi=0.5\varphi_*$.

different numerical prefactors. The prefactor of Frisch and Percus [41, 43] $c_0\cong 0.871$ agrees to our prefactor, if one inserts the correct value of the derivative of the Airy function: $A_i'(-2^{1/3}a_0)\cong 0.701211$. The prefactor obtained by Bagchi and Rice [42] is $c_0\cong 0.239$. The static structure factor for a packing fraction close to $\varphi_*\left(d\right)$ is shown in Fig. 3.4.

It can be seen, that it is nearly zero for $k<k_*\left(d\right)$, has one sharp diffraction peak at $k_*\left(d\right)$ and decays quite rapidly to one for $k>k_*\left(d\right)$, where it can be seen from Eq. (3.68) that $k_*(d)\sigma/d\cong 1/2$. It is obvious from the derivation of $\varphi_*\left(d\right)$, that for $\varphi\ll\varphi_*\left(d\right)$ the height of the first sharp diffraction peak of $S(k;d,\varphi)$ is given as

$$S\left(k_*(d);d,\varphi\right)\cong 1+\frac{\varphi}{\varphi_*\left(d\right)}. \tag{3.76}$$

In Fig. 3.5 the static structure factor is shown for φ of order $\varphi_c(d)\cong 0.22\cdot d^2 2^{-d}$, which will turn out to be the critical packing fraction of the MCT glass transition. Because $\varphi_c\left(d\right)$ is exponentially smaller than $\varphi_*\left(d\right)$, the static structure factor does not show any peak at this packing fraction anymore (cf. Eq. (3.76)).

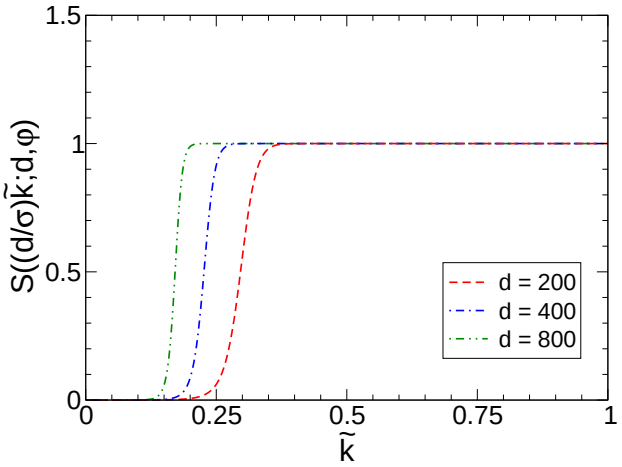

Figure 3.5: $S\left(k;d,\varphi\right)$ on the scale $\tilde{k}=k\sigma/d$ for $d=200$, 400, 800 and $\varphi=\varphi_c\left(d\right)$, i.e. the critical MCT packing fraction.

3.4 Numerical solution

We can now solve the MCT equations numerically by inserting the mode-coupling functional from Eqs. (3.36), (3.37) together with the static input from Eqs. (3.52) and (3.61) into Eq. (2.55) with the initial value from Eq. (2.56). It shall be noted that in the case of hard spheres the functional $\mathcal{F}_k$ for the zero order iterate $f_k^{(0)}\left(d,\varphi\right)$ from Eq. (2.56) exists only for a finite cut-off at $k_{\max}$. The integrals appearing in $\mathcal{F}_k\left[f_k^{(i)}\left(d,\varphi\right);d,\varphi\right]$ are replaced by Riemann sums with an upper cutoff $\sigma k_{\max}=\max(40d^{1/2};4d;0.2d^{3/2})$ and 500 gridpoints for $d<200$, 1000 gridpoints for $200\leq d\leq 600$ and 1500 gridpoints for $d>600$. The reason why we need more gridpoints in higher dimensions, is the oscillatory behaviour of the direct correlation function (cf. Figs. 3.14 and 3.15). This is also the reason, why we only have evaluated the MCT equations up to $d=800$.

The critical packing fraction $\varphi_c(d)$ is the packing fraction, where

$$f_k\left(d,\varphi\right)\begin{cases}=0 & ,\ \varphi<\varphi_c(d)\\ \neq 0 & ,\ \varphi\geq\varphi_c(d)\end{cases} \tag{3.77}$$

and the critical nonergodicity parameters are given by

$$f_k^c\left(d\right)\equiv f_k(d,\varphi_c(d)). \tag{3.78}$$

Because the real critical packing fraction and the critical nonergodicity parameters can

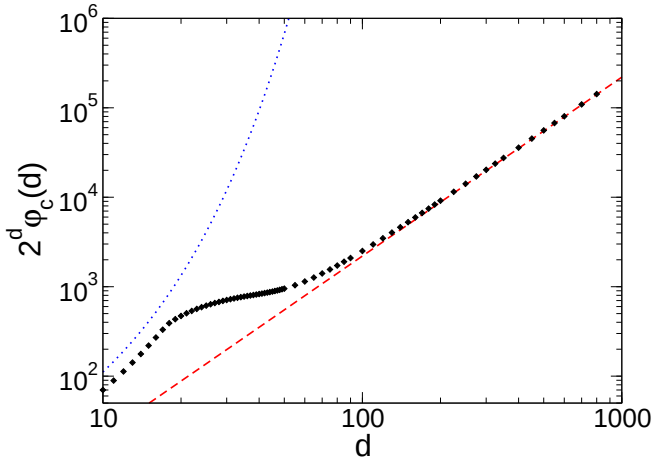

Figure 3.6: d dependence of the critical packing fraction $\varphi_c(d)$ on a log-log representation. The dashed red line is $2^d\varphi_c(d) \cong ad^2$. The dotted blue line is $\varphi_*(d)$ from Eq. (3.74).

never be computed numerically in finite time, we have evaluated $f_k^c(d)$ at a packing fraction $\hat{\varphi}_c(d)$ where $\lim_{i\to\infty} f_k^{(i)}(d, \hat{\varphi}_c(d)) = 0$ but

$$\min_i \left(\max_k \left| \frac{f_k^{(i+1)}(d, \hat{\varphi}_c(d)) - f_k^{(i)}(d, \hat{\varphi}_c(d))}{f_k^{(i+1)}(d, \hat{\varphi}_c(d))} \right| \right) < \varepsilon \tag{3.79}$$

with $\varepsilon = 10^{-7}$ for $d \leq 600$ and $\varepsilon = 10^{-5}$ for $d > 600$. It can be estimated that the relative difference between this packing fraction $\hat{\varphi}_c(d)$ and the real critical packing fraction $\varphi_c(d)$ is of order ε. It has been verified that the system really becomes nonergodic near this packing fraction, i.e. $f_k(d, \varphi) \neq 0$ for $\varphi > (1 + \varepsilon \cdot O(1))\hat{\varphi}_c(d)$. The critical nonergodicity parameters can then be approximated by

$$f_k^c(d) \cong f_k^{(i_0)}(d, \hat{\varphi}_c(d)) \tag{3.80}$$

where i_0 equals the iteration step, where

$$\max_k \left| \frac{f_k^{(i_0+1)}(d, \hat{\varphi}_c(d)) - f_k^{(i_0)}(d, \hat{\varphi}_c(d))}{f_k^{(i_0+1)}(d, \hat{\varphi}_c(d))} \right| \tag{3.81}$$

reaches a minimum[2] [44]. It has been verified that there are no visible differences in the

[2]It will become more clear in section 3.4.1, when we evaluate the exponent parameter λ, why we use this definition of the critical nonergodicity parameter.

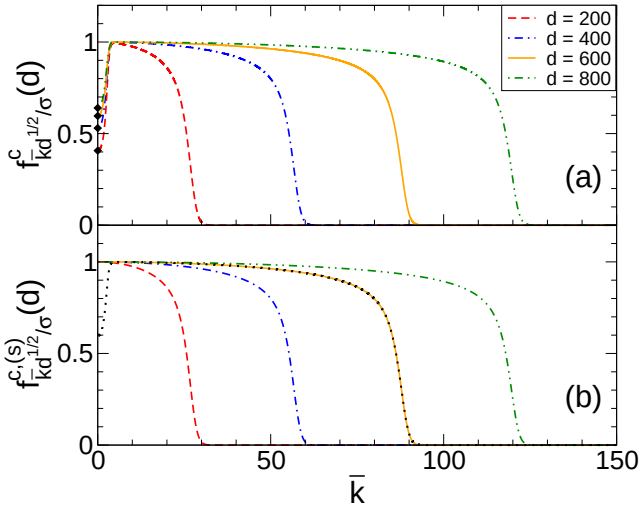

Figure 3.7: Critical nonergodicity parameters $f_k^c(d)$ (a) and $f_k^{c,(s)}(d)$ (b) for $d = 200$, 400, 600 and 800 on a scale $\bar{k} = k\sigma/\sqrt{d}$. Diamonds in (a) mark the numerical precise values for $f_0^c(d)$ and the dotted line in (b) presents $f_k^c(600)$.

critical nonergodicity parameters obtained by this procedure with different values of ε and that $f_k(d, \varphi_c(d) + \Delta\varphi)$ converges to $f_k^{(i_0)}(d, \hat{\varphi}_c(d))$ with order $\sqrt{\Delta\varphi}$. Additionally it has been verified that $f_{k_{\max}}^c(d) < 10^{-16}$ for all evaluated dimensions. By increasing $k_{\max}$ and the number of gridpoints the relative error of the critical packing fraction due to the discretization can be estimated to be smaller than 10^{-3} for $d \leq 600$.

The nonergodicity parameters always show numerical artifacts on the first few gridpoints in k space. This is a problem when trying to observe the characteristics of $f_k^c(d)$ for small wavenumbers, especially for high dimensions. So we interpolated $f_k^c(d)$ onto a much finer k-grid and performed one single iteration step equivalent to the one given in Eq. (2.55). This procedure improves the result for $f_k^c(d)$ by shifting the numerical artifacts to much smaller values of k.

From this procedure we obtain the critical packing fraction $\varphi_c(d)$ shown in Fig. 3.6. We find that for $d \lesssim 18$ the critical packing fraction $\varphi_c(d)$ follows the behaviour of the spinodal $\varphi_*(d)$ (cf. section 3.3.3). For $d \gtrsim 18$ the critical packing fraction is much smaller than the value $\varphi_*(d)$, at which the spinodal occurs. For $d \gtrsim 100$ the critical packing fraction can be well described by

$$\varphi_c(d) \cong a d^2 2^{-d}, \quad a \cong 0.22. \tag{3.82}$$

The critical nonergodicity parameters obtained by the method described above are

shown in Fig. 3.7. It is already very obvious, that both, $f_k^c(d)$ and $f_k^{c,(s)}(d)$ show a non-Gaussian k dependence. Additionally it becomes clear, that there are three characteristic k scales. $f_k^c(d)$ increases from $f_0^c(d)$ to its maximum value on a scale $k\sigma \sim \sqrt{d}$. Because $f_k^{c,(s)}(d)$ starts from its maximum value at $k = 0$, $f_k^c(d)$ and $f_k^{c,(s)}(d)$ differ from each other on this scale. They both develop a plateau on a scale $k\sigma \sim d$ and show a steep descent on a scale $k\sigma \sim d^{3/2}$. This decay to zero occurs around $k\sigma \cong \hat{k}_0 d^{3/2}$ where $\hat{k}_0 \cong 0.15$.

3.4.1 Exponent parameter λ

The stability matrix can be evaluated from Eq. (2.61) with Eq. (3.36) inserted. The result reads

$$A_{kp}^c = \frac{\Omega_{d-1}}{(4\pi)^d} \left(1 - f_k^c\right) \int_{|k-p|}^{k+p} \mathrm{d}q \;\; \left(V\left(k,p,q\right) + V\left(k,q,p\right)\right) f_q^c \left(1 - f_p^c\right). \tag{3.83}$$

The left and right eigenvectors to the eigenvalue unity are obtained by iterating Eqs. (2.62), i.e.

$$\begin{aligned} \hat{a}_p^{(i+1)} &= \int \mathrm{d}k \; \hat{a}_k^{(i)} A_{kp}^c \\ a_k^{(i+1)} &= \int \mathrm{d}p \; A_{kp}^c a_p^{(i)} \end{aligned} \tag{3.84}$$

with arbitrary initial values $\hat{a}_p^{(0)}$ and $a_k^{(0)}$. The nondegeneracy of the maximum eigenvalue 1 ensures that this series converges exponentially fast to the desired result. In can be seen in Fig. 3.8 that the largest eigenvalue shows the expected square-root singularity $(1 - E_0(\varphi)) \sim \sqrt{(\varphi - \varphi_c(d))/\varphi_c(d)}$.

The matrix defined in Eq. (2.69) can then be evaluated as

$$\begin{aligned} & A_{kpq} = \\ = \; & \frac{1}{2} \left(1 - f_k\right) \left(1 - f_p\right) \left(1 - f_q\right) \left(V\left(k,p,q\right) + V\left(q,k,p\right)\right) \\ & \cdot \theta\left(-k + p + q\right) \theta\left(k - p + q\right) \theta\left(k + p - q\right) \end{aligned} \tag{3.85}$$

so that the exponent parameter can be evaluated from Eq. (2.68). Numerically one cannot find the point of the glass transition so exactly, that the largest eigenvalue of the stability matrix really becomes equal to 1 (cf. Fig. 3.8). For the same reason one cannot find the true value for the exponent parameter λ exactly. Like any quantity,

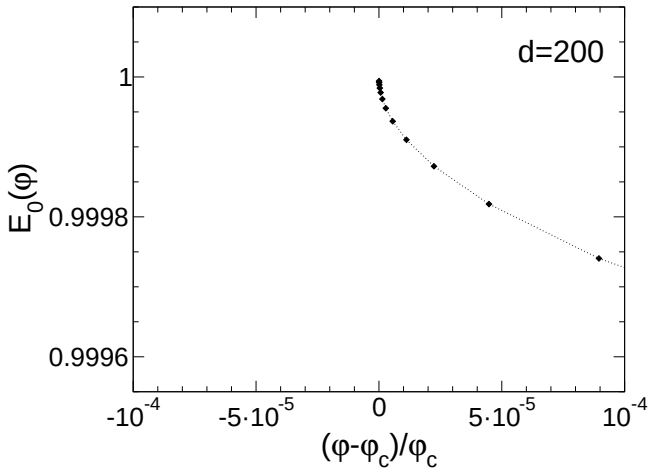

Figure 3.8: Numerical result for the largest eigenvalue $E_0(\varphi)$ of the stability matrix for packing fractions near the glass transition for $d = 200$. It can be seen that $1 - E_0(\varphi)$ shows a square-root singularity, i.e. $1 - E_0(\varphi) \sim \sqrt{(\varphi - \varphi_c(d))/\varphi_c(d)}$.

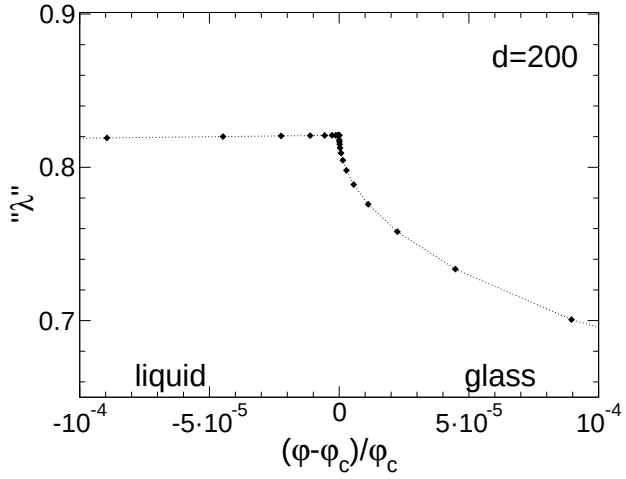

Figure 3.9: Numerical result for the exponent parameter λ evaluated at various packing fractions near the critical point for $d = 200$. For $\varphi > \varphi_c(d)$ we use $f_k(\varphi, d)$ instead of $f_k^c(d)$ to evaluate λ. For $\varphi < \varphi_c(d)$ the required nonergodicity paramaters $f_k^c(d)$ are evaluated from Eq. (3.80) with $\hat{\varphi}_c(d) = \varphi$.

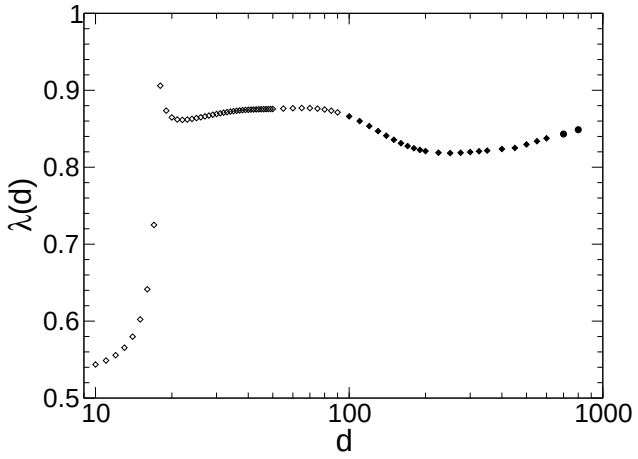

Figure 3.10: d dependence of the exponent parameter λ. The full symbols mark the regime where $\varphi_c(d)$ from Figure 3.6 follows the asymptotic result (3.82). The values for $d = 700$ and 800 depicted by full circles possibly have a larger relative error.

that depends on the nonergodicity parameters, the numerically determined exponent parameter λ shows a squareroot singularity, as can be seen in Fig. 3.9. From this figure it becomes clear, why we use Eq. (3.80) to define the critical nonergodicity parameters. It can be seen that there may be large numerical errors, if one inserts the usual nonergodicity parameters from the glassy side as critical nonergodicity parameter. In contrast to this, the numerical error becomes much smaller, if the nonergodicity parameters are evaluated with Eq. (3.80) on the liquid side of the glass transition, as can be seen if Fig. 3.9.

We found that this effect becomes more important for higher dimensions and one has to evaluate the nonergodicity parameters at packing fractions closer to the glass transition. Because then also the iteration scheme (cf. Eq. (2.55)) converges more slowly, it requires much more computing time for the evaluation of the exponent parameter λ at higher dimensions.

The numerical results for the d dependence of the exponent parameter λ can be seen in Fig. 3.10. The variation of λ for small dimensions d may be an artifact due to the incorrect static input, which is strictly speaking only valid in the limit $d \to \infty$. However, if we assume that the static input would be valid for such low dimensions, the cusplike behaviour of the exponent parameter around $d \cong 18$ is an evidence of a glass-glass transition. This will be investigated in detail in section 3.4.2. In Fig. 3.10 we also realize, that the exponent parameter does not converge to a constant value in

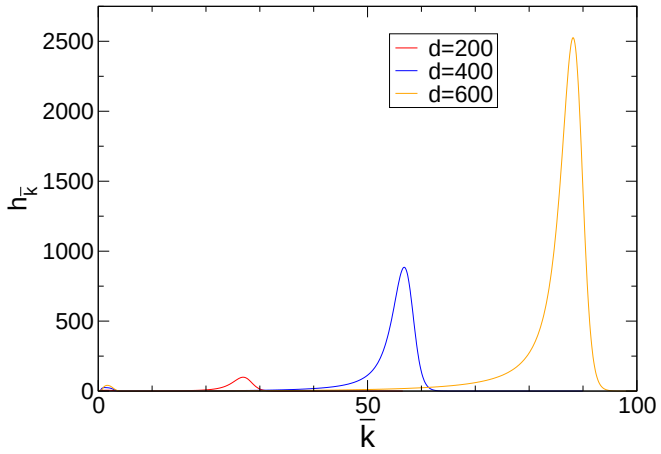

Figure 3.11: d dependence of the critical amplitudes h_k on a scale $\bar{k} = k\sigma/\sqrt{d}$

our range of dimensions. It is not clear, what happens in the limit $d \to \infty$.

The critical amplitudes, which can then be evaluated from Eq. (2.65), are shown in Fig. 3.11 for $d = 200$, 400 and 600. It can be seen that their magnitude increases for higher dimensions and that they have a maximum in the region, where the critical nonergodicity paramters decay from the value of the plateau to zero.

3.4.2 Glass-glass transition

We can now interpret the dimension d as continuous variable, i.e. d may also take non-integer values. From the numerical data we see that there is a slight kink in the critical packing fraction (blue full diamonds in Fig. 3.12) around $d \approx 17.7$. Additionally, there is a strong change in the critical nonergodicity parameters along the liquid-glass transition line at this dimension. This can be interpreted as the crossing of two A_2 singularity lines. One of the A_2 singularities can be continued into the glass (red empty diamonds in Fig. 3.12), the other A_2 line does not consist of the largest solutions, i.e. they are smaller than the physical ones (cf. Eq. (2.54c)). This means that at the line of A_2 singularities, which can be followed into the glass, a glass-glass transition occurs. As discussed in connection with Fig. 2.2, the line of A_2 singularities ends in an A_3 singularity, where $\lambda = 1$. This can be seen Fig. 3.13. The strong change in the critical nonergodicity parameters along the liquid-glass transition line becomes manifest in a jump in the value of λ.

The physical reason for a glass-glass transition is that the mechanism of the glass

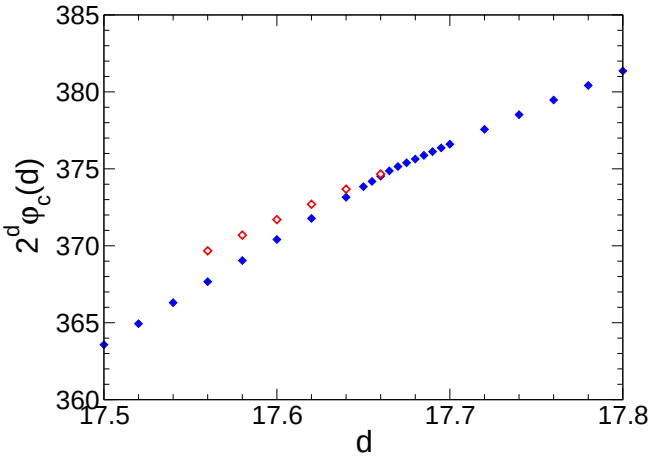

Figure 3.12: d dependence of the critical packing fraction $\varphi_c(d)$ of the liquid-glass transition (blue full diamonds) and glass-glass transition (red empty diamonds).

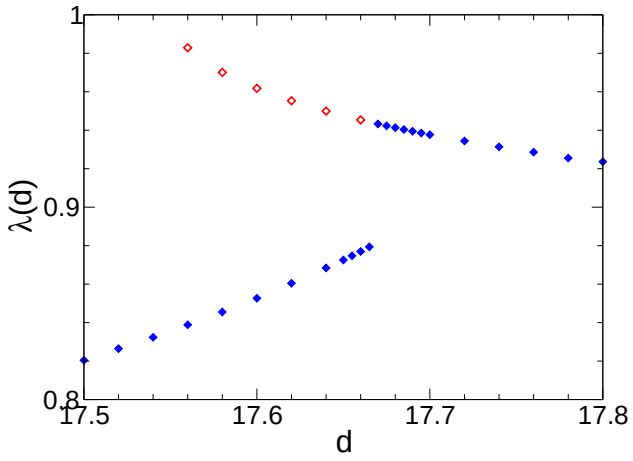

Figure 3.13: d dependence of the exponent parameter $\lambda(d)$ at the liquid-glass (blue full diamonds) and glass-glass transition (red empty diamonds).

transition changes. A change in the mechanism of the glass transition is also the reason for the glass-glass transition in colloidal systems with additional attractive interactions [10, 45]. From the fact, that the critical packing fraction of the glass transition follows the value of the spinodal, it becomes clear, that for $d \lesssim 17.7$ the glass transition is produced by a peak in the static structure factor. For $d \gtrsim 17.7$ this is not the case any more.

One may argue that for $d \approx 17$ it may not be justified to use Eq. (3.51) as static input for the MCT equations, because the approximations are only valid in the limit $d \to \infty$. However, even if one would insert the correct static input into the MCT equations, it can still be expected that a glass-glass transition occurs at some dimension, which may be different from the one we found here, because the fact, that the mechanism of the glass transition changes, remains valid. The mechanism which leads to the glass transition for higher dimension shall be investigated in the following section.

3.5 Analytical solution

Now we want to try to find an analytical explanation for the numerical results found in the previous section. First we show which approximations can be applied in the limit $d \to \infty$. With these approximations we can then evaluate the critical packing fraction and the shape of the critical nonergodicity parameters. Additionally, we also give an approximation of the $k \to 0$ value of the critical collective nonergodicity parameter. Then we also want to try to find an approximation for the self-part of the van Hove function. As Kirkpatrick and Wolynes have also tried to find the critical packing fraction for MCT, we want to compare their result with our result and we want to show, from where the differences between the two solutions come from. Finally we want to show that the convolution approximation becomes exact in the limit $d \to \infty$.

3.5.1 Approximations for $d \to \infty$

In this section we want to apply some approximations to the memory function, which are valid in the limit $d \to \infty$. To do so, we first rescale the vertex in Eq. (3.37) with

$$k = \tilde{k} d/\sigma, \tag{3.86}$$

where $\tilde{k}$ is of order 1 or larger. Quantities on this scale are denoted by a tilde (e.g. $\tilde{f}_{\tilde{k}}$). This rescaling is motivated by the fact that the direct correlation function can

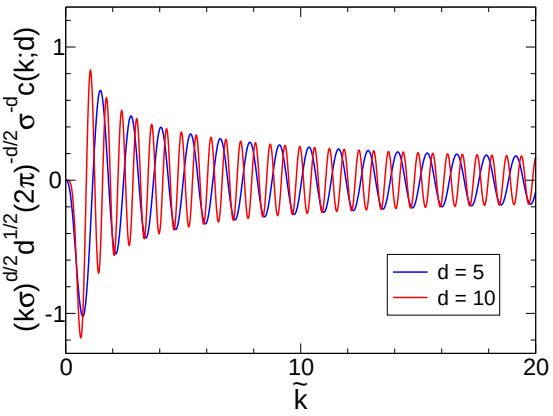

Figure 3.14: Rescaled direct correlation function $c(k;d)$ with a prefactor $(k\sigma)^{d/2}$ for $d = 5$ and $d = 10$.

be expanded more easily on this scale (cf. Eqs. (3.59), (3.60) and Figs. 3.14, 3.15). However, as it turns out, it is also important what happens on a scale $k\sigma = O(d^{3/2})$. This is not in contradiction to Eq. (3.86), because $\tilde{k} = O(d^{1/2})$ is still possible.

We realize from Eq. (3.60) and Fig. 3.14 that the mixed term $\sim c\,(\tilde{p}d/\sigma)\,c\,(\tilde{q}d/\sigma)$ oscillates faster and faster under an increase of d and can thus be neglected. Comparing Eqs. (3.37) and (3.42) we see, that neglecting this term is equivalent to

$$V(\tilde{k}d/\sigma, \tilde{p}d/\sigma, \tilde{q}d/\sigma) \to S\left(\tilde{k}d/\sigma\right) S\,(\tilde{q}d/\sigma)\, V^{(s)}(\tilde{k}d/\sigma, \tilde{p}d/\sigma, \tilde{q}d/\sigma) \tag{3.87}$$

where the symmetry in the integration between p and q in Eq. (3.36)

$$\begin{aligned} \int_0^\infty dp \int_{|k-p|}^{k+p} dq \cdots &= \int_0^\infty dp \int_0^\infty dq\; \theta\,(k-p+q)\,\theta\,(k+p-q)\,\theta\,(-k+p+q) \\ &= \int_0^\infty dq \int_{|k-q|}^{k+q} dp \cdots \end{aligned} \tag{3.88}$$

has been used. Because of the considerations at the end of section 3.3.3 (cf. Fig. 3.5) we can apply the replacement $S\left(\tilde{k}d/\sigma; d\right) \to 1$ for $d \to \infty$ and $\tilde{k}$ of order 1 or larger, i.e.

$$V(\tilde{k}d/\sigma, \tilde{p}d/\sigma, \tilde{q}d/\sigma) \to V^{(s)}(\tilde{k}d/\sigma, \tilde{p}d/\sigma, \tilde{q}d/\sigma) \tag{3.89}$$

and

$$V^{(s)}(k,p,q) \;\rightarrow\; n\frac{p\,q}{k^{d+2}}\left(4k^2p^2-\left(k^2+p^2-q^2\right)^2\right)^{\frac{d-3}{2}} \cdot\left(\left(k^2+p^2-q^2\right)c\left(p\right)\right)^2. \tag{3.90}$$

The factor $\left(4k^2p^2-\left(k^2+p^2-q^2\right)^2\right)^{\frac{d-3}{2}}\left(\left(k^2+p^2-q^2\right)c\left(p\right)\right)^2$ in Eq. (3.42) can then be rewritten as

$$\begin{aligned}&\left(4k^2p^2-\left(k^2+p^2-q^2\right)^2\right)^{\frac{d-3}{2}}\left(\left(k^2+p^2-q^2\right)c\left(p\right)\right)^2 = \\ =\;& \sigma^{-2d+2}d^{2d-2}\left(2\tilde{k}\tilde{p}\right)^{d-1}\left[1-\left(\frac{\tilde{k}^2+\tilde{p}^2-\tilde{q}^2}{2\tilde{k}\tilde{p}}\right)^2\right]^{\frac{d-3}{2}} \\ &\cdot\left(\frac{\tilde{k}^2+\tilde{p}^2-\tilde{q}^2}{2\tilde{k}\tilde{p}}\right)^2 c^2\left(\tilde{p}d/\sigma\right)\end{aligned} \tag{3.91}$$

where we can now apply the approximation

$$\left[1-\left(\frac{\tilde{k}^2+\tilde{p}^2-\tilde{q}^2}{2\tilde{k}\tilde{p}}\right)^2\right]^{\frac{d-3}{2}} \rightarrow \exp\left[-\frac{d}{2}\left(\frac{\tilde{k}^2+\tilde{p}^2-\tilde{q}^2}{2\tilde{k}\tilde{p}}\right)^2\right]. \tag{3.92}$$

This approximation is justified, because only regions with $\left(\frac{\tilde{k}^2+\tilde{p}^2-\tilde{q}^2}{2\tilde{k}\tilde{p}}\right) \ll 1$ lead to a non-neglectable contribution to $V(\tilde{k}d/\sigma, \tilde{p}d/\sigma, \tilde{q}d/\sigma)$. Then we use

$$x^2e^{-\frac{d}{2}x^2} \rightarrow \frac{\sqrt{\pi}}{4}\left(\frac{2}{d}\right)^{3/2}\left[\delta\left(x-\sqrt{\frac{2}{d}}\right)+\delta\left(x+\sqrt{\frac{2}{d}}\right)\right]. \tag{3.93}$$

This approximation is chosen in such a way, that the $\delta-$ distributions on the right hand side of Eq. (3.93) are nonzero where the left hand side of Eq. (3.93) has its maxima. Additionally, the integration over x leads to the same result on both sides of Eq. (3.93). This allows to perform the integration with respect to q in Eq. (3.36). From Eq. (3.60) and Fig. 3.15 we see that the square of the direct correlation function

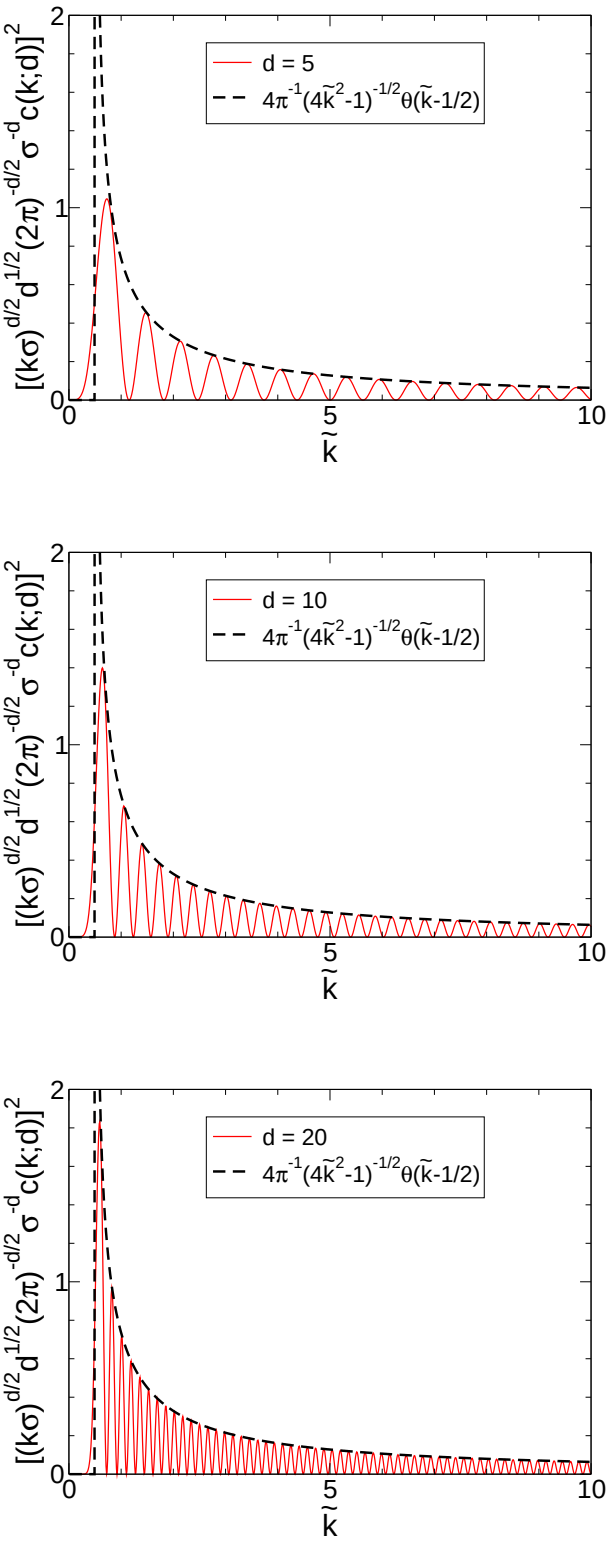

Figure 3.15: Rescaled square of the direct correlation function $c(k;d)$ with a prefactor $(k\sigma)^d$ and its envelope for various dimensions d.

can be approximated as:

$$\begin{aligned} & c^2\left(\tilde{p}d/\sigma\right) = (2\pi)^d \sigma^{2d} d^{-d} J_{d/2}^2\left[(d/2)\,2\tilde{p}\right]/\tilde{p}^d \\ \cong\ & 4\,(2\pi)^d \sigma^{2d} d^{-d} \left(\tilde{p}^d \pi d\sqrt{4\tilde{p}^2-1}\right)^{-1} \Theta\left(\tilde{p}-\frac{1}{2}\right) \\ & \cdot \cos^2\left[\frac{d}{2}\sqrt{4\tilde{p}^2-1} - \frac{d}{2}\arctan\sqrt{4\tilde{p}^2-1} - \frac{\pi}{4}\right]. \end{aligned} \tag{3.94}$$

where we also have made use of the fact that the direct correlation function becomes exponentially small for fixed $\tilde{p} < 1/2$ with increasing d (cf. Eq. (3.59)). Because $\cos^2[\ldots]$ oscillates faster and faster with increasing d, we can replace it with half of its average, i.e. $\cos^2[\ldots] \to \frac{1}{2}$. So we arrive at

$$\tilde{\mathcal{F}}_{\tilde{k}}\left[\tilde{f}_{\tilde{q}}\right] \cong \varphi \frac{2^d}{\tilde{k}^2 \pi d} \int_{\frac{1}{2}}^{\infty} d\tilde{p} \frac{\tilde{p}}{\sqrt{4\tilde{p}^2-1}} \tilde{f}_{\tilde{p}} \left(\tilde{f}_{\tilde{q}_-} + \tilde{f}_{\tilde{q}_+}\right) \tag{3.95}$$

with

$$\tilde{q}_\pm = \left[\tilde{k}^2 + \tilde{p}^2 \pm 2\sqrt{\frac{2}{d}}\tilde{k}\tilde{p}\right]^{1/2}. \tag{3.96}$$

3.5.2 Critical packing fraction

With Eq. (3.95) we can now evaluate the critical packing fraction $\varphi_c(d)$. We can define a point $\tilde{k}_0 \equiv \hat{k}_0 d^{1/2}$ such that $\tilde{f}^c_{\tilde{k}_0} = 1/2$. Because of Eq. (2.53) this is equivalent to

$$\tilde{\mathcal{F}}_{\tilde{k}_0}\left[\tilde{f}^c_{\tilde{q}}\right] = 1, \quad \varphi = \varphi_c(d). \tag{3.97}$$

Based on the numerical result we assume that $\tilde{f}^c_{\tilde{k}_0+\tilde{\delta}}$ decays very fast to zero with $\tilde{\delta} > 0$ and is about 1 for $\tilde{\delta} < 0$. $\tilde{f}_{\tilde{q}_+}$ can then be neglected compared to $\tilde{f}_{\tilde{q}_-}$ for $\tilde{k} = \tilde{k}_0$, which is of order one for $\tilde{p} = O(1)$ and becomes much smaller than 1 for $\tilde{p} \gg 1$. Additionally, we assume that $\tilde{f}^c_{\tilde{p}} \cong 1$ for $\tilde{p} = O(1)$. Then the integral in Eq. (3.95) is of order 1, i.e. order d^0. With these approximations and with $\varphi = \varphi_c(d)$ and $\tilde{k} = \hat{k}\sqrt{d}$ we obtain from Eq. (3.95)

$$1 \cong \tilde{\mathcal{F}}_{\tilde{k}_0}\left[\tilde{f}^c_{\tilde{q}}\right] \cong \pi^{-1}\varphi_c(d)\left(2^d/d^2\right)\hat{k}_0^{-2} O\left(d^0\right). \tag{3.98}$$

Because $\hat{k}_0$ is also of order d^0 we find that $\varphi_c(d)$ has to be

$$\varphi_c(d) \cong a \cdot d^2 2^{-d}. \tag{3.99}$$

From the numerical result we obtain for the constant $a \cong 0.22$.

3.5.3 Shape of the nonergodicity parameter

We can now also try to find an analytic approximation for the shape of the nonergodicity parameter. Same as in the previous section we assume again that $\tilde{f}_{\tilde{q}}^c \cong 0$ for $\tilde{q} > \tilde{k}_0$ and $\tilde{f}_{\tilde{q}}^c \cong 1$ for $\tilde{q} < \tilde{k}_0$. Then we obtain from Eq. (3.96) that $\tilde{q}_\pm$ is smaller than $\tilde{k}_0$ for

$$\tilde{p} < \mp\sqrt{2/d}\;\tilde{k} + \sqrt{(2/d)\,\tilde{k}^2 + \left(\tilde{k}_0^2 - \tilde{k}^2\right)} \cong \sqrt{\left(\tilde{k}_0^2 - \tilde{k}^2\right)}, \tag{3.100}$$

which is valid for $d \to \infty$ and $\tilde{k} \leq \tilde{k}_0$. From Eq. (3.95) we then obtain with $\varphi = \varphi_c\,(d)$

$$\tilde{\mathcal{F}}_{\tilde{k}}\left[\tilde{f}_{\tilde{q}}^c\right] \cong \frac{2ad}{\pi\tilde{k}^2}\int_{\frac{1}{2}}^{\sqrt{\tilde{k}_0^2-\tilde{k}^2}} \mathrm{d}\tilde{p}\;\tilde{p}\frac{1}{\sqrt{4\tilde{p}^2-1}}, \tag{3.101}$$

where the integration can be performed analytically as

$$\int_{\frac{1}{2}}^{\sqrt{\tilde{k}_0^2-\tilde{k}^2}} \mathrm{d}\tilde{p}\;\tilde{p}\frac{1}{\sqrt{4\tilde{p}^2-1}} = \frac{1}{2}\sqrt{\tilde{k}_0^2-\tilde{k}^2}. \tag{3.102}$$

Substituting $\tilde{k} = \hat{k}\sqrt{d}$ results in

$$\lim_{d\to\infty}\left(\tilde{\mathcal{F}}_{\sqrt{d}\,\hat{k}}\left[\tilde{f}_{\tilde{q}}^c\,(d)\,;d\right]/\sqrt{d}\right) = \hat{F}_0\left(\hat{k}\right) \tag{3.103}$$

with the master function:

$$\hat{F}_0\left(\hat{k}\right) \cong \begin{cases} a\pi^{-1}\hat{k}^{-2}\sqrt{\hat{k}_0^2-\hat{k}^2} & ,\ \hat{k} \leq \hat{k}_0 \\ 0 & ,\ \hat{k} > \hat{k}_0 \end{cases}. \tag{3.104}$$

Fig. 3.16 shows the convergence of the numerical results for $\tilde{\mathcal{F}}_{\sqrt{d}\,\hat{k}}\left[\tilde{f}_{\tilde{q}}^c\,(d)\,;d\right]/\sqrt{d}$ at the glass transition singularity to this master function. With Eqs. (2.53) and (3.103) the nonergodicity parameter itself can now be written as

$$\tilde{f}_{\tilde{k}}^c\,(d) \cong \frac{\sqrt{d}\hat{F}_0\left(\tilde{k}/\sqrt{d}\right)}{1+\sqrt{d}\hat{F}_0\left(\tilde{k}/\sqrt{d}\right)}, \tag{3.105}$$

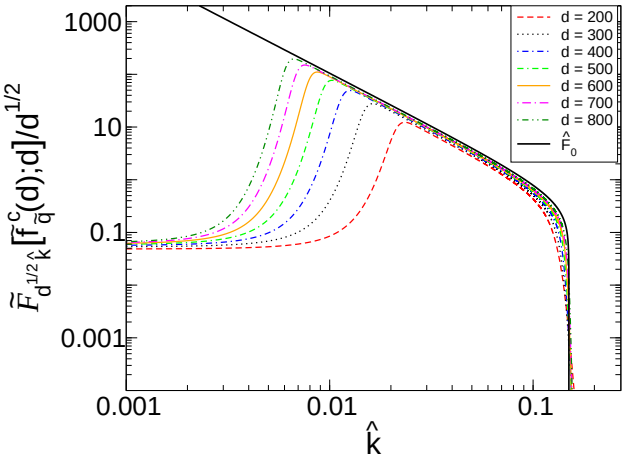

Figure 3.16: Numerical result for $\tilde{\mathcal{F}}_{\sqrt{d}\,\hat{k}}\left[\tilde{f}_k^c\,(d)\,;d\right]/\sqrt{d}$ as function of $\hat{k}$ for various dimensions d. The master function $\hat{F}_0(\hat{k})$ is shown as bold black line.

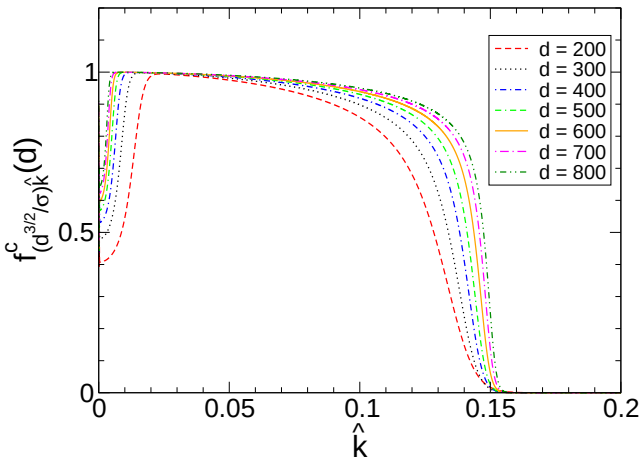

Figure 3.17: Numerical result for the critical nonergodicity parameters $f_k^c(d)$ on the scale $\hat{k} = k\sigma/d^{3/2}$ for various dimensions d.

i.e. on the scale $\hat{k} = k\sigma/d^{3/2}$ it is

$$\lim_{d\to\infty} f^c_{(d^{3/2}/\sigma)\hat{k}}(d) \equiv \hat{f}^c_{\hat{k}} = \Theta\left(\hat{k}_0 - \hat{k}\right). \tag{3.106}$$

The convergence of the numerical result for the critical nonergodicity parameters to this step function is shown in Fig. 3.17.

3.5.4 lim $k \to 0$

Now we want to investigate the limit $k \to 0$ of the nonergodicity parameter, in order to find out, if the dip for low values of k vanishes in the limit $d \to \infty$. Eqs. (3.36) and (3.37) cannot be evaluated directly, because both, the integrational volume in Eq. (3.36) and the denominator in Eq. (3.37) go to zero in this limit. One can now either do a Taylor expansion of these equations or start directly from Eqs. (2.48) and (2.49) again, i.e.

$$\mathcal{F}_k[f_q] = \int \frac{\mathrm{d}^d p}{(2\pi)^d} \frac{n}{2} \frac{S_k S_p S_{|\vec{k}-\vec{p}|}}{k^4} \left[\vec{k}\cdot\left(\vec{p}c(p) + \left(\vec{k}-\vec{p}\right)c\left(\left|\vec{k}-\vec{p}\right|\right)\right)\right]^2 f_p f_{|\vec{k}-\vec{p}|}. \tag{3.107}$$

In order to investigate the limit $k \to 0$ of this equation, we define the vector $\vec{k}$ to be

$$\vec{k} := \varepsilon \cdot \vec{k}_1 \tag{3.108}$$

and investigate the limit $\varepsilon \to 0$. It is then

$$c\left(\left|\vec{k}-\vec{p}\right|\right) = c(p) + \frac{\partial}{\partial\widetilde{\varepsilon}} c\left(\left|\widetilde{\varepsilon}\cdot\vec{k}_1 - \vec{p}\right|\right)\Big|_{\widetilde{\varepsilon}=0} \varepsilon + O\left(\varepsilon^2\right) \tag{3.109}$$

with

$$\begin{aligned}\frac{\partial}{\partial\varepsilon} c\left(\left|\varepsilon\cdot\vec{k}_1 - \vec{p}\right|\right)\Big|_{\varepsilon=0} &= c'(p)\,\frac{\partial}{\partial\varepsilon}\sqrt{\left(\varepsilon\cdot\vec{k}_1 - \vec{p}\right)^2}\Big|_{\varepsilon=0} \\ &= -c'(p)\,\frac{1}{p}\left(\vec{k}_1\cdot\vec{p}\right)\end{aligned} \tag{3.110}$$

i.e.

$$c\left(\left|\vec{k}-\vec{p}\right|\right) = c(p) - c'(p)\,\frac{1}{p}\left(\vec{k}\cdot\vec{p}\right) + O\left(k^2\right). \tag{3.111}$$

With this we obtain

$$\begin{aligned}
&\vec{k}\cdot\left(\vec{p}c\left(p\right)+\left(\vec{k}-\vec{p}\right)c\left(\left|\vec{k}-\vec{p}\right|\right)\right)=\\
=\;&\vec{k}\cdot\vec{p}c\left(p\right)+\vec{k}\cdot\left(\vec{k}-\vec{p}\right)\left(c\left(p\right)-c'\left(p\right)\frac{1}{p}\left(\vec{k}\cdot\vec{p}\right)+O\left(k^2\right)\right)\\
=\;&k^2c\left(p\right)+c'\left(p\right)\frac{1}{p}\left(\vec{k}\cdot\vec{p}\right)^2+O\left(k^3\right).
\end{aligned}\tag{3.112}$$

If we now insert this into Eq. (3.107) we get

$$\begin{aligned}
&\lim_{k\to 0}\mathcal{F}_k\left[f_q\right]=\\
=\;&\lim_{k\to 0}\int\frac{\mathrm{d}^dp}{\left(2\pi\right)^d}\frac{n}{2}\frac{S_0\left(S_p\right)^2}{k^4}\left[k^2c\left(p\right)+c'\left(p\right)\frac{1}{p}\left(\vec{k}\cdot\vec{p}\right)^2\right]^2\left(f_p\right)^2+O\left(k\right)\\
=\;&\lim_{k\to 0}\frac{n}{2}\frac{1}{\left(2\pi\right)^d}S_0\int_0^\infty\mathrm{d}p\;p^{d-1}S_p^2\left(f_p\right)^2\int\mathrm{d}\Omega_d^p\left[c\left(p\right)+pc'\left(p\right)\left(\frac{\vec{k}}{k}\cdot\frac{\vec{p}}{p}\right)^2\right]^2+O\left(k\right).
\end{aligned}\tag{3.113}$$

With

$$\int\mathrm{d}\Omega_d^p=\Omega_d\tag{3.114}$$

and

$$\int\mathrm{d}\Omega_d^p\left(\frac{\vec{k}}{k}\cdot\frac{\vec{p}}{p}\right)^2=\frac{1}{d}\int\mathrm{d}\Omega_d^p\sum_{i=1}^d\left(\vec{e}_i\cdot\frac{\vec{p}}{p}\right)^2=\frac{1}{d}\Omega_d\tag{3.115}$$

and also (cf. Eq. (3.20))

$$\int\mathrm{d}\Omega_d^p\left(\frac{\vec{k}}{k}\cdot\frac{\vec{p}}{p}\right)^4=\frac{3}{d\left(d+2\right)}\Omega_d\tag{3.116}$$

this yields[3]

$$\begin{aligned}
\lim_{k\to 0}\mathcal{F}_k\left[f_q\right]\;=\;&\frac{n}{2}\frac{\Omega_d}{\left(2\pi\right)^d}S_0\int_0^\infty\mathrm{d}p\;p^{d-1}S_p^2\left[c\left(p\right)^2+\frac{2p}{d}c'\left(p\right)c\left(p\right)+\frac{3p^2}{d\left(d+2\right)}c'\left(p\right)^2\right]\left(f_p\right)^2\\
&+O\left(k\right).
\end{aligned}\tag{3.117}$$

The $k\to 0$ value of the static structure factor follows from Eq. (3.65) as

$$S_0=\frac{1}{1+2^d\varphi}.\tag{3.118}$$

[3]Note that this result deviates from the one given in Ref. [17], which is probably due to a typographic error.

After inserting Ω_d from Eq. (3.10) and $c(k)$ from Eq. (3.57), i.e. also

$$c'(k) = (2\pi)^{\frac{d}{2}} \sigma^{d+1} \frac{1}{(\sigma k)^{\frac{d}{2}}} J_{\frac{d}{2}+1}(k\sigma) \tag{3.119}$$

and after rescaling with $k = \tilde{k}d/\sigma$ we obtain

$$\lim_{\tilde{k}\to 0} \tilde{\mathcal{F}}_{\tilde{k}} \left[\tilde{f}_{\tilde{q}}\right] = \frac{d}{2} \int_0^\infty \mathrm{d}\tilde{p}\ \tilde{p}^{d-1} \left[\tilde{c}(\tilde{p})^2 + \frac{2\tilde{p}}{d}\tilde{c}'(\tilde{p})\,\tilde{c}(\tilde{p}) + \frac{3\tilde{p}^2}{d^2}\tilde{c}'(\tilde{p})^2\right] \left(\tilde{f}_{\tilde{p}}\right)^2 \tag{3.120}$$

where we have used the approximation $S_{\tilde{p}} \cong 1$ and we have defined

$$\tilde{c}\left(\tilde{k}\right) = c\left(\tilde{k}d/\sigma\right) d^{d/2} \sigma^{-d} (2\pi)^{-\frac{d}{2}}, \tag{3.121}$$

i.e.

$$\begin{aligned} \tilde{c}\left(\tilde{k}\right) &= -\frac{1}{\tilde{k}^{\frac{d}{2}}} J_{\frac{d}{2}}\left(\tilde{k}d\right) \\ \tilde{c}'\left(\tilde{k}\right) &= \frac{d}{\tilde{k}^{\frac{d}{2}}} J_{\frac{d}{2}+1}\left(\tilde{k}d\right). \end{aligned} \tag{3.122}$$

We can now apply an integration by parts

$$\begin{aligned} \int_0^\infty \mathrm{d}p\ p^d \tilde{c}'(p)\,\tilde{c}(p) &= \underbrace{\left[p^d \tilde{c}(p)\,\tilde{c}(p)\right]_0^\infty}_{0} - \int_0^\infty \mathrm{d}p\ \tilde{c}(p)\left(p^{d-1} d\ \tilde{c}(p) + p^d\ \tilde{c}'(p)\right) \\ &= -\int_0^\infty \mathrm{d}p\ p^d \tilde{c}'(p)\,\tilde{c}(p) - \int_0^\infty \mathrm{d}p\ \tilde{c}(p)\, p^{d-1} d\ \tilde{c}(p) \end{aligned} \tag{3.123}$$

which means

$$\int_0^\infty dp\ p^d \tilde{c}'(p)\,\tilde{c}(p) = -\frac{d}{2} \int_0^\infty \mathrm{d}p\ p^{d-1} \tilde{c}(p)^2 \tag{3.124}$$

i.e. the first two terms in the square brackets in Eq. (3.120) vanish. This leads to

$$\lim_{\tilde{k}\to 0} \tilde{\mathcal{F}}_{\tilde{k}} \left[\tilde{f}_{\tilde{q}}\right] = \frac{d}{2} \int_0^\infty \mathrm{d}\tilde{p}\ \tilde{p}^{d-1} \left[\frac{3\tilde{p}^2}{d^2}\tilde{c}'(\tilde{p})^2\right] \left(\tilde{f}_{\tilde{p}}\right)^2. \tag{3.125}$$

With Eq. (3.122) and an approximation similar to the one following after Eq. (3.94) we obtain

$$\lim_{\tilde{k}\to 0} \tilde{\mathcal{F}}_{\tilde{k}} \left[\tilde{f}_{\tilde{q}}\right] \cong \frac{3}{2} \int_{\frac{1}{2}}^\infty \mathrm{d}\tilde{p}\ \tilde{p} \left[\frac{2}{\pi\sqrt{4\tilde{p}^2 - 1}}\right] \left(\tilde{f}_{\tilde{p}}\right)^2. \tag{3.126}$$

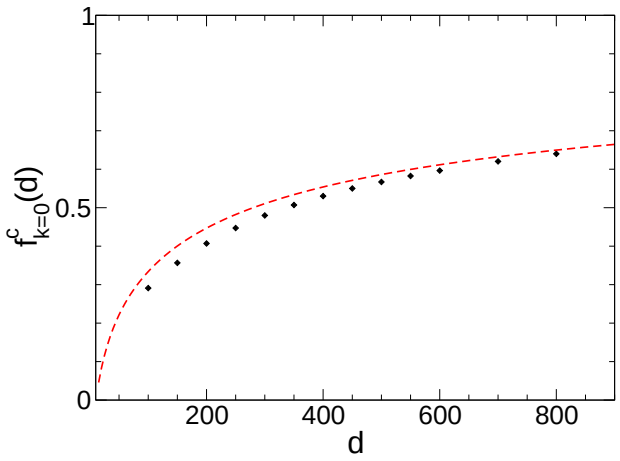

Figure 3.18: The numerical value of $\lim_{k\to 0} f_k^c(d)$ (diamonds) compared with the analytical result in Eq. 3.128 (dashed red line)

Using the results of the previous section we can now apply the approximation for the critical nonergodicity parameter, $\tilde{f}_{\tilde{q}}^c \cong 0$ for $\tilde{q} > \tilde{k}_0$ and $\tilde{f}_{\tilde{q}}^c \cong 1$ for $\tilde{q} < \tilde{k}_0$, which implies

$$\begin{aligned} \lim_{\tilde{k}\to 0} \tilde{\mathcal{F}}_{\tilde{k}} \left[\tilde{f}_{\tilde{q}}^c\right] &\cong \frac{3}{2\pi} \int_{\frac{1}{2}}^{\tilde{k}_0} \mathrm{d}\tilde{p} \\ &\cong \frac{3}{2\pi}\left(\tilde{k}_0 - \frac{1}{2}\right), \end{aligned} \tag{3.127}$$

where we have used that $2\tilde{p}/\left(\sqrt{4\tilde{p}^2-1}\right) \cong 1$ for large values of $\tilde{p}$. Inserting this into Eq. (2.53) we obtain

$$\lim_{\tilde{k}\to 0} \tilde{f}_{\tilde{k}}^c = \frac{\frac{3}{2\pi}\left(\tilde{k}_0 - \frac{1}{2}\right)}{1 + \frac{3}{2\pi}\left(\tilde{k}_0 - \frac{1}{2}\right)} \tag{3.128}$$

i.e.

$$\lim_{d\to\infty} \lim_{\tilde{k}\to 0} \tilde{f}_{\tilde{k}}^c = 1, \tag{3.129}$$

because $\tilde{k}_0 = \hat{k}_0\sqrt{d}$. This means that the dip for low values of k vanishes in the limit $d \to \infty$. The agreement between the numerically evaluated values for $\lim_{k\to 0} f_k^c(d)$ and the analytical formula (Eq. (3.128)) can be seen in Fig. 3.18.

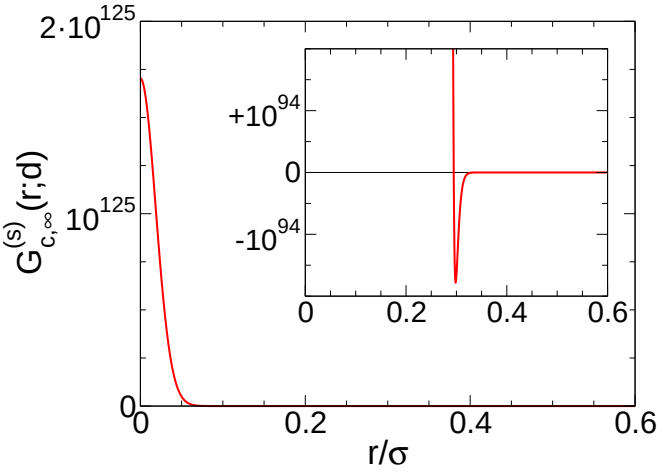

Figure 3.19: The self part of the van Hove function $G^c_{s,\infty}(r;d)$ evaluated from the numerical MCT solution for $d = 100$. The inset visualizes the existence of a negative dip. The amplitude of this dip is smaller than the maximum value of $G^c_{s,\infty}(r;d)$ by about 30 orders of magnitude.

3.5.5 Self-part of the van Hove function

Of special interest is also the self-part of the van Hove function (cf. Eq. (2.15))

$$G^{(s)}\left(\vec{r},t\right) = \frac{1}{n}\left\langle \rho^{(s)}\left(\vec{r}+\vec{r}_0,t+t_0\right)\rho^{(s)}\left(\vec{r}_0,t_0\right)\right\rangle \tag{3.130}$$

with

$$\rho^{(s)}\left(\vec{r},t\right) = \delta\left(\vec{r}-\vec{r}_i\left(t\right)\right), \tag{3.131}$$

where we have chosen an arbitrary particle i. It can be written as the Fourier transform of the self-nonergodicity parameter. At the glass transition it is

$$G^{(s)}_{c,\infty}(r;d) = (2\pi)^{-d/2}\, r^{-(d/2-1)} \int_0^\infty \mathrm{d}k\, J_{d/2-1}(kr) k^{d/2} f^{c,(s)}_k(d) \tag{3.132}$$

where Eq. (3.31) has been used. The numerical result for $G^{(s)}_{c,\infty}(r;d)$ for $d = 100$ is shown in Fig. 3.19. It can be seen that $G^{(s)}_{c,\infty}(r;100)$ has tiny negative dips, which cannot be true in reality as $G^{(s)}_{c,\infty}(r;d)$ should always be positive (cf. Eq. (3.130)). These dips are already present for $d = 3$. It has been argued by Ikeda and Miyazaki [46] that the relevant quantity may not be $G^{(s)}_{c,\infty}(r;d)$, but $r^{d-1}G^{(s)}_{c,\infty}(r;d)$, which would lead to a great increase of the magnitude of the dip. From this they conclude that MCT may

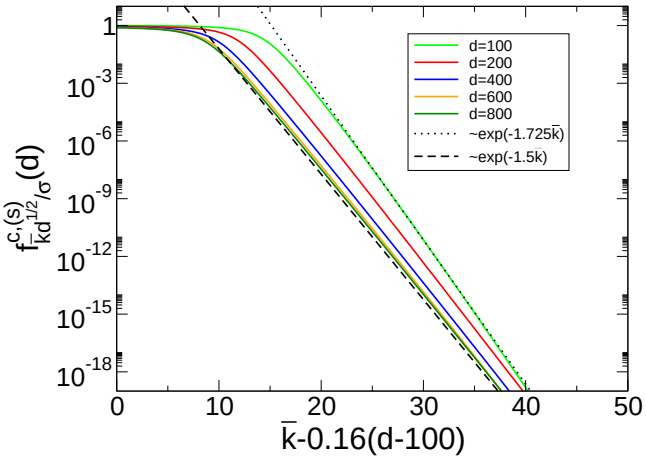

Figure 3.20: Illustration of the exponential decay of $f_k^{c,(s)}(d)$ for $k > k_0 = \hat{k}_0 d^{3/2}/\sigma$. The decay rate a converges for $d \to \infty$ to an asymptotic value $a_\infty \cong 1.5\sigma$. For $d = 100$ this asymptotic regime is not reached yet. It is $a \cong 1.725\sigma$ for $d = 100$.

become incorrect for high dimensions. Due to numerical problems we cannot evaluate $r^{d-1}G_{c,\infty}^{(s)}(r;d)$ directly. For large values of r the numerical errors become very large. Therefore, we want to give an analytical approximation for $G_{c,\infty}^{(s)}(r;d)$ in the following.

$f_k^{c,(s)}(d)$ seems to decay exponentially with k for $k > k_0$ (see Fig. 3.20), so that $k^{d/2} f_k^{c,(s)}(d)$, which appears as factor in the integrand in Eq. (3.132), can be approximated as

$$k^{d/2} f_k^{c,(s)}(d) \to \bar{g}_c^{(s)}(k;d) = k^{d/2} \exp[-a_d(k-k_0)/\sqrt{d}] \tag{3.133}$$

($a_\infty \cong 1.50\sigma$, $k_0 \cong 0.155\sigma^{-1}d^{3/2}$) for $d \to \infty$. The accuracy of this approximation can be seen in Fig. 3.21. Replacing $k^{d/2} f_k^{c,(s)}(d)$ in Eq. (3.132) by $\bar{g}_c^{(s)}(k;d)$ leads to $G_{c,\infty}^{(s)}(r;d) \to \bar{G}_{c,\infty}^{(s)}(r;d) = B_d/[1+(r/a_d)^2 d]^{(d+1)/2}$ ($0 < B_d \sim d^d$). This means that $G_{c,\infty}^{(s)}(r;d)$ becomes non-negative and a Gaussian on a scale $rd/\sigma = O(1)$ for $d \to \infty$ (see Fig. 3.22). By comparing Figs. 3.19 and 3.22 one realizes, that the $r \to 0$ value of $G_{c,\infty}^{(s)}(r;100)$ seems to deviate by one order of magnitude. In Fig. 3.23 it becomes clear, that this deviation only occurs for small values of r. It is probably due to the fact that d is not high enough yet. With this we have shown, that small deformations of $k^{d/2} f_k^{c,(s)}(d)$ can eliminate the negative dips for a non-Gaussian $f_k^{c,(s)}(d)$.

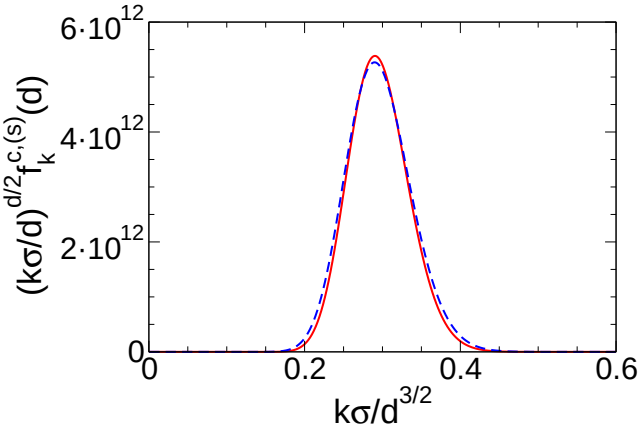

Figure 3.21: k dependence of $(k\sigma/d)^{d/2} f_k^{c,(s)}(d)$ (solid red line) from the numerical MCT solution and $(\sigma/d)^{d/2} \bar{g}_c^{(s)}(k;d)$ (dashed blue line) for $d = 100$.

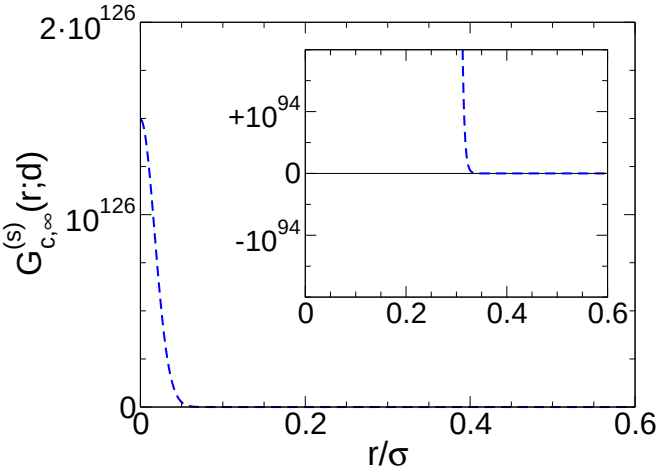

Figure 3.22: The self part of the van Hove function $G^c_{s,\infty}(r;d)$ evaluated for $d = 100$ with the approximation $k^{d/2} f_k^{c,(s)}(d) \to \bar{g}_c^{(s)}(k;d)$ (cf. Eq. (3.133)).

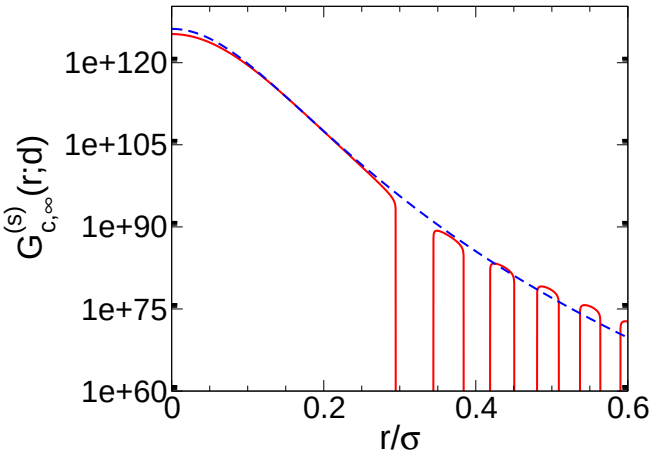

Figure 3.23: The self part of the van Hove function $G^c_{s,\infty}(r;d)$ evaluated for $d = 100$ from the numerical MCT solution (solid red line) and with the approximation $k^{d/2} f_k^{c,(s)}(d) \to \bar{g}_c^{(s)}(k;d)$ (dashed blue line) (cf. Eq. (3.133)) on a logarithmic scale.

3.5.6 Comparison with the theory of Kirkpatrick and Wolynes

There has been a previous work of Kirkpatrick and Wolynes [3], which claims that the critical MCT packing fraction is proportional to $d2^{-d}$, which deviates from our result (Eq. (3.99)). The main difference compared to our treatment of the problem is that they used a Gaussian function as an ansatz for the critical nonergodicity parameter and they only required Eq. (2.53) to be valid in the limit $k \to 0$. In this section we want to show, that we would obtain the same result for the critical packing fraction from our equations with this ansatz.

We start with Eq. (3.95) and apply the Vineyard approximation [47], i.e.

$$\phi^s_{\vec{q}}(t) \approx \phi_{\vec{q}}(t) \tag{3.134}$$

which leads to

$$\tilde{\mathcal{F}}_{\tilde{k}}\left[\tilde{f}^s_{\tilde{q}}\right] \cong \varphi \frac{2^d}{\tilde{k}^2 \pi d} \int_{\frac{1}{2}}^{\infty} \mathrm{d}\tilde{p} \frac{\tilde{p}}{\sqrt{4\tilde{p}^2 - 1}} \tilde{f}^s_{\tilde{p}} \left(\tilde{f}^s_{\tilde{q}_-} + \tilde{f}^s_{\tilde{q}_+}\right). \tag{3.135}$$

If we use a Gaussian function as an ansatz for $\tilde{f}^s_{\tilde{k}}$, i.e.

$$\tilde{f}^s_{\tilde{k}} = e^{-\tilde{k}^2/\alpha} \tag{3.136}$$

and consider the $k \to 0$ limit of Eq. (2.53) we obtain

$$\lim_{\tilde{k}\to 0} \tilde{k}^2 \frac{\tilde{f}^s_{\tilde{k}}}{1-\tilde{f}^s_{\tilde{k}}} = \lim_{\tilde{k}\to 0} \tilde{k}^2 \tilde{\mathcal{F}}_{\tilde{k}} \left[\tilde{f}^s_{\tilde{q}}\right]. \tag{3.137}$$

Inserting Eq. (3.136) into the left-hand side of Eq. (3.137) results in

$$\lim_{\tilde{k}\to 0} \tilde{k}^2 \frac{\tilde{f}^s_{\tilde{k}}}{1-\tilde{f}^s_{\tilde{k}}} = \alpha \tag{3.138}$$

i.e. Eq. (3.137) can be written as

$$\alpha = 2\varphi \frac{2^d}{\pi d} \int_{\frac{1}{2}}^{\infty} \mathrm{d}\tilde{p} \frac{\tilde{p}}{\sqrt{4\tilde{p}^2-1}} \left(\tilde{f}^s_{\tilde{p}}\right)^2. \tag{3.139}$$

With the ansatz given in Eq. (3.136) and

$$\int_{\frac{1}{2}}^{\infty} \mathrm{d}\tilde{p}\ \tilde{p} e^{-2\tilde{p}^2/a} \frac{1}{\sqrt{4\tilde{p}^2-1}} = \frac{1}{2}\sqrt{\frac{a\pi}{2}} e^{-\frac{1}{2a}} \tag{3.140}$$

we obtain

$$\alpha = \varphi \frac{2^d}{\pi d} \sqrt{\frac{\alpha\pi}{2}} e^{-\frac{1}{2\alpha}}. \tag{3.141}$$

This can also be written as

$$\alpha = \frac{1}{8}\varphi^2 \frac{2^{2d}}{\pi d^2} e^{-\frac{1}{\alpha}}. \tag{3.142}$$

The smallest packing fraction, for which this equation has a solution can be found by inserting the value of α, at which $\alpha e^{1/\alpha}$ has its minimum. This is at

$$\alpha_{KW} = 1. \tag{3.143}$$

From this one finds

$$\varphi^c_{KW} = \sqrt{8\pi e} d 2^{-d}, \tag{3.144}$$

which is (besides a factor of 2, which is probably an error in Ref. [3]) exactly the result of Kirkpatrick and Wolynes. From this we see, why the result of Kirkpatrick and Wolynes has a d dependence different from our result. They only use the $k \to 0$ limit of the MCT equations, which is, as we found out in the previous sections, not the important region for the glass transition. Additionally, the assumption of a Gaussian nonergodicity parameter is not justified.

3.5.7 Three-particle direct correlation function for $d \to \infty$

In this section we want to prove the following statement: for all packing fractions $\varphi\,(d)$ such that $2^d\varphi\,(d)$ does not increase exponentially or faster with d for $d \to \infty$, the static three-point correlation function $S^{(3)}(\vec{k},\vec{k}')$ reduces in the limit of high dimensions to $S\,(k)\,S\,(k')\,S(|\vec{k}+\vec{k}'|)$, i.e. the convolution approximation becomes exact. For this proof we use the Ornstein-Zernike equation for three-particle correlation functions [31]:

$$S^{(3)}\left(\vec{k},\vec{k}'\right) = S\,(k)\,S\,(k')\,S(|\vec{k}+\vec{k}'|)\left(1+n^2c^{(3)}(\vec{k},\vec{k}')\right). \tag{3.145}$$

So, we have to show that $n^2c^{(3)}(\vec{k},\vec{k}') \to 0$ for all $\vec{k},\ \vec{k}'$ for $d \to \infty$ and φ constrained as above. The explicit dependence of $c^{(3)}(\vec{k},\vec{k}')$ on $\vec{k},\vec{k}'$ does not have to be considered, as we can use for all $\vec{k},\ \vec{k}'$:

$$\begin{aligned} & n^2\left|c^{(3)}\left(\vec{k},\vec{k}'\right)\right| = \\ = \ & n^2\left|\int \mathrm{d}^d r \int \mathrm{d}^d r'\ e^{-i\vec{k}\vec{r}}e^{-i\vec{k}'\vec{r}'}c^{(3)}\left(\vec{r},\vec{r}'\right)\right| \\ \leq \ & n^2\int \mathrm{d}^d r \int \mathrm{d}^d r'\ \left|c^{(3)}\left(\vec{r},\vec{r}'\right)\right|. \end{aligned} \tag{3.146}$$

Now we can expand $c^{(3)}\left(\vec{r},\vec{r}'\right)$ into diagrams, where the lines are Mayer functions and the vertices are single particle densities. This expansion only consists of loop diagrams. We want to show now, that the contribution of each of these diagrams to $n^2\int d^d r \int d^d r'\ \left|c^{(3)}\left(\vec{r},\vec{r}'\right)\right|$ vanishes in the limit $d \to \infty$. To do so, we apply the theorem of Wyler, Rivier and Frisch [20]. This theorem states, that a loop diagram leads to an exponentially smaller contribution to an integral like the one appearing in the last line of Eq. (3.146), than a tree diagram of the same order. The simplest diagram in the expansion of $c^{(3)}\left(\vec{r},\vec{r}'\right)$ reads

$$\left|c_0^{(3)}\left(\vec{r},\vec{r}'\right)\right| = \theta\left(\sigma-r\right)\theta\left(\sigma-r'\right)\theta\left(\sigma-|\vec{r}-\vec{r}'|\right), \tag{3.147}$$

which can be inserted into Eq. (3.146)

$$\begin{aligned} & \left|c_0^{(3)}\left(\vec{k},\vec{k}'\right)\right| \leq \\ \leq \ & \int \mathrm{d}^d r \int \mathrm{d}^d r'\ \theta\left(\sigma-r\right)\theta\left(\sigma-r'\right)\theta\left(\sigma-|\vec{r}-\vec{r}'|\right). \end{aligned} \tag{3.148}$$

The integral occurring in Eq. (3.148) leads to an exponentially smaller contribution than the corresponding tree diagram of the same order [20]:

$$\begin{aligned} & \int \mathrm{d}^d r \int \mathrm{d}^d r' \; \theta\left(\sigma - r\right) \theta\left(\sigma - r'\right) \theta\left(\sigma - |\vec{r} - \vec{r}'|\right) \leq \\ \leq \; & \alpha^d \int \mathrm{d}^d r \int \mathrm{d}^d r' \; \theta\left(\sigma - r\right) \theta\left(\sigma - r'\right) \\ = \; & \alpha^d \left(V_d\left(\sigma\right)\right)^2 \end{aligned} \tag{3.149}$$

where $V_d\left(\sigma\right)$ is the volume of a d-dimensional sphere with radius σ and

$$\alpha < 1. \tag{3.150}$$

From Eqs. (3.148) and (3.149) we obtain:

$$n^2 \left| c_0^{(3)}\left(\vec{k}, \vec{k}'\right)\right| \leq \alpha^d \left(n V_d\left(\sigma\right)\right)^2. \tag{3.151}$$

Together with

$$\varphi = n V_d\left(\frac{\sigma}{2}\right) = 2^{-d} n V_d\left(\sigma\right) \tag{3.152}$$

this leads to

$$n^2 \left| c_0^{(3)}\left(\vec{k}, \vec{k}'\right)\right| \leq \alpha^d \left(2^d \varphi\right)^2, \tag{3.153}$$

i.e. for all packing fractions, where $2^d\varphi$ does not increasing exponentially or faster with d, we obtain from Eqs. (3.150), (3.153):

$$n^2 \left| c_0^{(3)}\left(\vec{k}, \vec{k}'\right)\right| \underset{d\to\infty}{\longrightarrow} 0 \quad \text{for all } \vec{k}, \vec{k}'. \tag{3.154}$$

The contribution of all other diagrams are also exponentially smaller than the corresponding tree diagrams [20], which leads to:

$$n^2 \left| c_i^{(3)}\left(\vec{k}, \vec{k}'\right)\right| \leq \alpha_i^d n^2 \left(V_d\left(\sigma\right)\right)^2 n^j \left(V_d\left(\sigma\right)\right)^j \tag{3.155}$$

where j is the number of vertices over which it has to be integrated in the corresponding diagram and α_i is always smaller than one. From this we obtain

$$n^2 \left| c_i^{(3)}\left(\vec{k}, \vec{k}'\right)\right| \leq \alpha_i^d \left(2^d \varphi\right)^{j+2} \tag{3.156}$$

or

$$n^2 \left| c_i^{(3)}\left(\vec{k}, \vec{k}'\right)\right| \underset{d\to\infty}{\longrightarrow} 0 \quad \text{for all } \vec{k}, \vec{k}' \text{ and all } i \tag{3.157}$$

provided $2^d\varphi(d)$ does not increase exponentially or faster with d. From Eq. (3.82) we see that this is the case for the critical MCT packing fraction.

3.6 Summary and conclusions

We found analytically and numerically that the critical collective and self nonergodicity parameters show a non-Gaussian k dependence up to $d = 800$, in contrast to the assumption of Kirkpatrick and Wolynes [3]. Instead we found that there are three different k scales ($k\sigma = O(d^{1/2})$, $O(d)$, $O(d^{3/2})$) on which the critical collective and self nonergodicity parameters behave differently. We have seen numerically that the self and collective nonergodicity parameters are different on the scale $k \sim d^{1/2}$, but become the same on a scale $k \sim d$. We could show analytically why this is the case and that they will eventually even become the same on the scale $k \sim d^{1/2}$, as the dip for low wavevectors disappears in the limit $d \to \infty$. Additionally, we proved that the nonergodicity parameters converge to a non-Gaussian master function on a scale $k \sim d^{3/2}$.

This non-Gaussian k dependence is also the reason, why the critical packing fraction scales with $d^2 2^{-d}$ as we have shown analytically, and not with $d2^{-d}$ as found by Kirkpatrick and Wolynes [3]. This means that the critical MCT-packing fraction is larger than the Kauzmann-packing fraction, found by Parisi and Zamponi [2, 22] to scale with $d\ln(d/2)2^{-d}$, which cannot be true. The possible reason is the small-cage expansion, applied by Parisi and Zamponi, where the movement of the particles within the cages is described by harmonic vibrations, corresponding to a Gaussian distribution, similar to the theory of Kirkpatrick and Wolynes [3].

We have seen that the static structure factor $S(k)$ at the glass transition is structureless for high dimensions, i.e. it does not have any sharp peak. This could imply that there is no intermediate-range order at the glass transition. This does not necessarily rule out caging as it could be enough to have a short-range order because the caged particle only has to interact with its nearest neighbours. $c(k)$ is not equal to zero as it would be in the ideal gas. Due to the high coordination numbers in high dimensions [21], this possibly does not lead necessarily to several shells with higher density around the caged particle. This, or maybe some properties of the high-dimensional Fourier transform, may lead to the fact that no sharp peak of the static structure factor is needed for the glass transition.

This is in fact similar to the colloidal gelation found in a system of hard spheres with an additional attractive Yukawa potential [45, 48, 49]. There it has been shown

that in the limit of an infinitely strong attractive part of the potential, the critical MCT packing fraction goes to zero like the squareroot of the inverse strength of this potential. It was also shown that in this limit $S(k) \to 1$ for all k and f_k^c becomes similar to $f_k^{c,(s)}$, same as in our result.

We have seen that there is a change in the mechanism of the glass transition at some dimension, leading to a glass-glass transition. For $d \lesssim 18$ the glass transition is dominated by a peak in the static structure factor. For $d \gtrsim 18$ the glass transition is produced by modes with wavevectors in a range close to where the nonergodicity parameters fall to zero.

We saw that the van Hove function may become a Gaussian in real space in the limit $d \to \infty$, even if the nonergodicity parameters are non-Gaussian in k space. Due to the involved structure of the high-dimensional Fourier transform this could mean, that the Gaussian approximation may be an appropriate assumption in real space, but not in k space.

The numerical results indicate that the critical exponents are not constant in our range of dimensions. It is not clear what happens for $d \to \infty$. Finally we have shown that the convolution approximation becomes exact for the critical MCT packing fraction in the limit of high dimensions.

4 Application of mode-coupling theory to liquids

The mode-coupling theory described in the previous chapters is a theory that was developed originally to give a description of the liquid-glass transition. But even if the strong separation of time scales should not be valid in simple liquids away from the glass transition, we can still compare the results of MCT for such systems with the results obtained by other methods. Previously the dynamics of simple liquids has been described by a two-step continued fraction, similar to Eq. (2.35), where the memory function has been approximated by an empirical ansatz. It turned out that a fit with a function consisting of a sum of two terms decaying exponentially in time with two different decay times, gave quite a good fit to the simulational and experimental data [4, 50–54], much better than a fit with only one exponential. This is in fact only a method of curve fitting and not a microscopic theory. Such a theory are the various versions of mode-coupling theory. In the older versions a three-step continued fraction for the density autocorrelation function has been used [55–57]. It was shown not long ago that the collective excitations of simple liquids away from the glass transition can be described by the two-step version, both, by the schematic model [58] and the full MCT model [24, 25], where the only input is the static structure factor. As we will see in the following there are quite some deviations between the application of the MCT described in section 2.3 onto simple liquids away from the glass transition and a computer simulation by Levesque et al. [4]. Because of this we also want to compare the results of the computer simulation with a modified mode-coupling theory, which shall be described in the second part of this chapter.

4.1 Standard mode-coupling theory

In this section we want to compare the predictions of MCT with a computer simulation of liquid argon, performed by Levesque et al. [4]. The pair potential between the atoms is of a Lennard-Jones type, i.e.

$$u(r) = 4\varepsilon \left(\left(\frac{\sigma}{r}\right)^{12} - \left(\frac{\sigma}{r}\right)^{6} \right). \tag{4.1}$$

The temperature used for the simulation was $T = 0.723\varepsilon/k_B$ and the density was $n = 0.844\sigma^{-3}$. This corresponds to Argon at 86.5 K with a density of $1.418\mathrm{g/cm}^3$. For the comparison with MCT we need the static structure factor as input. We used the static structure factor obtained from a molecular dynamics simulation of Verlet et al. [59] for a system in the same state. In this simulation they used a truncated Lennard-Jones potential, i.e. $u(r) = 0$ for $r > r_c$ with $r_c = 2.5\sigma$. This means that the simulated radial distribution function $g_{sim}(r)$ may also be wrong for $r > r_c$. In order to extend the validity of $g_{sim}(r)$ beyond r_c, they used a combination of the Ornstein-Zernike equation [29]

$$h(r) = c(r) + n \int \mathrm{d}^3 r' h(r') c(|\vec{r} - \vec{r}'|) \tag{4.2}$$

where $h(r) = g(r) - 1$ and as closure the Percus-Yevick equation [29]

$$c(r) = g(r) \left(e^{\beta u(r)} - 1 \right) \tag{4.3}$$

for $r > r_c$ and

$$g(r) = g_{sim}(r) \tag{4.4}$$

for $r < r_c$ [59]. For the numerical evaluation one introduces the quantity $H(r) = h(r) - c(r)$, which allows to rewrite Eq. (4.2) as

$$H(k) = \frac{n\,(c(k))^2}{1 - nc(k)} \tag{4.5}$$

and Eqs. (4.3) and (4.4) as

$$c(r) = \begin{cases} (H(r) + 1) \left(e^{-\beta u(r)} - 1 \right) & \text{for } r > r_c \\ g_{sim}(r) - 1 - H(r) & \text{for } r < r_c \end{cases} \tag{4.6}$$

which may then be solved self-consistently.

This structure factor is compared in Fig. 4.1 to the Percus Yevick structure factor

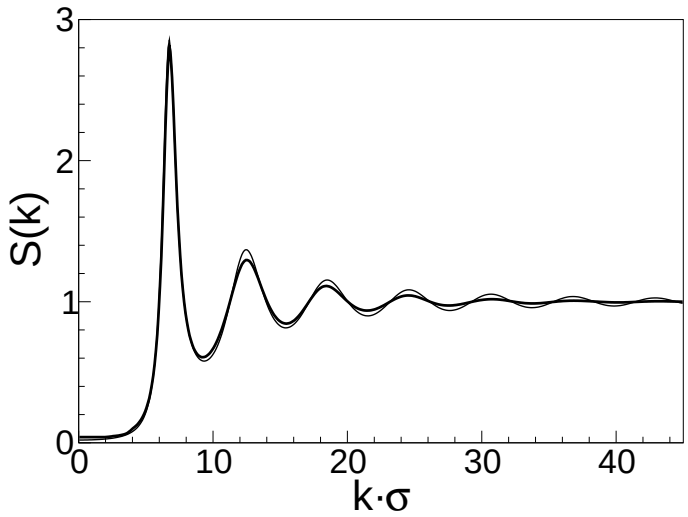

Figure 4.1: Thick line: Static structure factor of a simulation of Lennard-Jones Argon by Levesque et al. [4]. Thin line: Hard sphere PY static structure factor with $\sigma_{\text{eff}} = 1.026\sigma$ and $\varphi = 0.48$.

of hard spheres. As can be seen the simulated structure factor is very similar to the one of hard spheres with a packing fraction of $\varphi = 0.48$ and an effective hard-sphere diameter of $\sigma_{\text{eff}} = 1.026\sigma$.

With this static structure factor as input the MCT equations (cf. Eqs. (2.36), (2.46), (2.48) and (2.49), where we set $\nu_k = 0$, because there is no direct microscopic theory for it) can be solved with the standard methods [60]. As a result the dynamic structure factor $S(k,\omega)$ can be evaluated. As length scale we used the effective hard-sphere diameter σ_{eff} and as frequency scale the isothermal velocity v_T, divided by σ:

$$\omega_0 = \frac{v_T}{\sigma_{\text{eff}}} = \frac{v_{th}}{\sigma_{\text{eff}}\sqrt{S(k=0)}} = \frac{1}{\sigma_{\text{eff}}}\sqrt{\frac{k_B T}{m S(k=0)}} \tag{4.7}$$

with $S\,(k=0) = 1/24.7$ [4]. It should be noted that in these units the isothermal sound velocity is fixed to be equal to unity. In Fig. 4.2 we compare the results of the molecular dynamics simulation for the rescaled dynamic structure factor $\tilde{S}(k,\omega) \equiv S(k,\omega)/S(k)\cdot\omega_0$ (solid black line) with the result of MCT. It can be seen that there is some qualitative agreement between MCT and the computer simulation, but MCT does not agree well with the simulation at low frequencies.

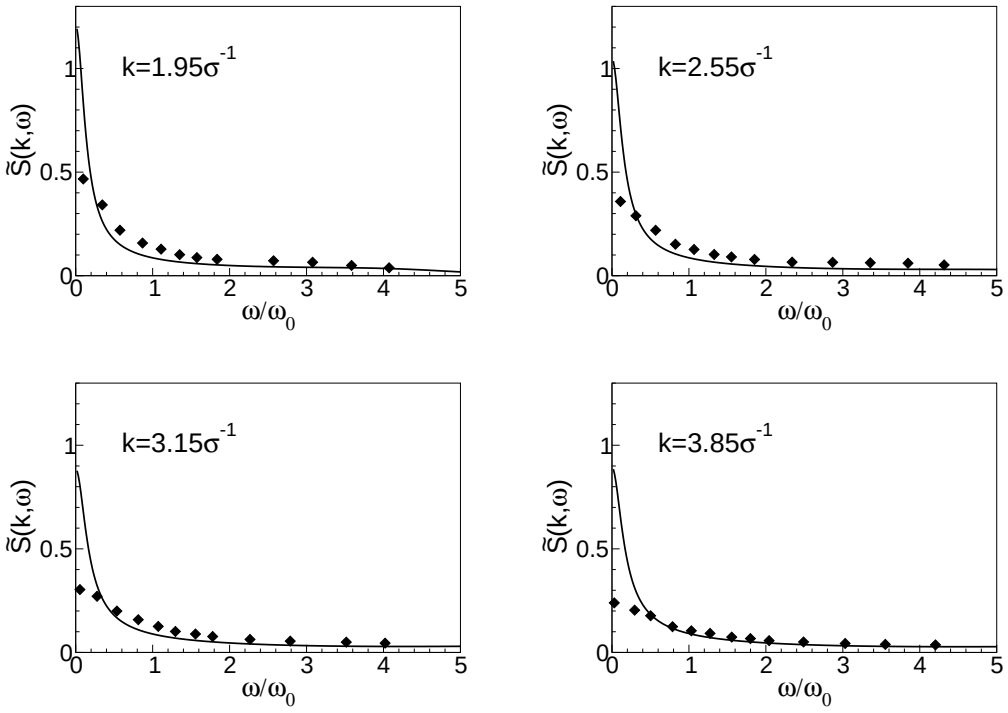

Figure 4.2: MCT result for $\tilde{S}(k,\omega) \equiv S(k,\omega)/S(k) \cdot \omega_0$ (line) compared with the result of a computer simulation by Levesque et al. (diamonds) [4].

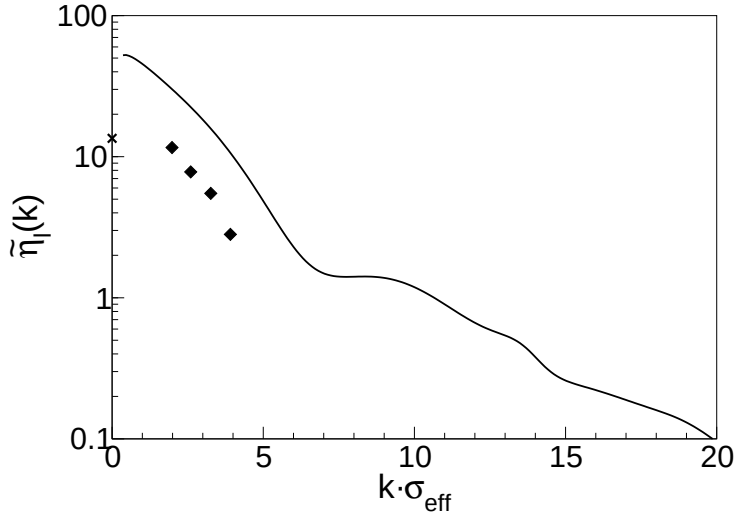

Figure 4.3: MCT result (line) for the viscosity $\tilde{\eta}_\ell(k)$ as defined in equation (4.8) compared with the simulation by Levesque et al. [4] (diamonds). The cross is the value determined by Naugle et al. [61].

The quantity $\tilde{S}(k,\omega=0)$ is proportional[1] to the so-called longitudinal k-dependent viscosity

$$\begin{aligned}\tilde{\eta}_\ell(k) &= \frac{1}{\pi n k_B T}\eta_\ell(k)\cdot\omega_0 = S(k,\omega=0)/S(k)^2\cdot\omega_0 \\ &= \tilde{S}(k,\omega=0)/S(k)\cdot\omega_0. \end{aligned} \tag{4.8}$$

For $k=0$ we have

$$\eta_\ell(k=0) = \eta_v + \frac{4}{3}\eta_s \tag{4.9}$$

where η_s is the usual shear viscosity and η_v is the bulk or volume viscosity. Because of this relation between the zero frequency limit of the dynamic structure factor and the generalized viscosity, there is also quite some deviation in the viscosity between the MCT result and the simulation, as can be seen in Fig. 4.3.

The quantitative deviation is related to the fact that MCT underestimates the critical packing fraction at which the glass transition occurs [1]. So the result of the unmodified MCT describes a state which is much closer to the glass transition. This leads to an overestimation of the viscosity.

In Fig. 4.4 we show the generalized sound dispersion defined by

$$\Omega^2(k) = \operatorname*{Max}_{\omega}\{\omega^2 S(k,\omega)\} \tag{4.10}$$

for MCT and compare it with the result of the computer simulation. We have also included the results of a different computer simulation of Lennard-Jones Argon by Rahman [63, 66] in a similar state ($T = 76$ K, $\rho = 1.408$ g/cm^3) as well as neutron-scattering data [64, 65]. As can be seen there is again at least some qualitative agreement.

Finally in Fig. 4.5 there is a comparison between the memory functions of MCT and the computer simulation by Levesque et al. [4]. The memory function of the computer simulation cannot be obtained directly. It can only be obtained by postulating a two relaxation time structure for the memory function

$$M_k(t) = A_1(k)e^{-t/\tau_1(k)} + A_2(k)e^{-t/\tau_2(k)}. \tag{4.11}$$

and by using the two relaxation times to obtain the best fit for the dynamic structure

[1] This relation is only valid if temperature fluctuations are not taken into account, as it is done here. If temperature fluctuations are existent, $S(k,\omega=0)$ becomes inversely proportional to $k^2\lambda$ at small k where λ is the thermal conductivity, see [62].

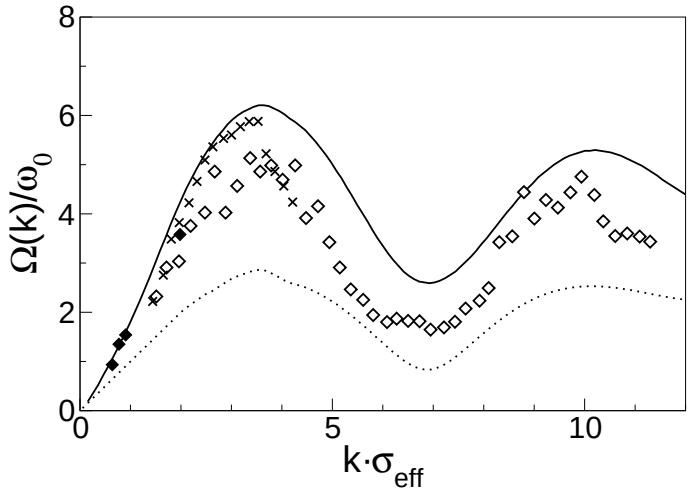

Figure 4.4: Generalised dispersion $\Omega(k)$ calculated from $S(k,\omega)$ via Eq. (4.10) for MCT (solid line), compared with the simulational results of Levesque et al. [4] (full diamonds) and Rahman [63] (empty diamonds). The crosses are neutron scattering results of de Schepper et al. [64, 65]. The dotted line is $\Omega_0(k)$ as given in Eq. (2.37).

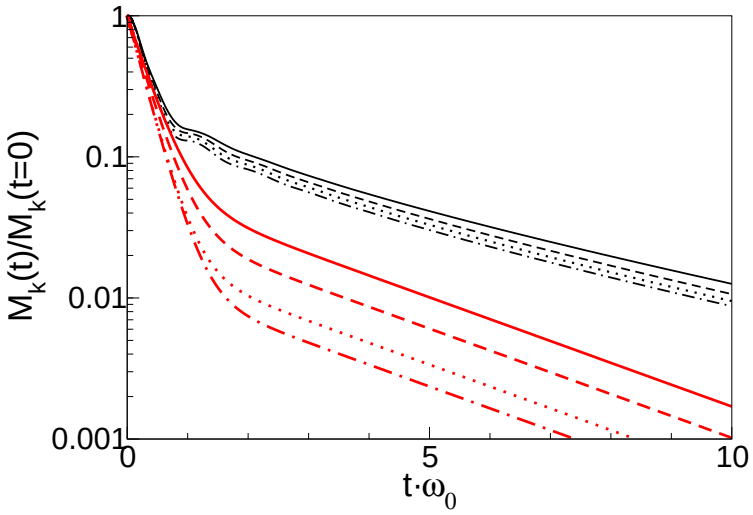

Figure 4.5: MCT result (thin black lines) for the memory function compared with the result of the computer simulation by Levesque et al. [4] (thick red lines) for $k\sigma = 1.95$ (solid lines), $k\sigma = 2.55$ (dashed lines), $k\sigma = 3.15$ (dotted lines), $k\sigma = 3.85$ (dash-dotted lines).

factor. In MCT the memory function is obtained directly by solving the mode-coupling equations. The quantitative deviation between simulation and MCT in the relaxation time can again be explained by the fact that MCT describes a state closer to the glass transition.

4.2 Modified mode-coupling theory

In order to improve the results of MCT we now try to use a modified version of MCT. This modified version of MCT is based on a theory of Sjögren and Götze [5, 67, 68] which is a generalization of MCT by additionally taking binary collisions into account. The original MCT equations (2.48) and (2.47) can be obtained within the theory of Sjögren and Götze by neglecting all terms which contain couplings to current-correlation functions and binary collision terms. If we now keep the binary collision terms instead of neglecting them, we obtain the new memory function [5]

$$M_k(t) = M_k^B(t) + \Omega_0^2(k)\left(\mathcal{F}_k[\phi_q(t)] - \mathcal{F}_k[\phi_q^B(t)]\right) \tag{4.12}$$

with the binary collision term

$$M_k^B(t) = \left(\omega_E^2 + \gamma^l(k) + \frac{k^2 k_B T}{m} nc(k)\right) e^{-t^2/\tau(k)^2} \tag{4.13}$$

and the Einstein frequency

$$\omega_E^2 = \frac{n}{3m}\int d^3r\; g(r)\,\vec{\nabla}^2 u(r) \tag{4.14}$$

and

$$\gamma^l(k) = -\frac{n}{m}\int d^3r\; e^{-i\vec{k}\vec{r}} g(r)\left(\frac{\vec{k}}{k}\cdot\vec{\nabla}\right)^2 u(r)\,. \tag{4.15}$$

The last term on the right hand side of Eq. (4.12) has to be subtracted to avoid taking the binary collisions into account twice, because they are already included in $M_k^B(t)$. To further simplify the theory we do not use the function $\phi_k^B(t)$ suggested by Sjögren et al. [5] as it contains the self part of the intermediate scattering function, which would have to be evaluated selfconsistently. Instead we use

$$\phi_k^B(t) = \exp\left(-\frac{k^2 t^2}{2}\frac{k_B T}{m S(k)}\right) \tag{4.16}$$

which fulfills the requirement of having the same short-time behaviour as $\phi_k(t)$ and decaying to zero for longer times. The product of the derivative of the pair potential

$$\nabla_\alpha \nabla_\beta u(r) = \frac{r_\alpha r_\beta}{r^2} u''(r) + \left(\delta_{\alpha\beta} - \frac{r_\alpha r_\beta}{r^2}\right) \frac{u'(r)}{r} \tag{4.17}$$

with $g(r)$ in Eqs. (4.14) and (4.15) can be simplified, because in Lennard-Jones systems $g(r)$ shows a peak, where $u''(r)$ is big and $u'(r)$ small so that [56, 69, 70]

$$g(r) \nabla_\alpha \nabla_\beta u(r) \cong \frac{r_\alpha r_\beta}{r^2} \frac{3}{4\pi} \frac{m}{nr^2} \omega_E^2 \delta(r - r_0) \tag{4.18}$$

where $r_0 \cong 1.04\sigma$ is the point where $r^2 g(r) u''(r)$ reaches a maximum and

$$\omega_E^2 \cong \frac{4\pi}{3} \frac{n}{m} \int_0^\infty dr\ r^2 g(r) u''(r) \tag{4.19}$$

$$\cong 288 \frac{\varepsilon}{m\sigma^2}. \tag{4.20}$$

Here ϵ and σ are Lennard-Jones units (see previous section). In this approximation Eq. (4.15) can be simplified as

$$\gamma^l(k) \cong -3\omega_0^2 \frac{2kr_0 \cos(kr_0) + (k^2 r_0^2 - 2) \sin(kr_0)}{(kr_0)^3}. \tag{4.21}$$

The decay time $\tau(k)$ entering the collisional term in Eq. (4.13) is assumed to be independent of k, and can be used as a fit parameter. By trying different values for this decay time we obtained a good agreement between our modified MCT calculations and the results of the simulation by using the following expression for the decay time:

$$\tau(k)^{-2} = \frac{u''(r_0)}{m} \cong 0.83\omega_E^2. \tag{4.22}$$

Another variation of MCT in order to improve the agreement between theory and the computer simulation is obtained by using a prefactor $A \neq 1$ in the equation for the memory function

$$M_k(t) = A\Omega_0^2(k) \mathcal{F}_k[\phi_q(t)]. \tag{4.23}$$

This prefactor can again be used as a fit parameter. Such a correction factor has already been applied by Fabbian et al. [71, 72] to account for neglecting the rotational degrees of freedom in a liquid composed of non-rotationally symmetric molecules. As the system we investigate here is a simple liquid, such a prefactor may have a different reason,

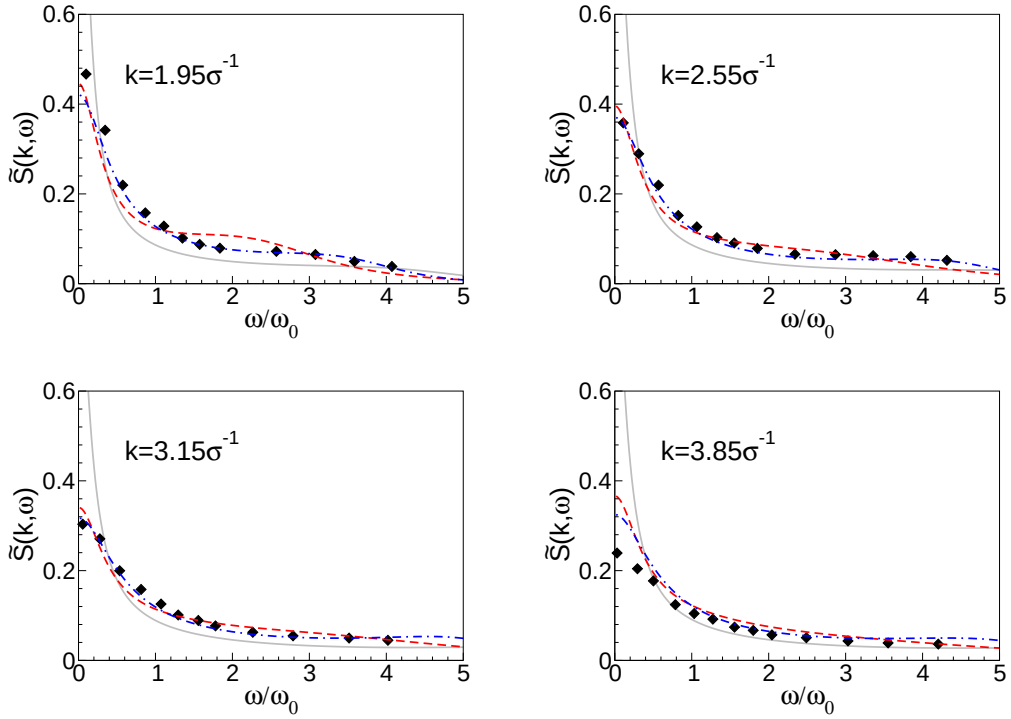

Figure 4.6: MCT result for $\tilde{S}(k,\omega) \equiv S(k,\omega)/S(k)\cdot\omega_0$ (lines) compared with the result of a computer simulation by Levesque et al. (diamonds) [4]. The red dashed line is the result of the modified theory (Eq. (4.12)), the blue dash-dotted line is the standard version of MCT with a prefactor (Eq. (4.23)) with $A = 0.65$ and the solid grey line is the result of the standard version of MCT (Eq. (2.48)).

presumably the approximations applied by MCT. In our calculations we obtained good agreement with the simulations for $A = 0.65$. This prefactor shifts the glass transition of hard spheres to a critical packing fraction of $\varphi_c = 0.566$ instead of $\varphi_c = 0.516$ [1].

It can be seen in Figures 4.6 to 4.8 that the agreement between the simulation and the modified version of MCT becomes much better than the original version of MCT (without a prefactor). This comes again at the prize of having an additional fit parameter. It has to be emphasized that the original version of MCT has no adjustable parameter at all, if one neglects ν_k. The mechanisms how the two variations of MCT, we used here, improve the agreement with the result of the simulation are quite different. The first version, described by Eq. (4.12), reduces the effect of the memory function by subtracting the third term in Eq. (4.12). The second version, described by Eq. (4.23), reduces the effect of the memory function by adding a simple prefactor. The advantage of the first version (Eq. (4.12)) is that it can somehow be justified, while the advantage

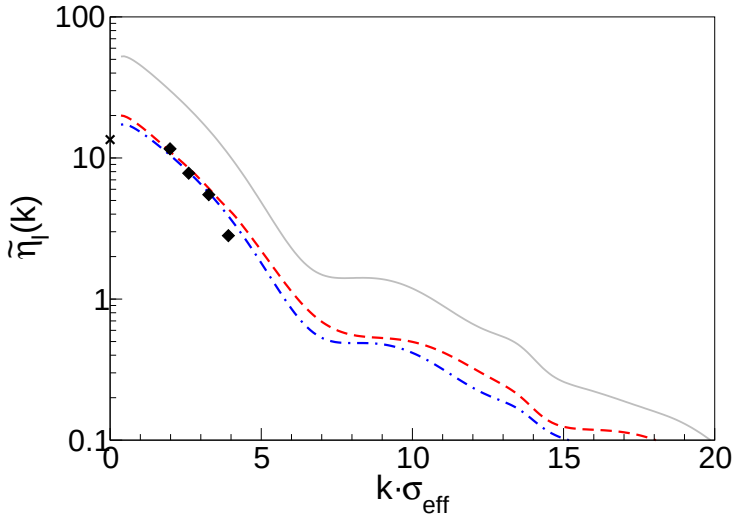

Figure 4.7: MCT result (lines) for the viscosity $\tilde{\eta}_\ell(k)$ as defined in equation (4.8) compared with the simulation by Levesque et al. [4] (diamonds). The cross is the value determined by Naugle et al. [61]. The same color code is used as in Fig. 4.6.

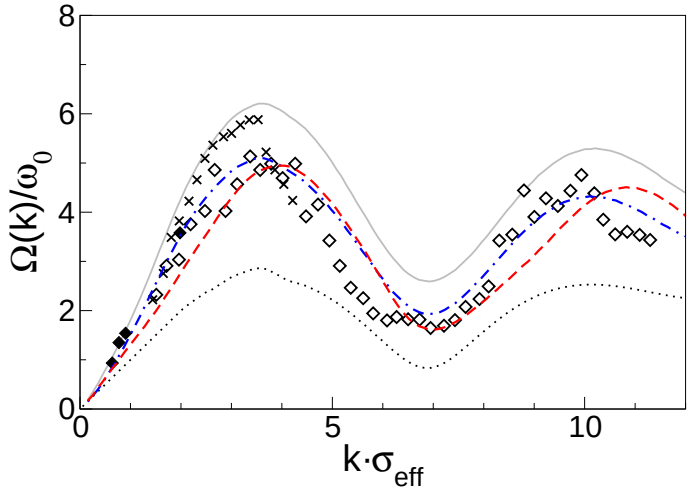

Figure 4.8: Generalised dispersion $\Omega(k)$ calculated from $S(k,\omega)$ via Eq. (4.10) for the three versions of MCT, compared with the simulational results of Levesque et al. [4] (full diamonds) and Rahman [63] (empty diamonds). The crosses are neutron scattering results of de Schepper et al. [64, 65]. The dotted line is $\Omega_0(k)$ as given in Eq. (2.37). The same color code is used as in Fig. 4.6.

of the second version (Eq. (4.23)) is that it is much simpler. It can be seen in Figures 4.6 to 4.8 that both can improve the agreement with the result of the simulation by about the same amount.

4.3 Summary and conclusions

We saw that MCT gives a sufficient description of the collective dynamics of a simple liquid far away from the glass transition in the case of liquid argon, which can be described by a Lennard-Jones potential. Some quantitative deviations cannot be avoided, since MCT does not have any adjustable parameters. This is a problem because one often finds a slightly different point of the glass transition, which also leads to a different dynamics close to it. We found that the agreement between the simulation and MCT can be improved by either taking binary collisions into account or multiplying the memory function with a phenomenological prefactor. This comes at the prize of having an adjustable parameter, i.e. not being a purely microscopic theory any more. Further investigations at different temperatures and densities would be interesting.

5 Mode-coupling theory with stress tensors

In this chapter we want to derive a theory for the correlation functions of stress tensors, similar to the original MCT, which is a theory for the correlation functions of the densities. The motivation for this theory is, that the original MCT only contains the static structure factor or the direct correlation function as input, but not correlation functions of the forces, i.e. correlation functions of the derivatives of the pair potential. This may be important as it was already mentioned in the introduction. There have been already theories for the density correlation function, which contain the derivative of the pair potential as input [55–57, 73]. This is done by applying again the Mori-Zwanzig formalism to the memory function of the original MCT. This leads to a continued fraction which is of one order higher than that of the original mode-coupling equations. The problem is, because of the structure of the equations, that this continued fraction cannot lead to a freezing of the correlation functions of the density modes (i.e. they always decay to zero for $t \to \infty$). Only the equations for the transverse currents then have a similar structure like the equations for the density modes in the original MCT. But it should not be possible in classical physical systems that correlation functions of the current modes freeze in, because then the currents would flow forever. This only happens in superfluid systems, which can only be described by the quantum properties of the system.

So now we want to construct a theory for a quantity, where it is physically reasonable that its autocorrelation function freezes in. This quantity can be the stress tensor. The stress tensor can be derived from momentum conservation similar to the continuity equation for densities (Eq. (2.22)) [74]

$$\partial_j \sigma_{ij}\left(\vec{r}, t\right) + m\frac{\partial}{\partial t} j_i\left(\vec{r}, t\right) = 0, \tag{5.1}$$

where $m\vec{j}\left(\vec{r}, t\right)$ is the momentum density. So the stress tensor may be written micro-

scopically as [74]

$$\sigma_{ij}\left(\vec{k}\right)=\sum_n\left\{mv_i^nv_j^n+\frac{1}{2}\sum_{m\neq n}\frac{\left(r_i^m-r_i^n\right)\left(r_j^m-r_j^n\right)}{|\vec{r}^m-\vec{r}^n|}\left.\frac{\partial u\left(r\right)}{\partial r}\right|_{r=|\vec{r}^n-\vec{r}^m|}\frac{e^{-i\vec{k}(\vec{r}^m-\vec{r}^n)}-1}{i\vec{k}\cdot\left(\vec{r}_m-\vec{r}_n\right)}\right\}e^{-i\vec{k}\vec{r}^n}. \tag{5.2}$$

For this quantity we want to derive mode-coupling equations.

5.1 Coordinate systems and spherical tensors

For simplicity we now transform the Cartesian coordinates into spherical coordinates. Tensors in spherical coordinates always depend on the direction of the z axis. Because we will later need different directions of the z axis, we also need different coordinate systems. In the standard coordinate system we chose $\vec{k}$ as the direction of the z axis. In the additional coordinate systems, denoted by a prime or a double prime, the z axis shall be in the direction of $\vec{q}$ or $\vec{k}-\vec{q}$ respectively, i.e.

$$\begin{aligned}\vec{e}_z &= \frac{\vec{k}}{k}\\ \vec{e}_{z'} &= \frac{\vec{q}}{q}\\ \vec{e}_{z''} &= \frac{\vec{k}-\vec{q}}{|\vec{k}-\vec{q}|}\end{aligned} \tag{5.3}$$

where the different coordinate systems are denoted by a prime of the respective index [75]. The direction of the x axis is chosen to be

$$\vec{e}_x=\vec{e}_{x'}=\vec{e}_{x''}=\frac{\vec{k}\times\vec{q}}{|\vec{k}\times\vec{q}|} \tag{5.4}$$

from which follows:

$$\begin{aligned}\vec{e}_y &= \vec{e}_z\times\vec{e}_x\\ \vec{e}_{y'} &= \vec{e}_{z'}\times\vec{e}_{x'}\\ \vec{e}_{y''} &= \vec{e}_{z''}\times\vec{e}_{x''}\end{aligned} \tag{5.5}$$

We can now define the spherical components $\sigma_m^l\left(\vec{k}\right)$ of the stress tensor. To discriminate between the different coordinate systems we also have to define the spherical tensors $\sigma_{m'}^{l'}\left(\vec{q}\right)$ and $\sigma_{m''}^{l''}\left(\vec{k}-\vec{q}\right)$. The advantage of this notation is that $\left\langle\sigma_m^l\left(\vec{k},t\right)\sigma_m^l\left(\vec{k}\right)\right\rangle=$

$\left\langle \sigma^{l'}_{m'}\left(\vec{q},t\right)\sigma^{l'}_{m'}\left(\vec{q}\right)\right\rangle$ if $\left|\vec{k}\right| = |\vec{q}|$. In contrast to this $\left\langle \sigma^{l}_{m}\left(\vec{k},t\right)\sigma^{l}_{m}\left(\vec{k}\right)\right\rangle$ is generally not equal to $\left\langle \sigma^{l}_{m}\left(\vec{q},t\right)\sigma^{l}_{m}\left(\vec{q}\right)\right\rangle$ even if $\left|\vec{k}\right| = |\vec{q}|$. So it is sufficient if we consider as dynamic variables the following spherical components of the stress tensor $\sigma^{l}_{m}\left(\vec{k}\right)$, where the relation to the Cartesian stress tensor $\sigma_{ij}\left(\vec{k}\right)$ is given as

$$\begin{aligned}
\sigma^{0}_{0}\left(\vec{k}\right) &= \frac{1}{\sqrt{3}}\left(\sigma_{xx}\left(\vec{k}\right)+\sigma_{yy}\left(\vec{k}\right)+\sigma_{zz}\left(\vec{k}\right)\right)\\
\sigma^{2}_{0}\left(\vec{k}\right) &= \frac{1}{\sqrt{6}}\left(2\sigma_{zz}\left(\vec{k}\right)-\sigma_{xx}\left(\vec{k}\right)-\sigma_{yy}\left(\vec{k}\right)\right)\\
\sigma^{2}_{-2}\left(\vec{k}\right) &= \frac{1}{2}\left(\sigma_{xx}\left(\vec{k}\right)-\sigma_{yy}\left(\vec{k}\right)\right)-\frac{1}{2}i\left(\sigma_{xy}\left(\vec{k}\right)+\sigma_{yx}\left(\vec{k}\right)\right)\\
\sigma^{2}_{2}\left(\vec{k}\right) &= \frac{1}{2}\left(\sigma_{xx}\left(\vec{k}\right)-\sigma_{yy}\left(\vec{k}\right)\right)+\frac{1}{2}i\left(\sigma_{xy}\left(\vec{k}\right)+\sigma_{yx}\left(\vec{k}\right)\right)\\
\sigma^{2}_{1}\left(\vec{k}\right) &= -\frac{1}{2}\left(\sigma_{zx}\left(\vec{k}\right)+\sigma_{xz}\left(\vec{k}\right)\right)-\frac{i}{2}\left(\sigma_{yz}\left(\vec{k}\right)+\sigma_{zy}\left(\vec{k}\right)\right)\\
\sigma^{2}_{-1}\left(\vec{k}\right) &= \frac{1}{2}\left(\sigma_{zx}\left(\vec{k}\right)+\sigma_{xz}\left(\vec{k}\right)\right)-\frac{i}{2}\left(\sigma_{yz}\left(\vec{k}\right)+\sigma_{zy}\left(\vec{k}\right)\right)
\end{aligned} \tag{5.6}$$

There are no components with spherical index $l = 1$ due to symmetry reasons. Now we consider the following linear combinations of $\sigma^{0}_{0}\left(\vec{k}\right)$ and $\sigma^{2}_{0}\left(\vec{k}\right)$:

$$\begin{aligned}
\sigma_{0}\left(\vec{k}\right) &= \frac{1}{\sqrt{3}}\left(\sqrt{2}\sigma^{0}_{0}\left(\vec{k}\right)-\sigma^{2}_{0}\left(\vec{k}\right)\right)=\frac{1}{\sqrt{2}}\left(\sigma_{xx}\left(\vec{k}\right)+\sigma_{yy}\left(\vec{k}\right)\right)\\
\widetilde{\sigma}_{0}\left(\vec{k}\right) &= \frac{1}{\sqrt{3}}\left(\sigma^{0}_{0}\left(\vec{k}\right)+\sqrt{2}\sigma^{2}_{0}\left(\vec{k}\right)\right)=\sigma_{zz}\left(\vec{k}\right).
\end{aligned} \tag{5.7}$$

Because $\sigma_{zz}\left(\vec{k}\right)$ can be written as time derivative of a current (cf. Eq. (5.1)), $\widetilde{\sigma}_{0}\left(\vec{k}\right)$ is expected to decay much faster to zero than $\sigma_{0}\left(\vec{k}\right)$. This was also indicated by a computer simulation by Visscher and Logan [76]. So we only keep $\sigma_{0}\left(\vec{k}\right)$ as slow variable. We can thus omit the index, which specifies the respective spherical index l.

So we only consider the following dynamic variables:

$$\begin{aligned}
\sigma_{-2}\left(\vec{k}\right) &:= \sigma_{-2}^2\left(\vec{k}\right) \\
\sigma_{-1}\left(\vec{k}\right) &:= \sigma_{-1}^2\left(\vec{k}\right) \\
\sigma_{0}\left(\vec{k}\right) &:= \frac{1}{\sqrt{3}}\left(\sqrt{2}\sigma_0^0\left(\vec{k}\right) - \sigma_0^2\left(\vec{k}\right)\right) \\
\sigma_{1}\left(\vec{k}\right) &:= \sigma_1^2\left(\vec{k}\right) \\
\sigma_{2}\left(\vec{k}\right) &:= \sigma_2^2\left(\vec{k}\right)
\end{aligned} \tag{5.8}$$

5.2 Derivation of the mode-coupling equations

So the respective correlation functions in which we are interested in are

$$\begin{aligned}
\phi_{m_1 m_2}\left(\vec{k},t\right) &= \frac{1}{V}\left\langle \sigma_{m_1}\left(\vec{k}\right)|e^{-i\mathcal{L}t}|\sigma_{m_2}\left(\vec{k}\right)\right\rangle \\
&= \delta_{m_1,m_2}\phi_{m_1}\left(\vec{k},t\right)
\end{aligned} \tag{5.9}$$

with

$$\phi_m\left(\vec{k},t\right) = \frac{1}{V}\left\langle \sigma_m\left(\vec{k}\right)|e^{-i\mathcal{L}t}|\sigma_m\left(\vec{k}\right)\right\rangle. \tag{5.10}$$

The property which is used here, i.e. that all nondiagonal elements of $\phi_{m_1 m_2}\left(\vec{k},t\right)$ vanish, is related to the rotational symmetry of an infinite system. Additionally we have due to symmetry reasons

$$\phi_m\left(\vec{k},t\right) = \phi_{-m}\left(\vec{k},t\right). \tag{5.11}$$

Eq. (5.10) can be transformed into Laplace space as

$$\hat{\phi}_m\left(\vec{k},z\right) = -\frac{1}{V}\left\langle \sigma_m\left(\vec{k}\right)|\left(z-\mathcal{L}\right)^{-1}|\sigma_m\left(\vec{k}\right)\right\rangle. \tag{5.12}$$

We can now apply the Mori-Zwanzig formalism described in section 2.2, from which we obtain

$$\hat{\phi}_m\left(\vec{k},z\right) = -\left(z-\Omega_m\left(\vec{k}\right)+M_m\left(\vec{k},z\right)\right)^{-1}\phi_m\left(\vec{k},0\right). \tag{5.13}$$

The frequency term appearing in Eq. (5.13) is

$$\begin{aligned} i\Omega_m\left(\vec{k}\right) &= \left\langle \sigma_m\left(\vec{k}\right)|\dot{\sigma}_m\left(\vec{k}\right)\right\rangle \left\langle \sigma_m\left(\vec{k}\right)|\sigma_m\left(\vec{k}\right)\right\rangle^{-1} \\ &= 0 \end{aligned} \tag{5.14}$$

where we have used the property [1]

$$\langle A|\,\mathcal{L}\,|A\rangle = 0 \tag{5.15}$$

which is valid if A has a specific time-reversal symmetry (i.e. either symmetric or antisymmetric). The memory kernel in Eq. (5.13) is

$$\begin{aligned} & M_m\left(\vec{k},z\right) = \\ = & -\left\langle \dot{\sigma}_m\left(\vec{k}\right)\right| Q_1\left(z-Q_1\mathcal{L}Q_1\right)^{-1}Q_1\left|\dot{\sigma}_m\left(\vec{k}\right)\right\rangle \left\langle \sigma_m\left(\vec{k}\right)|\sigma_m\left(\vec{k}\right)\right\rangle^{-1} \\ = & -\frac{1}{V}\left\langle \dot{\sigma}_m\left(\vec{k}\right)\right|\left(z-Q_1\mathcal{L}Q_1\right)^{-1}\left|\dot{\sigma}_m\left(\vec{k}\right)\right\rangle \phi_m^{-1}\left(\vec{k},0\right) \end{aligned} \tag{5.16}$$

where $P_1\left|\dot{\sigma}_m\left(\vec{k}\right)\right\rangle = 0$ (cf. Eq. (5.15)) was used. The projectors are here

$$P_1 = \sum_{m_1,m_2}\left|\sigma_{m_1}\left(\vec{k}\right)\right\rangle g_{m_1m_2}\left(\vec{k}\right)\left\langle \sigma_{m_2}\left(\vec{k}\right)\right| \tag{5.17}$$

and

$$Q_1 = 1 - P_1. \tag{5.18}$$

The normalization constant $g_{m_1m_2}\left(\vec{k}\right)$ in Eq. (5.17) can be determined by the condition

$$P_1^2 = P_1 \tag{5.19}$$

which is fulfilled by any projection operator. This means that it has to be valid

$$\sum_{m_3}\left\langle \sigma_{m_1}\left(\vec{k}\right)|\sigma_{m_3}\left(\vec{k}\right)\right\rangle g_{m_3m_2}\left(\vec{k}\right) = \delta_{m_1m_2} \tag{5.20}$$

or

$$g_{m_1m_2}\left(\vec{k}\right) = \delta_{m_1m_2}\left\langle \sigma_{m_1}\left(\vec{k}\right)|\sigma_{m_1}\left(\vec{k}\right)\right\rangle^{-1}. \tag{5.21}$$

This means that Eq. (5.17) can also be written as

$$P_1 = \sum_m \left|\sigma_m\left(\vec{k}\right)\right\rangle \left\langle\sigma_m\left(\vec{k}\right)|\sigma_m\left(\vec{k}\right)\right\rangle^{-1} \left\langle\sigma_m\left(\vec{k}\right)\right|. \tag{5.22}$$

Now we apply again the Mori-Zwanzig formalism to

$$\begin{aligned} \hat{D}_m\left(\vec{k},z\right) &= M_m\left(\vec{k},z\right)\phi_m\left(\vec{k},0\right) \\ &= -\frac{1}{V}\left\langle\dot{\sigma}_m\left(\vec{k}\right)\right|\left(z-Q_1\mathcal{L}Q_1\right)^{-1}\left|\dot{\sigma}_m\left(\vec{k}\right)\right\rangle \end{aligned} \tag{5.23}$$

i.e. we use Eq. (2.26) with

$$\begin{aligned} \left|\tilde{A}_m\right\rangle &= \left|\dot{\sigma}_m\left(\vec{k}\right)\right\rangle \\ \tilde{\mathcal{L}} &= Q_1\mathcal{L}Q_1. \end{aligned} \tag{5.24}$$

From Eqs. (2.28), (2.29) and (2.30) we obtain

$$\hat{D}_m\left(\vec{k},z\right) = -\frac{1}{V}\left(z+\tilde{M}_m\left(\vec{k},z\right)\right)^{-1}\left\langle\tilde{A}_m|\tilde{A}_m\right\rangle \tag{5.25}$$

with

$$\tilde{M}_m\left(\vec{k},z\right) = -\left\langle\tilde{A}_m\right|\tilde{\mathcal{L}}Q_2\left(z-Q_2\tilde{\mathcal{L}}Q_2\right)^{-1}Q_2\tilde{\mathcal{L}}\left|\tilde{A}_m\right\rangle / \left\langle\tilde{A}_m|\tilde{A}_m\right\rangle \tag{5.26}$$

where we have used Eq. (5.15) again. Combining Eqs. (5.13), (5.14), (5.23), and (5.25) we obtain

$$\hat{\phi}_m\left(\vec{k},z\right) = -\frac{\phi_m\left(\vec{k},0\right)}{z+\frac{\ddot{\phi}_m\left(\vec{k},0\right)/\phi_m\left(\vec{k},0\right)}{z+\tilde{M}_m\left(\vec{k},z\right)}}. \tag{5.27}$$

$\tilde{M}_m\left(\vec{k},z\right)$ is given by Eq. (5.26) with Eqs. (5.24) inserted

$$\begin{aligned} &\tilde{M}_m\left(\vec{k},z\right) = \\ &= -\left\langle\dot{\sigma}_m\left(\vec{k}\right)\right|\mathcal{L}Q_1Q_2\left(z-Q_2Q_1\mathcal{L}Q_1Q_2\right)^{-1}Q_2Q_1\mathcal{L}\left|\dot{\sigma}_m\left(\vec{k}\right)\right\rangle / \left\langle\tilde{A}_m|\tilde{A}_m\right\rangle \\ &= \frac{1}{V}\left\langle\sigma_m\left(\vec{k}\right)\right|\mathcal{L}^2Q_1\left(z-Q_2Q_1\mathcal{L}Q_1Q_2\right)^{-1}Q_1\mathcal{L}^2\left|\sigma_m\left(\vec{k}\right)\right\rangle / \ddot{\phi}_m\left(\vec{k},0\right) \end{aligned} \tag{5.28}$$

with the projectors from Eqs. (5.18), (5.22) and

$$\begin{aligned} P_2 &= \sum_m \left|\dot{\sigma}_m\left(\vec{k}\right)\right\rangle \left\langle \dot{\sigma}_m\left(\vec{k}\right)|\dot{\sigma}_m\left(\vec{k}\right)\right\rangle \left\langle \dot{\sigma}_m\left(\vec{k}\right)\right| \\ Q_2 &= 1 - P_2. \end{aligned} \tag{5.29}$$

In order to derive the second line of Eq. (5.28) from the first, we have again used Eq. (5.15). We note that Eq. (5.27) can be written in time space as

$$\frac{\partial^2}{\partial t^2}\phi_m\left(\vec{k},t\right) - \frac{\ddot{\phi}_m\left(\vec{k},0\right)}{\phi_m\left(\vec{k},0\right)}\phi_m\left(\vec{k},t\right) + \int_0^t \mathrm{d}t' \tilde{M}_m\left(\vec{k},t-t'\right)\dot{\phi}_m\left(\vec{k},t'\right) = 0. \tag{5.30}$$

Instead of projecting onto pairs of density modes, like in density MCT, we now project onto pairs of stress modes, i.e.

$$\begin{aligned} &\tilde{M}_m\left(\vec{k},z\right) \cong \\ \cong\ &\frac{1}{V}\left\langle \sigma_m\left(\vec{k}\right)\right| \mathcal{L}^2 Q_1 P_{\sigma\sigma}\left(\vec{k}\right)\left(z - Q_2Q_1\mathcal{L}Q_1Q_2\right)^{-1} P_{\sigma\sigma}\left(\vec{k}\right) Q_1\mathcal{L}^2 \left|\sigma_m\left(\vec{k}\right)\right\rangle / \ddot{\phi}_m\left(\vec{k},0\right) \end{aligned} \tag{5.31}$$

with

$$\begin{aligned} &P_{\sigma\sigma}\left(\vec{k}\right) = \\ = &\sum_{\substack{m_1',m_2'',\\ m_3''',m_4'''',\\ \vec{q},\vec{q}'}}{}' \left|\sigma_{m_1'}\left(\vec{q}\right)\sigma_{m_2''}\left(\vec{k}-\vec{q}\right)\right\rangle \langle\sigma\sigma|\sigma\sigma\rangle^{-1}_{m_1'm_2''m_3'''m_4''''\vec{q},\vec{k}-\vec{q},\vec{q}',\vec{k}-\vec{q}'} \\ &\left\langle \sigma_{m_3'''}\left(\vec{q}'\right)\sigma_{m_4''''}\left(\vec{k}-\vec{q}'\right)\right| \end{aligned} \tag{5.32}$$

where the prime in $\sum'$ again prevents double counting same as in Eq. (2.42). Additionally we also use in Eq. (5.31) the factorization approximation, already known from the density MCT

$$\begin{aligned} &\left\langle \sigma_{m_1'}\left(\vec{q}\right)\sigma_{m_2''}\left(\vec{k}-\vec{q}\right)\right| e^{-Q_2Q_1\mathcal{L}Q_1Q_2t}\left|\sigma_{m_3'''}\left(\vec{q}'\right)\sigma_{m_4''''}\left(\vec{k}-\vec{q}'\right)\right\rangle = \\ = &\left\langle \sigma_{m_1'}\left(\vec{q}\right)\right| e^{-i\mathcal{L}t}\left|\sigma_{m_3'''}\left(\vec{q}'\right)\right\rangle \left\langle \sigma_{m_2''}\left(\vec{k}-\vec{q}\right)\right| e^{-i\mathcal{L}t}\left|\sigma_{m_4''''}\left(\vec{k}-\vec{q}'\right)\right\rangle \\ = &\ V^2\delta_{\vec{q}\vec{q}'}\delta_{m_1'm_3'''}\phi_{m_1'}\left(\vec{q},t\right)\delta_{m_2''m_4''''}\phi_{m_2''}\left(\vec{k}-\vec{q},t\right). \end{aligned} \tag{5.33}$$

Accordingly we also obtain for the normalization term appearing in (5.32)

$$\begin{aligned} & \left\langle \sigma_{m_1'}\left(\vec{q}\right)\sigma_{m_2''}\left(\vec{k}-\vec{q}\right)|\sigma_{m_3'''}\left(\vec{q}'\right)\sigma_{m_4''''}\left(\vec{k}-\vec{q}'\right)\right\rangle = \\ = \; & V^2\delta_{\vec{q}\vec{q}'}\delta_{m_1'm_3'''}\phi_{m_1'}\left(\vec{q},t=0\right)\delta_{m_2''m_4''''}\phi_{m_2''}\left(\vec{k}-\vec{q},t=0\right) \end{aligned} \tag{5.34}$$

which also means that

$$\begin{aligned} & P_{\sigma\sigma}\left(\vec{k}\right) = \\ = \; & \frac{1}{V^2}\sum_{m_1',m_2'',\vec{q}}{}' \left|\sigma_{m_1'}\left(\vec{q}\right)\sigma_{m_2''}\left(\vec{k}-\vec{q}\right)\right\rangle \phi_{m_1'}^{-1}\left(\vec{q},t=0\right)\phi_{m_2''}^{-1}\left(\vec{k}-\vec{q},t=0\right) \\ & \left\langle \sigma_{m_1'}\left(\vec{q}\right)\sigma_{m_2''}\left(\vec{k}-\vec{q}\right)\right|. \end{aligned} \tag{5.35}$$

If we now insert Eq. (5.35) and (5.33) into Eq. (5.31) we obtain in time space (cf. also Eq. (2.26))

$$\tilde{M}_m\left(\vec{k},t\right) = \frac{1}{V}\sum_{\vec{q},m_2'',m_3'} \mathcal{V}_{m,m_2'',m_3'}\left(\vec{k},\vec{q}\right)\cdot\phi_{m_2''}\left(\vec{k}-\vec{q},t\right)\phi_{m_3'}\left(\vec{q},t\right) \tag{5.36}$$

with

$$\mathcal{V}_{m,m_2'',m_3'}\left(\vec{k},\vec{q}\right) = -\frac{1}{2\ddot{\phi}_m\left(\vec{k},t=0\right)}\left|\frac{V_{m,m_2'',m_3'}\left(\vec{k},\vec{q}\right)}{\phi_{m_2''}\left(\vec{k}-\vec{q},t=0\right)\phi_{m_3'}\left(\vec{q},t=0\right)}\right|^2. \tag{5.37}$$

So in order to evaluate the vertex $\mathcal{V}_{m,m_2'',m_3'}\left(\vec{k},\vec{q}\right)$ we need an explicit expression for the functions

$$\phi_m\left(\vec{k},t=0\right) = \frac{1}{V}\left\langle\sigma_m\left(\vec{k}\right)|\sigma_m\left(\vec{k}\right)\right\rangle \tag{5.38}$$

$$\ddot{\phi}_m\left(\vec{k},t=0\right) = -\frac{1}{V}\left\langle\sigma_m\left(\vec{k}\right)\right|\mathcal{L}^2\left|\sigma_m\left(\vec{k}\right)\right\rangle \tag{5.39}$$

$$V_{m,m_2'',m_3'}\left(\vec{k},\vec{q}\right) = \frac{1}{V}\left\langle\sigma_m\left(\vec{k}\right)\right|\mathcal{L}^2Q_1\left|\sigma_{m_2''}\left(\vec{k}-\vec{q}\right)\sigma_{m_3'}\left(\vec{q}\right)\right\rangle. \tag{5.40}$$

This will be worked out in the following section.

5.3 Evaluation of the Vertex

It was shown in a molecular-dynamics simulation by Balucani et al. that in the stress autocorrelation function at high viscosities the kinetic part plays a much less important role than the potential part [77]. For simplicity we will therefore neglect the kinetic part in the following. The potential part of the stress tensor may be rewritten as (see appendix A.1)

$$\begin{aligned}\sigma_m\left(\vec{k}\right) &= \sum_n \frac{1}{2}\sum_{m\neq n} \frac{\left(r_i^m - r_i^n\right)\left(r_j^m - r_j^n\right)}{|\vec{r}^m - \vec{r}^n|} \left.\frac{\partial u\left(r\right)}{\partial r}\right|_{r=|\vec{r}^n-\vec{r}^m|} \frac{e^{-i\vec{k}(\vec{r}^m-\vec{r}^n)}-1}{i\vec{k}\cdot\left(\vec{r}_m-\vec{r}_n\right)} e^{-i\vec{k}\vec{r}^n} \\ &= \frac{1}{V}\sum_{\vec{q}} \rho\left(\vec{k}-\vec{q}\right)\rho\left(\vec{q}\right) F_m\left(\vec{k},\vec{q}-\frac{\vec{k}}{2}\right) \end{aligned} \tag{5.41}$$

where $F_m\left(\vec{k},\vec{q}\right)$ is the spherical component of the Cartesian tensor

$$F_{ij}\left(\vec{k},\vec{q}\right) = \int \mathrm{d}^3 r\; e^{-i\vec{q}\vec{r}} \frac{r_i r_j}{r} \frac{\partial u\left(r\right)}{\partial r} \frac{\sin\left(\frac{\vec{k}\cdot\vec{r}}{2}\right)}{\vec{k}\cdot\vec{r}} \tag{5.42}$$

(cf. Eqs. (5.6) and (5.8)), where it can be seen easily that the relation

$$F_m\left(\vec{k},\vec{q}\right) = F_m\left(\vec{k},-\vec{q}\right) \tag{5.43}$$

holds. From Eq. (5.41) we obtain for the term required in (5.38)

$$\begin{aligned}&\left\langle \sigma_m\left(\vec{k}\right)|\sigma_m\left(\vec{k}\right)\right\rangle = \\ &= \frac{1}{V^2}\sum_{\vec{k}_1,\vec{k}_2} F_m^*\left(\vec{k},\vec{k}_1-\frac{\vec{k}}{2}\right) F_m\left(\vec{k},\vec{k}_2-\frac{\vec{k}}{2}\right) \\ &\quad\cdot\left\langle \rho^*\left(\vec{k}-\vec{k}_1\right)\rho^*\left(\vec{k}_1\right)\rho\left(\vec{k}-\vec{k}_2\right)\rho\left(\vec{k}_2\right)\right\rangle . \end{aligned} \tag{5.44}$$

The time derivative of the stress tensor can be evaluated from Eq. (5.41) together with Eq. (2.23) and Eq. (5.43). The result reads

$$\begin{aligned}&i\mathcal{L}\sigma_m\left(\vec{k}\right) = \\ &= -i\frac{2}{V}\sum_{\vec{q}} \vec{q}\cdot\vec{j}\left(\vec{q}\right)\rho\left(\vec{k}-\vec{q}\right) F_m\left(\vec{k},\vec{q}-\frac{\vec{k}}{2}\right) . \end{aligned} \tag{5.45}$$

From this we can evaluate the term required in Eq. (5.39)

$$\begin{aligned}
&\left\langle \sigma_m\left(\vec{k}\right)\middle|\,\mathcal{L}^2\left|\sigma_m\left(\vec{k}\right)\right\rangle = \right.\\
= \;& \frac{4}{V^2}\frac{k_BT}{m}\sum_{\vec{k}_1,\vec{k}_2}\vec{k}_1\cdot\vec{k}_2F_m^*\left(\vec{k},\vec{k}_1-\frac{\vec{k}}{2}\right)F_m\left(\vec{k},\vec{k}_2-\frac{\vec{k}}{2}\right)\\
&\cdot\left\langle\rho\left(\vec{k}_2-\vec{k}_1\right)\rho\left(\vec{k}_1-\vec{k}\right)\rho\left(\vec{k}-\vec{k}_2\right)\right\rangle. \qquad (5.46)
\end{aligned}$$

We have used here

$$\left\langle j_i\left(\vec{k}_1\right)j_j\left(\vec{k}_2\right)\cdots\right\rangle = \delta_{ij}\frac{k_BT}{m}\left\langle\rho\left(\vec{k}_1+\vec{k}_2\right)\cdots\right\rangle \qquad (5.47)$$

where $\cdots$ may only contain density modes (and not currents). This relation can be derived from Eqs. (2.2) and (2.4). Now we can also evaluate the term

$$\begin{aligned}
&V_{m,m_2'',m_3'}\left(\vec{k},\vec{q}\right) =\\
= \;& \frac{1}{V}\left\langle\sigma_m\left(\vec{k}\right)\middle|\,\mathcal{L}^2Q_1\left|\sigma_{m_2''}\left(\vec{k}-\vec{q}\right)\sigma_{m_3'}\left(\vec{q}\right)\right\rangle\right.\\
= \;& \frac{1}{V}\left\langle\sigma_m\left(\vec{k}\right)\middle|\,\mathcal{L}^2\left|\sigma_{m_2''}\left(\vec{k}-\vec{q}\right)\sigma_{m_3'}\left(\vec{q}\right)\right\rangle\right.\\
&-\frac{1}{V}\left\langle\sigma_m\left(\vec{k}\right)\middle|\,\mathcal{L}^2P_1\left|\sigma_{m_2''}\left(\vec{k}-\vec{q}\right)\sigma_{m_3'}\left(\vec{q}\right)\right\rangle\right.\\
= \;& V^1_{m,m_2'',m_3'}\left(\vec{k},\vec{q}\right)-V^2_{m,m_2'',m_3'}\left(\vec{k},\vec{q}\right) \qquad (5.48)
\end{aligned}$$

with

$$V^1_{m,m_2'',m_3'}\left(\vec{k},\vec{q}\right) = \frac{1}{V}\left\langle\sigma_m\left(\vec{k}\right)\middle|\,\mathcal{L}^2\left|\sigma_{m_2''}\left(\vec{k}-\vec{q}\right)\sigma_{m_3'}\left(\vec{q}\right)\right\rangle\right. \qquad (5.49)$$

and

$$V^2_{m,m_2'',m_3'}\left(\vec{k},\vec{q}\right) = \frac{1}{V}\left\langle\sigma_m\left(\vec{k}\right)\middle|\,\mathcal{L}^2P_1\left|\sigma_{m_2''}\left(\vec{k}-\vec{q}\right)\sigma_{m_3'}\left(\vec{q}\right)\right\rangle\right. . \qquad (5.50)$$

Eq. (5.49) can be evaluated with Eqs. (5.45) and (5.47) as

$$\begin{aligned}
&V^1_{m,m_2'',m_3'}\left(\vec{k},\vec{q}\right) =\\
= \;& \frac{4}{V^4}\frac{k_BT}{m}\sum_{\vec{k}_1,\vec{k}_2,\vec{k}_3}F_m^*\left(\vec{k},\vec{k}_1-\frac{\vec{k}}{2}\right)F_{m_2''}\left(\vec{k}-\vec{q},\vec{k}_2-\frac{\vec{k}-\vec{q}}{2}\right)F_{m_3'}\left(\vec{q},\vec{k}_3-\frac{\vec{q}}{2}\right)\cdot\\
&\vec{k}_1\cdot\vec{k}_2\left\langle\rho\left(\vec{k}_3\right)\rho\left(\vec{k}_2-\vec{k}_1\right)\rho\left(\vec{k}_1-\vec{k}\right)\rho\left(\vec{k}-\vec{q}-\vec{k}_2\right)\rho\left(\vec{q}-\vec{k}_3\right)\right\rangle\\
&+\left\{m_2''\leftrightarrow m_3',\vec{q}\leftrightarrow\vec{k}-\vec{q}\right\}. \qquad (5.51)
\end{aligned}$$

Eq. (5.50) can be evaluated with Eq. (5.22) as

$$V^2_{m,m''_2,m'_3}\left(\vec{k},\vec{q}\right) = \frac{1}{V}\frac{\left\langle \sigma_m\left(\vec{k}\right)\middle|\,\mathcal{L}^2\,\middle|\sigma_m\left(\vec{k}\right)\right\rangle}{\left\langle \sigma_m\left(\vec{k}\right)|\sigma_m\left(\vec{k}\right)\right\rangle}\left\langle \sigma_m\left(\vec{k}\right)|\sigma_{m''_2}\left(\vec{k}-\vec{q}\right)\sigma_{m'_3}\left(\vec{q}\right)\right\rangle \tag{5.52}$$

where $\left\langle \sigma_m\left(\vec{k}\right)|\sigma_m\left(\vec{k}\right)\right\rangle$ and $\left\langle \sigma_m\left(\vec{k}\right)\middle|\,\mathcal{L}^2\,\middle|\sigma_m\left(\vec{k}\right)\right\rangle$ are already given in Eqs. (5.44) and (5.46). The last factor in Eq. (5.52) can then be evaluated with Eq. (5.41) as

$$\begin{aligned}
&\left\langle \sigma_m\left(\vec{k}\right)|\sigma_{m''_2}\left(\vec{k}-\vec{q}\right)\sigma_{m'_3}\left(\vec{q}\right)\right\rangle = \\
= \;& \frac{1}{V^3}\sum_{\vec{k}_1,\vec{k}_2,\vec{k}_3} F^*_m\left(\vec{k},\vec{k}_1-\frac{\vec{k}}{2}\right)F_{m''_2}\left(\vec{k}-\vec{q},\vec{k}_2-\frac{\vec{k}-\vec{q}}{2}\right)F_{m'_3}\left(\vec{q},\vec{k}_3-\frac{\vec{q}}{2}\right)\cdot \\
&\cdot\left\langle \rho^*\left(\vec{k}-\vec{k}_1\right)\rho^*\left(\vec{k}_1\right)\rho\left(\vec{k}-\vec{q}-\vec{k}_2\right)\rho\left(\vec{k}_2\right)\rho\left(\vec{q}-\vec{k}_3\right)\rho\left(\vec{k}_3\right)\right\rangle .
\end{aligned} \tag{5.53}$$

5.3.1 Transformation into real space

We now transform these equations into real space in order to replace the static correlation functions $\langle\rho(\vec{k}_1)\rho(\vec{k}_2)\cdots\rho(\vec{k}_n)\rangle$ by the distribution functions $g^{(n)}(\vec{r}_1,\cdots,\vec{r}_n)$. With

$$\begin{aligned}
F_{ij}\left(\vec{k},\vec{r}\right) &= \frac{1}{(2\pi)^3}\int \mathrm{d}^3q \;\; F_{ij}\left(\vec{k},\vec{q}\right)e^{i\vec{q}\vec{r}} \\
&= \frac{r_i r_j}{r}\frac{\partial u\left(r\right)}{\partial r}\frac{\sin\left(\frac{\vec{k}\cdot\vec{r}}{2}\right)}{\vec{k}\cdot\vec{r}}
\end{aligned} \tag{5.54}$$

(cf. Eq. (5.42)) and

$$\begin{aligned}
&\frac{1}{(2\pi)^3}\int \mathrm{d}^3q\;\vec{q}\;F_m\left(\vec{k},\vec{q}\right)e^{i\vec{q}\vec{r}} \\
=\;& -i\vec{\nabla}_r\frac{1}{(2\pi)^3}\int \mathrm{d}^3q\;F_m\left(\vec{k},\vec{q}\right)e^{i\vec{q}\vec{r}} \\
=\;& -i\vec{\nabla}_r F_m\left(\vec{k},\vec{r}\right)
\end{aligned} \tag{5.55}$$

and the respective relation for the complex conjugate we obtain (see appendix A.2, Eq. (A.2))

$$\begin{aligned}
&\left\langle \sigma_m\left(\vec{k}\right) | \sigma_m\left(\vec{k}\right)\right\rangle = \\
= &\int \mathrm{d}^3r_1\mathrm{d}^3r_2\mathrm{d}^3r_3\mathrm{d}^3r_4\; e^{i\frac{\vec{k}}{2}(\vec{r}_1+\vec{r}_2-\vec{r}_3-\vec{r}_4)} F_m^*\left(\vec{k},\vec{r}_1-\vec{r}_2\right) F_m\left(\vec{k},\vec{r}_3-\vec{r}_4\right) \\
&\cdot\left\langle \rho\left(\vec{r}_1\right)\rho\left(\vec{r}_2\right)\rho\left(\vec{r}_3\right)\rho\left(\vec{r}_4\right)\right\rangle
\end{aligned} \tag{5.56}$$

and (see Eq. (A.3))

$$\begin{aligned}
&\left\langle \sigma_m\left(\vec{k}\right)\middle| \mathcal{L}^2 \middle|\sigma_m\left(\vec{k}\right)\right\rangle = \\
= &\; 4\frac{k_BT}{m}\int \mathrm{d}^3r_1\mathrm{d}^3r_2\mathrm{d}^3r_3\; e^{i\frac{\vec{k}}{2}(\vec{r}_1-\vec{r}_2)} \left(i\vec{\nabla}_r+\frac{\vec{k}}{2}\right) F_m^*\left(\vec{k},\vec{r}\right)\Big|_{\vec{r}=\vec{r}_1-\vec{r}_3} \cdot \\
&\cdot\left(-i\vec{\nabla}_{r'}+\frac{\vec{k}}{2}\right) F_m\left(\vec{k},\vec{r}'\right)\Big|_{\vec{r}'=\vec{r}_2-\vec{r}_3} \left\langle \rho\left(\vec{r}_1\right)\rho\left(\vec{r}_2\right)\rho\left(\vec{r}_3\right)\right\rangle
\end{aligned} \tag{5.57}$$

and (see Eq. (A.4))

$$\begin{aligned}
&V^1_{m,m_2'',m_3'}\left(\vec{k},\vec{q}\right) = \\
= &\; \frac{4k_BT}{m}\int \mathrm{d}^3r_1\mathrm{d}^3r_2\mathrm{d}^3r_3\mathrm{d}^3r_4\mathrm{d}^3r_5\; e^{i\frac{\vec{q}}{2}(\vec{r}_2+\vec{r}_3-\vec{r}_5-\vec{r}_1)} e^{i\frac{\vec{k}-\vec{q}}{2}(\vec{r}_3-\vec{r}_4)} F_{m_3'}\left(\vec{q},\vec{r}_5-\vec{r}_1\right)\cdot \\
&\cdot\left(i\vec{\nabla}_r+\frac{\vec{k}}{2}\right) F_m^*\left(\vec{k},\vec{r}\right)\Big|_{\vec{r}=\vec{r}_3-\vec{r}_2} \left(-i\vec{\nabla}_{r'}+\frac{\vec{k}-\vec{q}}{2}\right) F_{m_2''}\left(\vec{k}-\vec{q},\vec{r}'\right)\Big|_{\vec{r}'=\vec{r}_4-\vec{r}_2} \cdot \\
&\cdot\left\langle \rho\left(\vec{r}_1\right)\rho\left(\vec{r}_2\right)\rho\left(\vec{r}_3\right)\rho\left(\vec{r}_4\right)\rho\left(\vec{r}_5\right)\right\rangle + \\
&+\left\{m_2''\leftrightarrow m_3', \vec{q}\leftrightarrow\vec{k}-\vec{q}\right\}.
\end{aligned} \tag{5.58}$$

and (see Eq. (A.5))

$$\begin{aligned}
&\left\langle \sigma_m\left(\vec{k}\right) | \sigma_{m_2''}\left(\vec{k}-\vec{q}\right)\sigma_{m_3'}\left(\vec{q}\right)\right\rangle = \\
= &\int \mathrm{d}^3r_1\mathrm{d}^3r_2\mathrm{d}^3r_3\mathrm{d}^3r_4\mathrm{d}^3r_5\mathrm{d}^3r_6\; e^{i\frac{\vec{q}}{2}(\vec{r}_1+\vec{r}_2-\vec{r}_5-\vec{r}_6)} e^{i\frac{\vec{k}-\vec{q}}{2}(\vec{r}_1+\vec{r}_2-\vec{r}_3-\vec{r}_4)}\cdot \\
&\cdot F_m^*\left(\vec{k},\vec{r}_1-\vec{r}_2\right) F_{m_2''}\left(\vec{k}-\vec{q},\vec{r}_3-\vec{r}_4\right) F_{m_3'}\left(\vec{q},\vec{r}_5-\vec{r}_6\right)\cdot \\
&\cdot\left\langle \rho\left(\vec{r}_1\right)\rho\left(\vec{r}_2\right)\rho\left(\vec{r}_3\right)\rho\left(\vec{r}_4\right)\rho\left(\vec{r}_5\right)\rho\left(\vec{r}_6\right)\right\rangle.
\end{aligned} \tag{5.59}$$

It is important to note that $\langle \rho(\vec{r}_1)\,\rho(\vec{r}_2)\cdots\rho(\vec{r}_n)\rangle$ consists of a configurational average of a product of n independent densities

$$\rho(\vec{r}) = \sum_{i=1}^{N} \delta\left(\vec{r} - \vec{r}^{\,i}\right) \tag{5.60}$$

while in the n-particle distribution function $g^{(n)}(\vec{r}_1, \vec{r}_2 \cdots \vec{r}_n)$ the summation is modified in such a way [29], that all terms in the multiple sums, where the same particle appears more than once, are omitted. This means that $\langle \rho(\vec{r}_1)\,\rho(\vec{r}_2)\cdots\rho(\vec{r}_n)\rangle$ contains additionally to the n-particle distribution function also m-particle distribution functions with $m < n$. With this Eq. (5.56) can be rewritten as

$$\begin{aligned}
&\left\langle \sigma_m\left(\vec{k}\right) | \sigma_m\left(\vec{k}\right)\right\rangle = \\
= &\int \mathrm{d}^3r_1\mathrm{d}^3r_2\mathrm{d}^3r_3\mathrm{d}^3r_4\ \cos\left(\frac{\vec{k}}{2}\left(\vec{r}_1+\vec{r}_2-\vec{r}_3-\vec{r}_4\right)\right) F_m^*\left(\vec{k}, \vec{r}_1-\vec{r}_2\right) \\
&\cdot F_m\left(\vec{k}, \vec{r}_3-\vec{r}_4\right)\rho^4 g^{(4)}\left(\vec{r}_1,\vec{r}_2,\vec{r}_3,\vec{r}_4\right) \\
&+4\int \mathrm{d}^3r_1\mathrm{d}^3r_2\mathrm{d}^3r_4\ \cos\left(\frac{\vec{k}}{2}\left(\vec{r}_2-\vec{r}_4\right)\right) F_m^*\left(\vec{k}, \vec{r}_1-\vec{r}_2\right) F_m\left(\vec{k}, \vec{r}_1-\vec{r}_4\right) \\
&\cdot\rho^3 g^{(3)}\left(\vec{r}_1,\vec{r}_2,\vec{r}_4\right) \\
&+2\int \mathrm{d}^3r_1\mathrm{d}^3r_2\ F_m^*\left(\vec{k}, \vec{r}_1-\vec{r}_2\right) F_m\left(\vec{k}, \vec{r}_1-\vec{r}_2\right)\rho^2 g^{(2)}\left(\vec{r}_1,\vec{r}_2\right)
\end{aligned} \tag{5.61}$$

where we have used the symmetry $F_m\left(\vec{k}\,, -\vec{r}\right) = F_m\left(\vec{k}, \vec{r}\right)$. From Eq. (5.57) we obtain (see appendix A.3)

$$\begin{aligned}
&\left\langle \sigma_m\left(\vec{k}\right)\middle|\,\mathcal{L}^2\,\middle|\sigma_m\left(\vec{k}\right)\right\rangle \\
= &\ 4\frac{k_BT}{m}\frac{1}{V}\int \mathrm{d}^3r_1\mathrm{d}^3r_2\mathrm{d}^3r_3\ Y_m\left(\vec{k}, \vec{r}_1, \vec{r}_2, \vec{r}_3\right)\rho^3 g^{(3)}\left(\vec{r}_1,\vec{r}_2,\vec{r}_3\right) \\
&+4\frac{k_BT}{m}\frac{1}{V}\int \mathrm{d}^3r_1\mathrm{d}^3r_3\ Y_m\left(\vec{k}, \vec{r}_1, \vec{r}_1, \vec{r}_3\right)\rho^2 g^{(2)}\left(\vec{r}_1,\vec{r}_3\right)
\end{aligned} \tag{5.62}$$

with

$$
\begin{aligned}
& Y_m\left(\vec{k},\vec{r}_1,\vec{r}_2,\vec{r}_3\right) = \\
= \;& \cos\left(\frac{\vec{k}}{2}\left(\vec{r}_1-\vec{r}_2\right)\right)\vec{\nabla}_r F_m^*\left(\vec{k},\vec{r}\right)\Big|_{\vec{r}=\vec{r}_1-\vec{r}_3}\vec{\nabla}_{r'}F_m\left(\vec{k},\vec{r}'\right)\Big|_{\vec{r}'=\vec{r}_2-\vec{r}_3} \\
& +\cos\left(\frac{\vec{k}}{2}\left(\vec{r}_1-\vec{r}_2\right)\right)\frac{k^2}{4}\,F_m^*\left(\vec{k},\vec{r}\right)\Big|_{\vec{r}=\vec{r}_1-\vec{r}_3}F_m\left(\vec{k},\vec{r}'\right)\Big|_{\vec{r}'=\vec{r}_2-\vec{r}_3} \\
& -\sin\left(\frac{\vec{k}}{2}\left(\vec{r}_1-\vec{r}_2\right)\right)\frac{\vec{k}}{2}\cdot\vec{\nabla}_r F_m^*\left(\vec{k},\vec{r}\right)\Big|_{\vec{r}=\vec{r}_1-\vec{r}_3}F_m\left(\vec{k},\vec{r}'\right)\Big|_{\vec{r}'=\vec{r}_2-\vec{r}_3} \\
& +\sin\left(\frac{\vec{k}}{2}\left(\vec{r}_1-\vec{r}_2\right)\right)F_m^*\left(\vec{k},\vec{r}\right)\Big|_{\vec{r}=\vec{r}_1-\vec{r}_3}\frac{\vec{k}}{2}\cdot\vec{\nabla}_{r'}F_m\left(\vec{k},\vec{r}'\right)\Big|_{\vec{r}'=\vec{r}_2-\vec{r}_3}. \qquad (5.63)
\end{aligned}
$$

Eq. (5.58) can be rewritten as (see appendix A.3)

$$
\begin{aligned}
& V^1_{m,m_2'',m_3'}\left(\vec{k},\vec{q}\right) = \\
= \;& \frac{1}{V}\int \mathrm{d}^3r_1\mathrm{d}^3r_2\mathrm{d}^3r_3\mathrm{d}^3r_4\mathrm{d}^3r_5\; X_{m,m_2'',m_3'}\left(\vec{k},\vec{q},\vec{r}_1,\vec{r}_2,\vec{r}_3,\vec{r}_4,\vec{r}_5\right)\cdot\rho^5 g^{(5)}\left(\vec{r}_1,\vec{r}_2,\vec{r}_3,\vec{r}_4,\vec{r}_5\right) \\
& +2\frac{1}{V}\int \mathrm{d}^3r_1\mathrm{d}^3r_3\mathrm{d}^3r_4\mathrm{d}^3r_5\; X_{m,m_2'',m_3'}\left(\vec{k},\vec{q},\vec{r}_1,\vec{r}_1,\vec{r}_3,\vec{r}_4,\vec{r}_5\right)\cdot\rho^4 g^{(4)}\left(\vec{r}_1,\vec{r}_3,\vec{r}_4,\vec{r}_5\right)+ \\
& +2\frac{1}{V}\int \mathrm{d}^3r_1\mathrm{d}^3r_2\mathrm{d}^3r_4\mathrm{d}^3r_5\; X_{m,m_2'',m_3'}\left(\vec{k},\vec{q},\vec{r}_1,\vec{r}_2,\vec{r}_1,\vec{r}_4,\vec{r}_5\right)\cdot\rho^4 g^{(4)}\left(\vec{r}_1,\vec{r}_2,\vec{r}_4,\vec{r}_5\right)+ \\
& +2\frac{1}{V}\int \mathrm{d}^3r_1\mathrm{d}^3r_2\mathrm{d}^3r_3\mathrm{d}^3r_5\; X_{m,m_2'',m_3'}\left(\vec{k},\vec{q},\vec{r}_1,\vec{r}_2,\vec{r}_3,\vec{r}_1,\vec{r}_5\right)\cdot\rho^4 g^{(4)}\left(\vec{r}_1,\vec{r}_2,\vec{r}_3,\vec{r}_5\right)+ \\
& +\frac{1}{V}\int \mathrm{d}^3r_1\mathrm{d}^3r_2\mathrm{d}^3r_3\mathrm{d}^3r_5\; X_{m,m_2'',m_3'}\left(\vec{k},\vec{q},\vec{r}_1,\vec{r}_2,\vec{r}_3,\vec{r}_3,\vec{r}_5\right)\cdot\rho^4 g^{(4)}\left(\vec{r}_1,\vec{r}_2,\vec{r}_3,\vec{r}_5\right)+ \\
& +2\frac{1}{V}\int \mathrm{d}^3r_1\mathrm{d}^3r_2\mathrm{d}^3r_5\; X_{m,m_2'',m_3'}\left(\vec{k},\vec{q},\vec{r}_1,\vec{r}_2,\vec{r}_1,\vec{r}_1,\vec{r}_5\right)\cdot\rho^3 g^{(3)}\left(\vec{r}_1,\vec{r}_2,\vec{r}_5\right)+ \\
& +2\frac{1}{V}\int \mathrm{d}^3r_1\mathrm{d}^3r_3\mathrm{d}^3r_5\; X_{m,m_2'',m_3'}\left(\vec{k},\vec{q},\vec{r}_1,\vec{r}_1,\vec{r}_3,\vec{r}_3,\vec{r}_5\right)\cdot\rho^3 g^{(3)}\left(\vec{r}_1,\vec{r}_3,\vec{r}_5\right)+ \\
& +2\frac{1}{V}\int \mathrm{d}^3r_1\mathrm{d}^3r_3\mathrm{d}^3r_4\; X_{m,m_2'',m_3'}\left(\vec{k},\vec{q},\vec{r}_1,\vec{r}_1,\vec{r}_3,\vec{r}_4,\vec{r}_3\right)\cdot\rho^3 g^{(3)}\left(\vec{r}_1,\vec{r}_3,\vec{r}_4\right)+ \\
& +2\frac{1}{V}\int \mathrm{d}^3r_1\mathrm{d}^3r_3\mathrm{d}^3r_4\; X_{m,m_2'',m_3'}\left(\vec{k},\vec{q},\vec{r}_1,\vec{r}_1,\vec{r}_3,\vec{r}_4,\vec{r}_4\right)\cdot\rho^3 g^{(3)}\left(\vec{r}_1,\vec{r}_3,\vec{r}_4\right)+ \\
& +2\frac{1}{V}\int \mathrm{d}^3r_1\mathrm{d}^3r_2\mathrm{d}^3r_4\; X_{m,m_2'',m_3'}\left(\vec{k},\vec{q},\vec{r}_1,\vec{r}_2,\vec{r}_1,\vec{r}_4,\vec{r}_4\right)\cdot\rho^3 g^{(3)}\left(\vec{r}_1,\vec{r}_2,\vec{r}_4\right)+ \\
& +2\frac{1}{V}\int \mathrm{d}^3r_1\mathrm{d}^3r_2 X_{m,m_2'',m_3'}\left(\vec{k},\vec{q},\vec{r}_1,\vec{r}_2,\vec{r}_1,\vec{r}_1,\vec{r}_2\right)\cdot\rho^2 g^{(2)}\left(\vec{r}_1,\vec{r}_2\right) \\
& +\left\{m_2''\leftrightarrow m_3',\vec{q}\leftrightarrow\vec{k}-\vec{q}\right\} \qquad (5.64)
\end{aligned}
$$

with

$$\begin{aligned}
& X_{m,m_2'',m_3'}\left(\vec{k},\vec{q},\vec{r}_1,\vec{r}_2,\vec{r}_3,\vec{r}_4,\vec{r}_5\right) = \\
= \; & 4\frac{k_BT}{m}\cos\left(\frac{\vec{q}}{2}\left(\vec{r}_2+\vec{r}_3-\vec{r}_5-\vec{r}_1\right)+\frac{\vec{k}-\vec{q}}{2}\left(\vec{r}_3-\vec{r}_4\right)\right) \\
& \cdot\tilde{X}_{m,m_2'',m_3'}\left(\vec{k},\vec{q},\vec{r}_1,\vec{r}_2,\vec{r}_3,\vec{r}_4,\vec{r}_5\right)+ \\
& +4\frac{k_BT}{m}\sin\left(\frac{\vec{q}}{2}\left(\vec{r}_2+\vec{r}_3-\vec{r}_5-\vec{r}_1\right)+\frac{\vec{k}-\vec{q}}{2}\left(\vec{r}_3-\vec{r}_4\right)\right) \\
& \cdot\tilde{Y}_{m,m_2'',m_3'}\left(\vec{k},\vec{q},\vec{r}_1,\vec{r}_2,\vec{r}_3,\vec{r}_4,\vec{r}_5\right)
\end{aligned} \tag{5.65}$$

and

$$\begin{aligned}
& \tilde{X}_{m,m_2'',m_3'}\left(\vec{k},\vec{q},\vec{r}_1,\vec{r}_2,\vec{r}_3,\vec{r}_4,\vec{r}_5\right) = \\
= \; & \frac{k^2}{4}F_{m_3'}\left(\vec{q},\vec{r}_5-\vec{r}_1\right)F_m^*\left(\vec{k},\vec{r}_3-\vec{r}_2\right)F_{m_2''}\left(\vec{k}-\vec{q},\vec{r}_4-\vec{r}_2\right)+ \\
& +F_{m_3'}\left(\vec{q},\vec{r}_5-\vec{r}_1\right)\vec{\nabla}_r F_m^*\left(\vec{k},\vec{r}\right)\Big|_{\vec{r}=\vec{r}_3-\vec{r}_2}\cdot\vec{\nabla}_{r'}F_{m_2''}\left(\vec{k}-\vec{q},\vec{r}'\right)\Big|_{\vec{r}'=\vec{r}_4-\vec{r}_2}
\end{aligned} \tag{5.66}$$

and

$$\begin{aligned}
& \tilde{Y}_{m,m_2'',m_3'}\left(\vec{k},\vec{q},\vec{r}_1,\vec{r}_2,\vec{r}_3,\vec{r}_4,\vec{r}_5\right) = \\
= \; & -F_{m_3'}\left(\vec{q},\vec{r}_5-\vec{r}_1\right)\frac{\vec{k}}{2}\cdot\vec{\nabla}_r F_m^*\left(\vec{k},\vec{r}\right)\Big|_{\vec{r}=\vec{r}_3-\vec{r}_2}\cdot F_{m_2''}\left(\vec{k}-\vec{q},\vec{r}'\right)\Big|_{\vec{r}'=\vec{r}_4-\vec{r}_2} \\
& +F_{m_3'}\left(\vec{q},\vec{r}_5-\vec{r}_1\right)F_m^*\left(\vec{k},\vec{r}\right)\Big|_{\vec{r}=\vec{r}_3-\vec{r}_2}\cdot\frac{\vec{k}}{2}\cdot\vec{\nabla}_{r'}F_{m_2''}\left(\vec{k}-\vec{q},\vec{r}'\right)\Big|_{\vec{r}'=\vec{r}_4-\vec{r}_2}
\end{aligned} \tag{5.67}$$

where $\tilde{X}$ and $\tilde{Y}$ have the symmetry

$$\begin{aligned}
\tilde{X}_{m,m_2'',m_3'}\left(\vec{k},\vec{q},\vec{r}_1,\vec{r}_2,\vec{r}_3,\vec{r}_4,\vec{r}_5\right) &= \tilde{X}_{m,m_2'',m_3'}\left(\vec{k},\vec{q},-\vec{r}_1,-\vec{r}_2,-\vec{r}_3,-\vec{r}_4,-\vec{r}_5\right) \\
\tilde{Y}_{m,m_2'',m_3'}\left(\vec{k},\vec{q},\vec{r}_1,\vec{r}_2,\vec{r}_3,\vec{r}_4,\vec{r}_5\right) &= -\tilde{Y}_{m,m_2'',m_3'}\left(\vec{k},\vec{q},-\vec{r}_1,-\vec{r}_2,-\vec{r}_3,-\vec{r}_4,-\vec{r}_5\right).
\end{aligned}$$

Eq. (5.52) can finally be written with Eq. (5.59) as

$$
\begin{aligned}
& V^2_{m,m_2'',m_3'}\left(\vec{k},\vec{q}\right) = \\
= \; & \frac{\ddot{\phi}_m\left(\vec{k},t=0\right)}{\phi_m\left(\vec{k},t=0\right)}\frac{1}{V}\int \mathrm{d}^3r_1\mathrm{d}^3r_2\mathrm{d}^3r_3\mathrm{d}^3r_4\mathrm{d}^3r_5\mathrm{d}^3r_6 \; e^{i\frac{\vec{q}}{2}(\vec{r}_1+\vec{r}_2-\vec{r}_5-\vec{r}_6)}e^{i\frac{\vec{k}-\vec{q}}{2}(\vec{r}_1+\vec{r}_2-\vec{r}_3-\vec{r}_4)} \cdot \\
& \cdot F^*_m\left(\vec{k},\vec{r}_1-\vec{r}_2\right)F_{m_2''}\left(\vec{k}-\vec{q},\vec{r}_3-\vec{r}_4\right)F_{m_3'}\left(\vec{q},\vec{r}_5-\vec{r}_6\right) \\
& \cdot \left\langle \rho\left(\vec{r}_1\right)\rho\left(\vec{r}_2\right)\rho\left(\vec{r}_3\right)\rho\left(\vec{r}_4\right)\rho\left(\vec{r}_5\right)\rho\left(\vec{r}_6\right)\right\rangle \\
= \; & \frac{\ddot{\phi}_m\left(\vec{k},t=0\right)}{\phi_m\left(\vec{k},t=0\right)}\frac{1}{V}\int \mathrm{d}^3r_1\mathrm{d}^3r_2\mathrm{d}^3r_3\mathrm{d}^3r_4\mathrm{d}^3r_5\mathrm{d}^3r_6 \\
& \cdot \cos\left(\frac{\vec{q}}{2}\left(\vec{r}_1+\vec{r}_2-\vec{r}_5-\vec{r}_6\right)+\frac{\vec{k}-\vec{q}}{2}\left(\vec{r}_1+\vec{r}_2-\vec{r}_3-\vec{r}_4\right)\right)\cdot \\
& \cdot F^*_m\left(\vec{k},\vec{r}_1-\vec{r}_2\right)F_{m_2''}\left(\vec{k}-\vec{q},\vec{r}_3-\vec{r}_4\right)F_{m_3'}\left(\vec{q},\vec{r}_5-\vec{r}_6\right) \\
& \cdot \left\langle \rho\left(\vec{r}_1\right)\rho\left(\vec{r}_2\right)\rho\left(\vec{r}_3\right)\rho\left(\vec{r}_4\right)\rho\left(\vec{r}_5\right)\rho\left(\vec{r}_6\right)\right\rangle
\end{aligned}
\tag{5.68}
$$

which finally reads

$$
V^2_{m,m_2'',m_3'}\left(\vec{k},\vec{q}\right) = \frac{1}{2}\left(\tilde{V}^2_{m,m_2'',m_3'}\left(\vec{k},\vec{q}\right)+\tilde{V}^2_{m,m_3',m_2''}\left(\vec{k},\vec{k}-\vec{q}\right)\right) \tag{5.69}
$$

with

$$
\begin{aligned}
& \frac{\tilde{V}^2_{m,m_2'',m_3'}\left(\vec{k},\vec{q}\right)}{\frac{\ddot{\phi}_m\left(\vec{k},t=0\right)}{\phi_m\left(\vec{k},t=0\right)}} = \\
= \; & \frac{1}{V}\int \mathrm{d}^3r_1\mathrm{d}^3r_2\mathrm{d}^3r_3\mathrm{d}^3r_4\mathrm{d}^3r_5\mathrm{d}^3r_6 \; \cos\left(\frac{\vec{q}}{2}\left(\vec{r}_1+\vec{r}_2-\vec{r}_5-\vec{r}_6\right)+\frac{\vec{k}-\vec{q}}{2}\left(\vec{r}_1+\vec{r}_2-\vec{r}_3-\vec{r}_4\right)\right)\cdot \\
& \cdot F^*_m\left(\vec{k},\vec{r}_1-\vec{r}_2\right)F_{m_2''}\left(\vec{k}-\vec{q},\vec{r}_3-\vec{r}_4\right)F_{m_3'}\left(\vec{q},\vec{r}_5-\vec{r}_6\right)\rho^6 g^{(6)}\left(\vec{r}_1,\vec{r}_2,\vec{r}_3,\vec{r}_4,\vec{r}_5,\vec{r}_6\right)+ \\
& +8\frac{1}{V}\int \mathrm{d}^3r_1\mathrm{d}^3r_2\mathrm{d}^3r_4\mathrm{d}^3r_5\mathrm{d}^3r_6 \; \cos\left(\frac{\vec{q}}{2}\left(\vec{r}_1+\vec{r}_2-\vec{r}_5-\vec{r}_6\right)+\frac{\vec{k}-\vec{q}}{2}\left(\vec{r}_2-\vec{r}_4\right)\right)\cdot \\
& \cdot F^*_m\left(\vec{k},\vec{r}_1-\vec{r}_2\right)F_{m_2''}\left(\vec{k}-\vec{q},\vec{r}_1-\vec{r}_4\right)F_{m_3'}\left(\vec{q},\vec{r}_5-\vec{r}_6\right)\rho^5 g^{(5)}\left(\vec{r}_1,\vec{r}_2,\vec{r}_4,\vec{r}_5,\vec{r}_6\right)+ \\
& +4\frac{1}{V}\int \mathrm{d}^3r_1\mathrm{d}^3r_2\mathrm{d}^3r_3\mathrm{d}^3r_4\mathrm{d}^3r_6 \; \cos\left(\frac{\vec{q}}{2}\left(\vec{r}_1+\vec{r}_2-\vec{r}_3-\vec{r}_6\right)+\frac{\vec{k}-\vec{q}}{2}\left(\vec{r}_1+\vec{r}_2-\vec{r}_3-\vec{r}_4\right)\right)\cdot \\
& \cdot F^*_m\left(\vec{k},\vec{r}_1-\vec{r}_2\right)F_{m_2''}\left(\vec{k}-\vec{q},\vec{r}_3-\vec{r}_4\right)F_{m_3'}\left(\vec{q},\vec{r}_3-\vec{r}_6\right)\rho^5 g^{(5)}\left(\vec{r}_1,\vec{r}_2,\vec{r}_3,\vec{r}_4,\vec{r}_6\right)+
\end{aligned}
$$

$$
\begin{aligned}
&+8\frac{1}{V}\int \mathrm{d}^3r_1\mathrm{d}^3r_2\mathrm{d}^3r_4\mathrm{d}^3r_6\ \cos\left(\frac{\vec{q}}{2}\left(\vec{r}_2-\vec{r}_6\right)+\frac{\vec{k}-\vec{q}}{2}\left(\vec{r}_2-\vec{r}_4\right)\right)\cdot\\
&\cdot F_m^*\left(\vec{k},\vec{r}_1-\vec{r}_2\right)F_{m_2''}\left(\vec{k}-\vec{q},\vec{r}_1-\vec{r}_4\right)F_{m_3'}\left(\vec{q},\vec{r}_1-\vec{r}_6\right)\rho^4 g^{(4)}\left(\vec{r}_1,\vec{r}_2,\vec{r}_4,\vec{r}_6\right)+\\
&+4\frac{1}{V}\int \mathrm{d}^3r_1\mathrm{d}^3r_2\mathrm{d}^3r_5\mathrm{d}^3r_6\ \cos\left(\frac{\vec{q}}{2}\left(\vec{r}_1+\vec{r}_2-\vec{r}_5-\vec{r}_6\right)\right)\cdot\\
&\cdot F_m^*\left(\vec{k},\vec{r}_1-\vec{r}_2\right)F_{m_2''}\left(\vec{k}-\vec{q},\vec{r}_1-\vec{r}_2\right)F_{m_3'}\left(\vec{q},\vec{r}_5-\vec{r}_6\right)\rho^4 g^{(4)}\left(\vec{r}_1,\vec{r}_2,\vec{r}_5,\vec{r}_6\right)+\\
&+16\frac{1}{V}\int \mathrm{d}^3r_1\mathrm{d}^3r_2\mathrm{d}^3r_4\mathrm{d}^3r_6\ \cos\left(\frac{\vec{q}}{2}\left(\vec{r}_1+\vec{r}_2-\vec{r}_4-\vec{r}_6\right)+\frac{\vec{k}-\vec{q}}{2}\left(\vec{r}_2-\vec{r}_4\right)\right)\cdot\\
&\cdot F_m^*\left(\vec{k},\vec{r}_1-\vec{r}_2\right)F_{m_2''}\left(\vec{k}-\vec{q},\vec{r}_1-\vec{r}_4\right)F_{m_3'}\left(\vec{q},\vec{r}_4-\vec{r}_6\right)\rho^4 g^{(4)}\left(\vec{r}_1,\vec{r}_2,\vec{r}_4,\vec{r}_6\right)+\\
&+2\frac{1}{V}\int \mathrm{d}^3r_1\mathrm{d}^3r_2\mathrm{d}^3r_3\mathrm{d}^3r_4\ \cos\left(\frac{\vec{k}}{2}\left(\vec{r}_1+\vec{r}_2-\vec{r}_3-\vec{r}_4\right)\right)\cdot\\
&+8\frac{1}{V}\int \mathrm{d}^3r_1\mathrm{d}^3r_2\mathrm{d}^3r_4\mathrm{d}^3r_6\ \cos\left(\frac{\vec{q}}{2}\left(\vec{r}_1-\vec{r}_6\right)+\frac{\vec{k}-\vec{q}}{2}\left(\vec{r}_2-\vec{r}_4\right)\right)\cdot\\
&\cdot F_m^*\left(\vec{k},\vec{r}_1-\vec{r}_2\right)F_{m_2''}\left(\vec{k}-\vec{q},\vec{r}_1-\vec{r}_4\right)F_{m_3'}\left(\vec{q},\vec{r}_2-\vec{r}_6\right)\rho^4 g^{(4)}\left(\vec{r}_1,\vec{r}_2,\vec{r}_4,\vec{r}_6\right)+\\
&+8\frac{1}{V}\int \mathrm{d}^3r_1\mathrm{d}^3r_2\mathrm{d}^3r_4\mathrm{d}^3r_6\ \cos\left(\frac{\vec{q}}{2}\left(\vec{r}_1-\vec{r}_6\right)+\frac{\vec{k}-\vec{q}}{2}\left(\vec{r}_2-\vec{r}_4\right)\right)\cdot\\
&\cdot F_m^*\left(\vec{k},\vec{r}_1-\vec{r}_2\right)F_{m_2''}\left(\vec{k}-\vec{q},\vec{r}_1-\vec{r}_4\right)F_{m_3'}\left(\vec{q},\vec{r}_2-\vec{r}_6\right)\rho^4 g^{(4)}\left(\vec{r}_1,\vec{r}_2,\vec{r}_4,\vec{r}_6\right)+\\
&+8\frac{1}{V}\int \mathrm{d}^3r_1\mathrm{d}^3r_2\mathrm{d}^3r_4\ \cos\left(\frac{\vec{q}}{2}\left(\vec{r}_1-\vec{r}_4\right)+\frac{\vec{k}-\vec{q}}{2}\left(\vec{r}_2-\vec{r}_4\right)\right)\cdot\\
&\cdot F_m^*\left(\vec{k},\vec{r}_1-\vec{r}_2\right)F_{m_2''}\left(\vec{k}-\vec{q},\vec{r}_1-\vec{r}_4\right)F_{m_3'}\left(\vec{q},\vec{r}_2-\vec{r}_4\right)\rho^3 g^{(3)}\left(\vec{r}_1,\vec{r}_2,\vec{r}_4\right)+\\
&+16\frac{1}{V}\int \mathrm{d}^3r_1\mathrm{d}^3r_2\mathrm{d}^3r_6\ \cos\left(\frac{\vec{q}}{2}\left(\vec{r}_2-\vec{r}_6\right)\right)\cdot\\
&\cdot F_m^*\left(\vec{k},\vec{r}_1-\vec{r}_2\right)F_{m_2''}\left(\vec{k}-\vec{q},\vec{r}_1-\vec{r}_2\right)F_{m_3'}\left(\vec{q},\vec{r}_1-\vec{r}_6\right)\rho^3 g^{(3)}\left(\vec{r}_1,\vec{r}_2,\vec{r}_6\right)+\\
&+8\frac{1}{V}\int \mathrm{d}^3r_1\mathrm{d}^3r_2\mathrm{d}^3r_4\ \cos\left(\frac{\vec{k}}{2}\left(\vec{r}_2-\vec{r}_4\right)\right)\cdot\\
&\cdot F_m^*\left(\vec{k},\vec{r}_1-\vec{r}_2\right)F_{m_2''}\left(\vec{k}-\vec{q},\vec{r}_1-\vec{r}_4\right)F_{m_3'}\left(\vec{q},\vec{r}_1-\vec{r}_4\right)\rho^3 g^{(3)}\left(\vec{r}_1,\vec{r}_2,\vec{r}_4\right)+\\
&+4\frac{1}{V}\int \mathrm{d}^3r_1\mathrm{d}^3r_2\cdot F_{m_1}^*\left(\vec{k},\vec{r}_1-\vec{r}_2\right)F_{m_2''}\left(\vec{k}-\vec{q},\vec{r}_1-\vec{r}_2\right)F_{m_3'}\left(\vec{q},\vec{r}_1-\vec{r}_2\right)\\
&\cdot\rho^2 g^{(2)}\left(\vec{r}_1,\vec{r}_2\right)
\end{aligned}
\tag{5.70}
$$

The standard spherical tensors are complex quantities. Because we prefer to use real quantities, we use the following linear combinations

$$\begin{aligned}\sigma_{\hat{0}}\left(\vec{k}\right) &= \sigma_0\left(\vec{k}\right) \\ &= \frac{1}{\sqrt{2}}\left(\sigma_{xx}\left(\vec{k}\right)+\sigma_{yy}\left(\vec{k}\right)\right) \end{aligned} \tag{5.71}$$

$$\begin{aligned}\sigma_{\hat{1}}\left(\vec{k}\right) &= \frac{i}{\sqrt{2}}\left(\sigma_1\left(\vec{k}\right)+\sigma_{-1}\left(\vec{k}\right)\right) \\ &= \frac{1}{\sqrt{2}}\left(\sigma_{yz}\left(\vec{k}\right)+\sigma_{zy}\left(\vec{k}\right)\right) \end{aligned} \tag{5.72}$$

$$\begin{aligned}\sigma_{-\hat{1}}\left(\vec{k}\right) &= \frac{1}{\sqrt{2}}\left(-\sigma_1\left(\vec{k}\right)+\sigma_{-1}\left(\vec{k}\right)\right) \\ &= \frac{1}{\sqrt{2}}\left(\sigma_{zx}\left(\vec{k}\right)+\sigma_{xz}\left(\vec{k}\right)\right) \end{aligned} \tag{5.73}$$

$$\begin{aligned}\sigma_{\hat{2}}\left(\vec{k}\right) &= \frac{1}{\sqrt{2}}\left(\sigma_2\left(\vec{k}\right)+\sigma_{-2}\left(\vec{k}\right)\right) \\ &= \frac{1}{\sqrt{2}}\left(\sigma_{xx}\left(\vec{k}\right)-\sigma_{yy}\left(\vec{k}\right)\right) \end{aligned} \tag{5.74}$$

$$\begin{aligned}\sigma_{-\hat{2}}\left(\vec{k}\right) &= \frac{1}{\sqrt{2}i}\left(\sigma_2\left(\vec{k}\right)-\sigma_{-2}\left(\vec{k}\right)\right) \\ &= \frac{1}{\sqrt{2}}\left(\sigma_{xy}\left(\vec{k}\right)+\sigma_{yx}\left(\vec{k}\right)\right). \end{aligned} \tag{5.75}$$

and similar relations for a coordinate system with a prime or a double prime. It can be seen easily, that they represent a complete orthonormal system again. Additionally, it can be shown that with these new linear combinations it is valid

$$\begin{aligned}&\left\langle \sigma_{\hat{m}}\left(\vec{k}\right)\middle| A \middle|\sigma_{\hat{m}}\left(\vec{k}\right)\right\rangle = \left\langle \sigma_{-\hat{m}}\left(\vec{k}\right)\middle| A \middle|\sigma_{-\hat{m}}\left(\vec{k}\right)\right\rangle = \\ = \;&\left\langle \sigma_{m}\left(\vec{k}\right)\middle| A \middle|\sigma_{m}\left(\vec{k}\right)\right\rangle = \left\langle \sigma_{-m}\left(\vec{k}\right)\middle| A \middle|\sigma_{-m}\left(\vec{k}\right)\right\rangle \end{aligned} \tag{5.76}$$

where A may be any operator with full spherical symmetry and thus

$$\phi_{\hat{m}}\left(\vec{k},t\right) = \phi_{-\hat{m}}\left(\vec{k},t\right) = \phi_{m}\left(\vec{k},t\right) = \phi_{-m}\left(\vec{k},t\right). \tag{5.77}$$

This means that all the previous equations still remain valid with the spherical indices m replaced by $\hat{m}$. We now want to evaluate the terms explicitly. In order to do this we need an explicit representation of the coordinate systems described in Eqs. (5.3), (5.4) and (5.5). If we now choose without loss of generality

$$\vec{e}_x = \begin{pmatrix} 1 \\ 0 \\ 0 \end{pmatrix}, \quad \vec{e}_y = \begin{pmatrix} 0 \\ 1 \\ 0 \end{pmatrix}, \quad \vec{e}_z = \begin{pmatrix} 0 \\ 0 \\ 1 \end{pmatrix} \tag{5.78}$$

we obtain from Eqs. (5.3) and (5.4)

$$\vec{k} = \begin{pmatrix} 0 \\ 0 \\ k \end{pmatrix}, \quad \vec{q} = \begin{pmatrix} 0 \\ q_y \\ q_z \end{pmatrix}, \quad \vec{k} - \vec{q} = \begin{pmatrix} 0 \\ -q_y \\ k - q_z \end{pmatrix} \tag{5.79}$$

and thus from Eqs. (5.3), (5.4) and (5.5)

$$\vec{e}_{x'} = \begin{pmatrix} 1 \\ 0 \\ 0 \end{pmatrix}, \quad \vec{e}_{y'} = \frac{1}{|\vec{q}|} \begin{pmatrix} 0 \\ q_z \\ -q_y \end{pmatrix}, \quad \vec{e}_{z'} = \frac{1}{|\vec{q}|} \begin{pmatrix} 0 \\ q_y \\ q_z \end{pmatrix} \tag{5.80}$$

$$\vec{e}_{x''} = \begin{pmatrix} 1 \\ 0 \\ 0 \end{pmatrix}, \quad \vec{e}_{y''} = \frac{1}{|\vec{k} - \vec{q}|} \begin{pmatrix} 0 \\ k - q_z \\ q_y \end{pmatrix}, \quad \vec{e}_{z''} = \frac{1}{|\vec{k} - \vec{q}|} \begin{pmatrix} 0 \\ -q_y \\ k - q_z \end{pmatrix}. \tag{5.81}$$

We now want to evaluate $F_{\hat{m}}\left(\vec{k}, \vec{r}\right)$, $F_{\hat{m}'}\left(\vec{q}, \vec{r}\right)$ and $F_{\hat{m}''}\left(\vec{k} - \vec{q}, \vec{r}\right)$ which is required for Eqs. (5.61), (5.63), (5.66), (5.67) and (5.70). In a Cartesian representation they can be written as

$$\begin{aligned} F_{ij}\left(\vec{k}, \vec{r}\right) &= \frac{r_i r_j}{r} \frac{\partial u\left(r\right)}{\partial r} \frac{\sin\left(\frac{\vec{k}\cdot\vec{r}}{2}\right)}{\vec{k}\cdot\vec{r}} \\ F_{i'j'}\left(\vec{q}, \vec{r}\right) &= \frac{r_{i'} r_{j'}}{r} \frac{\partial u\left(r\right)}{\partial r} \frac{\sin\left(\frac{\vec{q}\cdot\vec{r}}{2}\right)}{\vec{k}\cdot\vec{r}} \\ F_{i''j''}\left(\vec{k} - \vec{q}, \vec{r}\right) &= \frac{r_{i''} r_{j''}}{r} \frac{\partial u\left(r\right)}{\partial r} \frac{\sin\left(\frac{(\vec{k}-\vec{q})\cdot\vec{r}}{2}\right)}{\left(\vec{k} - \vec{q}\right)\cdot\vec{r}} \end{aligned} \tag{5.82}$$

where $r_{i'}$ and $r_{i''}$ can be evaluated as

$$\begin{aligned} r_{i'} &= \vec{r} \cdot \vec{e}_{i'} = \sum_j r_j \left(\vec{e}_{i'}\right)_j \\ r_{i''} &= \vec{r} \cdot \vec{e}_{i''} = \sum_j r_j \left(\vec{e}_{i''}\right)_j \end{aligned} \tag{5.83}$$

We then have for the respective linear combinations, which are required for the terms in spherical coordinates

$$\begin{aligned} \left(r_i r_j\right)_{\tilde{m}=0} &= \frac{1}{\sqrt{2}} \left(r_x r_x + \left(\frac{r_y p_z - r_z p_y}{|\vec{p}|} \right)^2 \right) \\ \left(r_i r_j\right)_{\tilde{m}=1} &= \frac{\sqrt{2} \left(r_y p_z - r_z p_y\right) \left(p_y r_y + p_z r_z\right)}{|\vec{p}|^2} \\ \left(r_i r_j\right)_{\tilde{m}=-1} &= \frac{\sqrt{2} \left(p_y r_y + p_z r_z\right) r_x}{|\vec{p}|} \\ \left(r_i r_j\right)_{\tilde{m}=2} &= \frac{1}{\sqrt{2}} \left(r_x r_x - \left(\frac{r_y p_z - r_z p_y}{|\vec{p}|} \right)^2 \right) \\ \left(r_i r_j\right)_{\tilde{m}=-2} &= \frac{\sqrt{2} \left(r_y p_z - r_z p_y\right) r_x}{|\vec{p}|} \end{aligned} \tag{5.84}$$

where we have to choose for $\tilde{m} = \hat{m}$: $\vec{p} = \vec{k}$, for $\tilde{m} = \hat{m}'$: $\vec{p} = \vec{q}$ and for $\tilde{m} = \hat{m}''$: $\vec{p} = \vec{k} - \vec{q}$. For the evaluation of Eqs. (5.63), (5.66) and (5.67) we require additionally $\partial_s F_{\hat{m}} \left(\vec{k}, \vec{r}\right)$, $\partial_s F_{\hat{m}'} \left(\vec{q}, \vec{r}\right)$ and $\partial_s F_{\hat{m}''} \left(\vec{k} - \vec{q}, \vec{r}\right)$. In a Cartesian representation this can again be written as

$$\begin{aligned} &\partial_s F_{ij} \left(\vec{k}, \vec{r}\right) = \\ = \; & \frac{\delta_{is} r_j + \delta_{sj} r_i}{r} \frac{\partial u\left(r\right)}{\partial r} \frac{\sin\left(\frac{\vec{k}\cdot\vec{r}}{2}\right)}{\vec{k}\cdot\vec{r}} \\ & + \frac{r_i r_j}{r} \left(\frac{r_s}{r} \frac{\sin\left(\frac{\vec{k}\cdot\vec{r}}{2}\right)}{\vec{k}\cdot\vec{r}} \left(\frac{\partial^2 u\left(r\right)}{\partial r^2} - \frac{1}{r} \frac{\partial u\left(r\right)}{\partial r} \right) \right. \\ & \left. + \frac{k_s}{\vec{k}\cdot\vec{r}} \frac{\partial u\left(r\right)}{\partial r} \left(\frac{1}{2} \cos\left(\frac{\vec{k}\cdot\vec{r}}{2} \right) - \frac{\sin\left(\frac{\vec{k}\cdot\vec{r}}{2}\right)}{\vec{k}\cdot\vec{r}} \right) \right) \end{aligned} \tag{5.85}$$

and similar equations for $\partial_s F_{i'j'} \left(\vec{q}, \vec{r}\right)$ and $\partial_s F_{i''j''} \left(\vec{k} - \vec{q}, \vec{r}\right)$. If we now define the

following base vectors as

$$\vec{e}_x\left(\vec{p}\right) = \begin{pmatrix} 1 \\ 0 \\ 0 \end{pmatrix}, \quad \vec{e}_y\left(\vec{p}\right) = \frac{1}{|\vec{p}|}\begin{pmatrix} 0 \\ p_z \\ -p_y \end{pmatrix}, \quad \vec{e}_z\left(\vec{p}\right) = \frac{1}{|\vec{p}|}\begin{pmatrix} 0 \\ p_y \\ p_z \end{pmatrix} \tag{5.86}$$

we can rewrite the terms required in 5.85 as spherical tensors

$$\begin{aligned}
\left(\delta_{is}r_j + \delta_{sj}r_i\right)_{\tilde{m}=0} &= \sqrt{2}\left(\left(\vec{e}_x\left(\vec{p}\right)\right)_s r_x + \left(\vec{e}_y\left(\vec{p}\right)\right)_s \frac{p_z r_y - p_y r_z}{|\vec{p}|}\right) \\
\left(\delta_{is}r_j + \delta_{sj}r_i\right)_{\tilde{m}=1} &= \sqrt{2}\left(\left(\vec{e}_y\left(\vec{p}\right)\right)_s \frac{p_y r_y + p_z r_z}{|\vec{p}|} + \left(\vec{e}_z\left(\vec{p}\right)\right)_s \frac{p_z r_y - p_y r_z}{|\vec{p}|}\right) \\
\left(\delta_{is}r_j + \delta_{sj}r_i\right)_{\tilde{m}=-1} &= \sqrt{2}\left(\left(\vec{e}_x\left(\vec{p}\right)\right)_s \frac{p_y r_y + p_z r_z}{|\vec{p}|} + \left(\vec{e}_z\left(\vec{p}\right)\right)_s r_x\right) \\
\left(\delta_{is}r_j + \delta_{sj}r_i\right)_{\tilde{m}=2} &= \sqrt{2}\left(\left(\vec{e}_x\left(\vec{p}\right)\right)_s r_x - \left(\vec{e}_y\left(\vec{p}\right)\right)_s \frac{p_z r_y - p_y r_z}{|\vec{p}|}\right) \\
\left(\delta_{is}r_j + \delta_{sj}r_i\right)_{\tilde{m}=-2} &= \sqrt{2}\left(\left(\vec{e}_x\left(\vec{p}\right)\right)_s \frac{p_z r_y - p_y r_z}{|\vec{p}|} + \left(\vec{e}_y\left(\vec{p}\right)\right)_s r_x\right)
\end{aligned} \tag{5.87}$$

where we again have to choose for $\tilde{m} = \hat{m}$: $\vec{p} = \vec{k}$, for $\tilde{m} = \hat{m}'$: $\vec{p} = \vec{q}$ and for $\tilde{m} = \hat{m}''$: $\vec{p} = \vec{k} - \vec{q}$.

5.3.2 Low-density approximation

Unfortunately we cannot evaluate Eqs. (5.38)–(5.40), because they also require multipoint distribution functions such as $g^{(5)}(\vec{r}_1, \vec{r}_2, \vec{r}_3, \vec{r}_4, \vec{r}_5)$ and $g^{(6)}(\vec{r}_1, \vec{r}_2, \vec{r}_3, \vec{r}_4, \vec{r}_5, \vec{r}_6)$, which cannot be evaluated easily. We thus apply a low density approximation, i.e. $\rho \to 0$, which means that the higher order distribution functions can be neglected because they have a higher power of the density as a prefactor. This approximation is probably not really valid, because the glass transition is not a low density phenomenon. However, we still apply it because we do not see any other way to really evaluate the multipoint distribution functions. In this approximation the equations can be summarized as follows:

$$\hat{\phi}_{\hat{m}}\left(\vec{k}, z\right) = -\frac{\phi_{\hat{m}}\left(\vec{k}, 0\right)}{z + \frac{\ddot{\phi}_{\hat{m}}\left(\vec{k},0\right)/\phi_{\hat{m}}\left(\vec{k},0\right)}{z + \tilde{M}_{\hat{m}}\left(\vec{k},z\right)}} \tag{5.88}$$

or respectively in time space

$$\frac{\partial^2}{\partial t^2}\phi_{\hat{m}}\left(\vec{k},t\right)-\frac{\ddot{\phi}_{\hat{m}}\left(\vec{k},0\right)}{\phi_{\hat{m}}\left(\vec{k},0\right)}\phi_{\hat{m}}\left(\vec{k},t\right)+\int_0^t \mathrm{d}t'\tilde{M}_{\hat{m}}\left(\vec{k},t-t'\right)\dot{\phi}_{\hat{m}}\left(\vec{k},t'\right)=0 \tag{5.89}$$

with

$$\tilde{M}_{\hat{m}}\left(\vec{k},t\right)=\frac{1}{V}\sum_{\vec{q},\hat{m}_2'',\hat{m}_3'}\mathcal{V}_{\hat{m},\hat{m}_2'',\hat{m}_3'}\left(\vec{k},\vec{q}\right)\cdot\phi_{\hat{m}_2''}\left(\vec{k}-\vec{q},t\right)\phi_{\hat{m}_3'}\left(\vec{q},t\right) \tag{5.90}$$

with

$$\mathcal{V}_{\hat{m},\hat{m}_2'',\hat{m}_3'}\left(\vec{k},\vec{q}\right)=-\frac{1}{2\ddot{\phi}_{\hat{m}}\left(\vec{k},t=0\right)}\left|\frac{V_{\hat{m},\hat{m}_2'',\hat{m}_3'}\left(\vec{k},\vec{q}\right)}{\phi_{\hat{m}_2''}\left(\vec{k}-\vec{q},t=0\right)\phi_{\hat{m}_3'}\left(\vec{q},t=0\right)}\right|^2. \tag{5.91}$$

where

$$\begin{aligned}&\phi_{\hat{m}}\left(\vec{k},t=0\right)=\\ =\;&\frac{1}{V}\left\langle\sigma_{\hat{m}}\left(\vec{k}\right)|\sigma_{\hat{m}}\left(\vec{k}\right)\right\rangle\\ =\;&2\int\mathrm{d}^3r\;F_{\hat{m}}^*\left(\vec{k},\vec{r}\right)F_{\hat{m}}\left(\vec{k},\vec{r}\right)\rho^2g^{(2)}\left(\vec{r}\right)\end{aligned} \tag{5.92}$$

and

$$\begin{aligned}&\ddot{\phi}_{\hat{m}}\left(\vec{k},t=0\right)=\\ =\;&-\frac{1}{V}\left\langle\sigma_{\hat{m}}\left(\vec{k}\right)\middle|\,\mathcal{L}^2\left|\sigma_{\hat{m}}\left(\vec{k}\right)\right.\right\rangle\\ =\;&-4\frac{k_BT}{m}\int\mathrm{d}^3r\;Y_{\hat{m}}\left(\vec{k},\vec{r}\right)\rho^2g^{(2)}\left(\vec{r}\right)\end{aligned} \tag{5.93}$$

with

$$\begin{aligned}Y_{\hat{m}}\left(\vec{k},\vec{r}\right)\;=\;&\vec{\nabla}_rF_{\hat{m}}^*\left(\vec{k},\vec{r}\right)\cdot\vec{\nabla}_rF_{\hat{m}}\left(\vec{k},\vec{r}\right)\\ &+\frac{k^2}{4}F_{\hat{m}}^*\left(\vec{k},\vec{r}\right)F_{\hat{m}}\left(\vec{k},\vec{r}\right)\end{aligned} \tag{5.94}$$

and

$$V_{\hat{m},\hat{m}_2'',\hat{m}_3'}\left(\vec{k},\vec{q}\right)=V^1_{\hat{m},\hat{m}_2'',\hat{m}_3'}\left(\vec{k},\vec{q}\right)-V^2_{\hat{m},\hat{m}_2'',\hat{m}_3'}\left(\vec{k},\vec{q}\right) \tag{5.95}$$

$$V^1_{\hat{m}_1\hat{m}''_2\hat{m}'_3}\left(\vec{k},\vec{q}\right) = 8\frac{k_BT}{m}\int \mathrm{d}^3r\ \tilde{X}_{\hat{m}_1\hat{m}''_2\hat{m}'_3}\left(\vec{k},\vec{q},\vec{r}\right)\cdot\rho^2 g^{(2)}\left(\vec{r}\right) + \\ +8\frac{k_BT}{m}\int \mathrm{d}^3r\ \tilde{X}_{\hat{m}_1\hat{m}'_3\hat{m}''_2}\left(\vec{k},\vec{k}-\vec{q},\vec{r}\right)\cdot\rho^2 g^{(2)}\left(\vec{r}\right) \quad (5.96)$$

with

$$\tilde{X}_{\hat{m}_1\hat{m}''_2\hat{m}'_3}\left(\vec{k},\vec{q},\vec{r}\right) = \frac{k^2}{4}F_{\hat{m}'_3}\left(\vec{q},\vec{r}\right)F^*_{\hat{m}_1}\left(\vec{k},\vec{r}\right)F_{\hat{m}''_2}\left(\vec{k}-\vec{q},\vec{r}\right) + \\ +F_{\hat{m}'_3}\left(\vec{q},\vec{r}\right)\vec{\nabla}_r F^*_{\hat{m}_1}\left(\vec{k},\vec{r}\right)\cdot\vec{\nabla}_r F_{\hat{m}''_2}\left(\vec{k}-\vec{q},\vec{r}\right) \quad (5.97)$$

and

$$V^2_{\hat{m}_1\hat{m}''_2\hat{m}'_3}\left(\vec{k},\vec{q}\right) = \\ = 2\frac{\ddot{\phi}_{\hat{m}_1}\left(\vec{k},t=0\right)}{\phi_{\hat{m}_1}\left(\vec{k},t=0\right)}\int \mathrm{d}^3r\cdot F^*_{\hat{m}_1}\left(\vec{k},\vec{r}\right)F_{\hat{m}''_2}\left(\vec{k}-\vec{q},\vec{r}\right)F_{\hat{m}'_3}\left(\vec{q},\vec{r}\right)\rho^2 g^{(2)}\left(\vec{r}\right) + \\ +\left\{\hat{m}''_2\leftrightarrow\hat{m}'_3,\vec{q}\leftrightarrow\vec{k}-\vec{q}\right\}. \quad (5.98)$$

This can be transformed into bipolar coordinates (cf. section 3.1.3) as

$$\tilde{M}_{\hat{m}}\left(k,t\right) = \frac{1}{\left(2\pi\right)^2}\int_0^\infty \mathrm{d}p\int_{|k-p|}^{k+p}\mathrm{d}q\sum_{\hat{m}_2,\hat{m}_3}\frac{p\ q}{k}\tilde{\mathcal{V}}_{\hat{m},\hat{m}_2,\hat{m}_3}\left(k,p,q\right)\cdot\tilde{\phi}_{\hat{m}_2}\left(p,t\right)\tilde{\phi}_{\hat{m}_3}\left(q,t\right) \quad (5.99)$$

with

$$\tilde{\mathcal{V}}_{\hat{m},\hat{m}_2,\hat{m}_3}\left(k,p,q\right) = \mathcal{V}_{\hat{m},\hat{m}''_2,\hat{m}'_3}\left(k\ \vec{e}_z, q\cos\vartheta\ \vec{e}_z + q\sin\vartheta\ \vec{e}_y\right) \quad (5.100)$$

and

$$\cos\vartheta = \frac{k^2+q^2-p^2}{2kq} \quad (5.101)$$

$$\sin\vartheta = \sqrt{1-\cos^2\vartheta} \quad (5.102)$$

and

$$\tilde{\phi}_{\hat{m}}\left(k,t\right) = \phi_{\hat{m}}\left(k\ \vec{e}_z,t\right). \quad (5.103)$$

Unfortunately the computing time required to solve these equations is still too large to find for example the point of the liquid-glass transition. This is due to the fact, that in the normal MCT the vertex is just a simple algebraic expression (cf. Eq. (3.37)), while in the theory with stress tensors the vertex still contains a three-dimensional

integral (Eqs. (5.96) and (5.98)). This can be reduced similarly to Eq. (4.18) to a two-dimensional integral. Additionally, the integrand in Eqs. (5.96) and (5.98) contains terms of the form $\sin\left(\frac{\vec{k}\cdot\vec{r}}{2}\right)/\vec{k}\cdot\vec{r}$ (cf. Eq. (5.82)), which oscillates very fast if $|\vec{k}|$ is large. This requires a lot of computing time, because this integral has to be evaluated for every $\hat{m}$, $\hat{m}_2$, $\hat{m}_3$, k, p and q.

5.4 Summary and conclusions

We have derived the mode-coupling equations for the correlation functions of the spherical components of the stress tensor. They have the same structure as the standard MCT equations for the correlation functions of the density. They are thus expected to have the same possibility of showing a glass transition singularity. The memory function contains the derivative of the pair potential and higher order distribution functions such as $g^{(n)}(\vec{r}_1, ..., \vec{r}_n)$ with $n = 1, ..., 6$, which are required as input. Unfortunately it turned out that even with the questionable approximation of neglecting all higher order distribution functions with $n > 2$, the equations are still too complex to be solved numerically.

A Appendix

A.1 Rewriting of the stress tensor

The stress tensor from Eq. (5.2) can be rewritten as

$$
\begin{aligned}
\sigma_{ij}\left(\vec{k}\right) &= \sum_n \frac{1}{2} \sum_{m \neq n} \frac{\left(r_i^m - r_i^n\right)\left(r_j^m - r_j^n\right)}{|\vec{r}^m - \vec{r}^n|} \left.\frac{\partial u\left(r\right)}{\partial r}\right|_{r=|\vec{r}^n - \vec{r}^m|} \frac{e^{-i\vec{k}(\vec{r}^m - \vec{r}^n)} - 1}{i\vec{k}\cdot\left(\vec{r}_m - \vec{r}_n\right)} e^{-i\vec{k}\vec{r}^n} \\
&= \sum_n \sum_{m \neq n} \int \mathrm{d}^3 r \; \delta\left(\vec{r} + \vec{r}^n - \vec{r}^m\right) \frac{r_i r_j}{r} \frac{\partial u\left(r\right)}{\partial r} \frac{e^{-i\vec{k}\vec{r}} - 1}{2i\vec{k}\cdot\vec{r}} e^{-i\vec{k}\vec{r}^n} \\
&= \sum_n \sum_{m \neq n} \frac{1}{\left(2\pi\right)^3} \int \mathrm{d}^3 r \int \mathrm{d}^3 q \; e^{i\left(\frac{\vec{k}}{2} + \vec{q}\right)\left(\vec{r} + \vec{r}^n - \vec{r}^m\right)} \frac{r_i r_j}{r} \frac{\partial u\left(r\right)}{\partial r} \frac{e^{-i\vec{k}\vec{r}} - 1}{2i\vec{k}\cdot\vec{r}} e^{-i\vec{k}\vec{r}^n} \\
&= \sum_n \sum_{m \neq n} \frac{1}{\left(2\pi\right)^3} \int \mathrm{d}^3 q \; e^{-i\left(\frac{\vec{k}}{2} - \vec{q}\right)\vec{r}^n} e^{-i\left(\frac{\vec{k}}{2} + \vec{q}\right)\vec{r}^m} \\
&\quad \cdot \left(\int \mathrm{d}^3 r \; e^{-i\vec{q}\vec{r}} \frac{r_i r_j}{r} \frac{\partial u\left(r\right)}{\partial r} \frac{e^{-i\frac{\vec{k}}{2}\vec{r}} - e^{i\frac{\vec{k}}{2}\vec{r}}}{2i\vec{k}\cdot\vec{r}} \right) \\
&= \sum_n \sum_{m \neq n} \frac{1}{\left(2\pi\right)^3} \int \mathrm{d}^3 q \; e^{-i\left(\frac{\vec{k}}{2} - \vec{q}\right)\vec{r}^n} e^{-i\left(\frac{\vec{k}}{2} + \vec{q}\right)\vec{r}^m} F_{ij}\left(\vec{k}, \vec{q}\right) \\
&= \sum_{n,m} \frac{1}{\left(2\pi\right)^3} \int \mathrm{d}^3 q \; e^{-i\left(\frac{\vec{k}}{2} - \vec{q}\right)\vec{r}^n} e^{-i\left(\frac{\vec{k}}{2} + \vec{q}\right)\vec{r}^m} F_{ij}\left(\vec{k}, \vec{q}\right) \\
&\quad - \sum_n \frac{1}{\left(2\pi\right)^3} \int \mathrm{d}^3 q e^{-i\vec{k}\vec{r}^n} F_{ij}\left(\vec{k}, \vec{q}\right)
\end{aligned}
$$

$$
\begin{aligned}
&= \frac{1}{(2\pi)^3}\int \mathrm{d}^3q\rho\left(\frac{\vec{k}}{2}-\vec{q}\right)\rho\left(\frac{\vec{k}}{2}+\vec{q}\right)F_{ij}\left(\vec{k},\vec{q}\right)\\
&\quad -\rho\left(\vec{k}\right)\frac{1}{(2\pi)^3}\underbrace{\int \mathrm{d}^3qF_{ij}\left(\vec{k},\vec{q}\right)}_{0}\\
&= \frac{1}{V}\sum_{\vec{q}}\rho\left(\frac{\vec{k}}{2}-\vec{q}\right)\rho\left(\frac{\vec{k}}{2}+\vec{q}\right)F_{ij}\left(\vec{k},\vec{q}\right)\\
&= \frac{1}{V}\sum_{\vec{q}}\rho\left(\vec{k}-\vec{q}\right)\rho\left(\vec{q}\right)F_{ij}\left(\vec{k},\vec{q}-\frac{\vec{k}}{2}\right). \qquad \text{(A.1)}
\end{aligned}
$$

A.2 Transformation into real space

In this section we want to give a derivation of the results used in Eqs. (5.56), (5.57), (5.58) and (5.59). With Eqs. (5.54) and (5.55) and the respective relations for the complex conjugate we obtain from Eq. (5.44)

$$
\begin{aligned}
&\left\langle\sigma_m\left(\vec{k}\right)|\sigma_m\left(\vec{k}\right)\right\rangle =\\
&= \frac{1}{V^2}\sum_{\vec{k}_1,\vec{k}_2}F_m^*\left(\vec{k},\vec{k}_1-\frac{\vec{k}}{2}\right)F_m\left(\vec{k},\vec{k}_2-\frac{\vec{k}}{2}\right)\left\langle\rho^*\left(\vec{k}-\vec{k}_1\right)\rho^*\left(\vec{k}_1\right)\rho\left(\vec{k}-\vec{k}_2\right)\rho\left(\vec{k}_2\right)\right\rangle\\
&= \frac{1}{V^2}\sum_{\vec{k}_1,\vec{k}_2}F_m^*\left(\vec{k},\vec{k}_1\right)F_m\left(\vec{k},\vec{k}_2\right)\\
&\quad \cdot\left\langle\rho^*\left(\frac{\vec{k}}{2}-\vec{k}_1\right)\rho^*\left(\frac{\vec{k}}{2}+\vec{k}_1\right)\rho\left(\frac{\vec{k}}{2}-\vec{k}_2\right)\rho\left(\frac{\vec{k}}{2}+\vec{k}_2\right)\right\rangle\\
&= \frac{1}{V^2}\int \mathrm{d}^3r_1\mathrm{d}^3r_2\mathrm{d}^3r_3\mathrm{d}^3r_4\sum_{\vec{k}_1,\vec{k}_2}F_m^*\left(\vec{k},\vec{k}_1\right)F_m\left(\vec{k},\vec{k}_2\right)e^{i\left(\frac{\vec{k}}{2}-\vec{k}_1\right)\vec{r}_1}e^{i\left(\frac{\vec{k}}{2}+\vec{k}_1\right)\vec{r}_2}\\
&\quad \cdot e^{-i\left(\frac{\vec{k}}{2}-\vec{k}_2\right)\vec{r}_3}e^{-i\left(\frac{\vec{k}}{2}+\vec{k}_2\right)\vec{r}_4}\left\langle\rho\left(\vec{r}_1\right)\rho\left(\vec{r}_2\right)\rho\left(\vec{r}_3\right)\rho\left(\vec{r}_4\right)\right\rangle\\
&= \frac{1}{V^2}\int \mathrm{d}^3r_1\mathrm{d}^3r_2\mathrm{d}^3r_3\mathrm{d}^3r_4\ e^{i\frac{\vec{k}}{2}\left(\vec{r}_1+\vec{r}_2-\vec{r}_3-\vec{r}_4\right)}\sum_{\vec{k}_1,\vec{k}_2}F_m^*\left(\vec{k},\vec{k}_1\right)F_m\left(\vec{k},\vec{k}_2\right)\\
&\quad \cdot e^{-i\vec{k}_1\left(\vec{r}_1-\vec{r}_2\right)}e^{i\vec{k}_2\left(\vec{r}_3-\vec{r}_4\right)}\left\langle\rho\left(\vec{r}_1\right)\rho\left(\vec{r}_2\right)\rho\left(\vec{r}_3\right)\rho\left(\vec{r}_4\right)\right\rangle\\
&= \int \mathrm{d}^3r_1\mathrm{d}^3r_2\mathrm{d}^3r_3\mathrm{d}^3r_4\ e^{i\frac{\vec{k}}{2}\left(\vec{r}_1+\vec{r}_2-\vec{r}_3-\vec{r}_4\right)}F_m^*\left(\vec{k},\vec{r}_1-\vec{r}_2\right)F_m\left(\vec{k},\vec{r}_3-\vec{r}_4\right)\\
&\quad \cdot\left\langle\rho\left(\vec{r}_1\right)\rho\left(\vec{r}_2\right)\rho\left(\vec{r}_3\right)\rho\left(\vec{r}_4\right)\right\rangle \qquad \text{(A.2)}
\end{aligned}
$$

and from Eq. (5.46) we obtain

$$
\begin{aligned}
&\left\langle \sigma_m\left(\vec{k}\right)\middle|\,\mathcal{L}^2\,\middle|\sigma_m\left(\vec{k}\right)\right\rangle = \\
= \;& \frac{4k_BT}{m}\frac{1}{V^2}\sum_{\vec{k}_1,\vec{k}_2}\vec{k}_1\cdot\vec{k}_2 F_m^*\left(\vec{k},\vec{k}_1-\frac{\vec{k}}{2}\right)F_m\left(\vec{k},\vec{k}_2-\frac{\vec{k}}{2}\right) \\
& \cdot\left\langle\rho\left(\vec{k}_1-\vec{k}\right)\rho\left(\vec{k}-\vec{k}_2\right)\rho\left(\vec{k}_2-\vec{k}_1\right)\right\rangle \\
= \;& \frac{4k_BT}{m}\frac{1}{V^2}\int \mathrm{d}^3r_1\mathrm{d}^3r_2\mathrm{d}^3r_3\sum_{\vec{k}_1,\vec{k}_2}\left(\vec{k}_1+\frac{\vec{k}}{2}\right)\cdot\left(\vec{k}_2+\frac{\vec{k}}{2}\right)F_m^*\left(\vec{k},\vec{k}_1\right)F_m\left(\vec{k},\vec{k}_2\right) \\
& \cdot\left\langle\rho\left(\vec{k}_1-\frac{\vec{k}}{2}\right)\rho\left(\vec{k}-\frac{\vec{k}_2}{2}\right)\rho\left(\vec{k}_2-\vec{k}_1\right)\right\rangle \\
= \;& \frac{4k_BT}{m}\frac{1}{V^2}\int \mathrm{d}^3r_1\mathrm{d}^3r_2\mathrm{d}^3r_3\sum_{\vec{k}_1,\vec{k}_2}\left(\vec{k}_1+\frac{\vec{k}}{2}\right)\cdot\left(\vec{k}_2+\frac{\vec{k}}{2}\right)F_m^*\left(\vec{k},\vec{k}_1\right)F_m\left(\vec{k},\vec{k}_2\right) \\
& \cdot e^{-i\left(\vec{k}_1-\frac{\vec{k}}{2}\right)\vec{r}_1}e^{-i\left(\frac{\vec{k}}{2}-\vec{k}_2\right)\vec{r}_2}e^{-i\left(\vec{k}_2-\vec{k}_1\right)\vec{r}_3}\left\langle\rho\left(\vec{r}_1\right)\rho\left(\vec{r}_2\right)\rho\left(\vec{r}_3\right)\right\rangle \\
= \;& \frac{4k_BT}{m}\int \mathrm{d}^3r_1\mathrm{d}^3r_2\mathrm{d}^3r_3 e^{i\frac{\vec{k}}{2}\left(\vec{r}_1-\vec{r}_2\right)}\left(\frac{1}{(2\pi)^3}\right)^2\int \mathrm{d}^3k_1\;\left(\vec{k}_1+\frac{\vec{k}}{2}\right)F_m^*\left(\vec{k},\vec{k}_1\right)e^{-i\vec{k}_1\left(\vec{r}_1-\vec{r}_3\right)}\cdot \\
& \cdot\int \mathrm{d}^3k_2\;\left(\vec{k}_2+\frac{\vec{k}}{2}\right)F_m\left(\vec{k},\vec{k}_2\right)e^{i\vec{k}_2\left(\vec{r}_2-\vec{r}_3\right)}\left\langle\rho\left(\vec{r}_1\right)\rho\left(\vec{r}_2\right)\rho\left(\vec{r}_3\right)\right\rangle \\
= \;& \frac{4k_BT}{m}\int \mathrm{d}^3r_1\mathrm{d}^3r_2\mathrm{d}^3r_3\; e^{i\frac{\vec{k}}{2}\left(\vec{r}_1-\vec{r}_2\right)}\left(i\vec{\nabla}_r+\frac{\vec{k}}{2}\right)F_m^*\left(\vec{k},\vec{r}\right)\Big|_{\vec{r}=\vec{r}_1-\vec{r}_3} \\
& \cdot\left(-i\vec{\nabla}_{r'}+\frac{\vec{k}}{2}\right)F_m\left(\vec{k},\vec{r}'\right)\Big|_{\vec{r}'=\vec{r}_2-\vec{r}_3}\left\langle\rho\left(\vec{r}_1\right)\rho\left(\vec{r}_2\right)\rho\left(\vec{r}_3\right)\right\rangle
\end{aligned}
\tag{A.3}
$$

and from Eq. (5.51) we obtain

$$
\begin{aligned}
& V^1_{m,m_2'',m_3'}\left(\vec{k},\vec{q}\right) = \\
= \;& \frac{4k_BT}{m}\frac{1}{V^4}\sum_{\vec{k}_1,\vec{k}_2,\vec{k}_3}\vec{k}_1\cdot\vec{k}_2 F_m^*\left(\vec{k},\vec{k}_1-\frac{\vec{k}}{2}\right)F_{m_2''}\left(\vec{k}-\vec{q},\vec{k}_2-\frac{\vec{k}-\vec{q}}{2}\right) \\
& \cdot F_{m_3'}\left(\vec{q},\vec{k}_3-\frac{\vec{q}}{2}\right)\left\langle\rho\left(\vec{k}_3\right)\rho\left(\vec{k}_2-\vec{k}_1\right)\rho^*\left(\vec{k}-\vec{k}_1\right)\rho\left(\vec{k}-\vec{q}-\vec{k}_2\right)\rho\left(\vec{q}-\vec{k}_3\right)\right\rangle \\
& + \left\{m_2''\leftrightarrow m_3', \vec{q}\leftrightarrow\vec{k}-\vec{q}\right\} \\
= \;& \frac{4k_BT}{m}\frac{1}{V^4}\sum_{\vec{k}_1,\vec{k}_2,\vec{k}_3}F_m^*\left(\vec{k},\vec{k}_1\right)F_{m_2''}\left(\vec{k}-\vec{q},\vec{k}_2\right)F_{m_3'}\left(\vec{q},\vec{k}_3\right)\left(\vec{k}_1+\frac{\vec{k}}{2}\right)\cdot\left(\vec{k}_2+\frac{\vec{k}-\vec{q}}{2}\right) \\
& \cdot\left\langle\rho\left(\vec{k}_3+\frac{\vec{q}}{2}\right)\rho\left(\vec{k}_2-\vec{k}_1-\frac{\vec{q}}{2}\right)\rho\left(\vec{k}_1-\frac{\vec{k}}{2}\right)\rho\left(\frac{\vec{k}-\vec{q}}{2}-\vec{k}_2\right)\rho\left(\frac{\vec{q}}{2}-\vec{k}_3\right)\right\rangle \\
& + \left\{m_2''\leftrightarrow m_3', \vec{q}\leftrightarrow\vec{k}-\vec{q}\right\} \\
= \;& \frac{4k_BT}{m}\frac{1}{V^4}\sum_{\vec{k}_1,\vec{k}_2,\vec{k}_3}F_m^*\left(\vec{k},\vec{k}_1\right)F_{m_2''}\left(\vec{k}-\vec{q},\vec{k}_2\right)F_{m_3'}\left(\vec{q},\vec{k}_3\right)\left(\vec{k}_1+\frac{\vec{k}}{2}\right)\cdot\left(\vec{k}_2+\frac{\vec{k}-\vec{q}}{2}\right)\cdot \\
& \cdot\int \mathrm{d}^3r_1\mathrm{d}^3r_2\mathrm{d}^3r_3\mathrm{d}^3r_4\mathrm{d}^3r_5\; e^{-i\left(\vec{k}_3+\frac{\vec{q}}{2}\right)\vec{r}_1}e^{-i\left(\vec{k}_2-\vec{k}_1-\frac{\vec{q}}{2}\right)\vec{r}_2}e^{-i\left(\vec{k}_1-\frac{\vec{k}}{2}\right)\vec{r}_3}e^{-i\left(\frac{\vec{k}-\vec{q}}{2}-\vec{k}_2\right)\vec{r}_4}e^{-i\left(\frac{\vec{q}}{2}-\vec{k}_3\right)\vec{r}_5}\cdot \\
& \cdot\left\langle\rho\left(\vec{r}_1\right)\rho\left(\vec{r}_2\right)\rho\left(\vec{r}_3\right)\rho\left(\vec{r}_4\right)\rho\left(\vec{r}_5\right)\right\rangle + \left\{m_2''\leftrightarrow m_3', \vec{q}\leftrightarrow\vec{k}-\vec{q}\right\} \\
= \;& \frac{4k_BT}{Vm}\int \mathrm{d}^3r_1\mathrm{d}^3r_2\mathrm{d}^3r_3\mathrm{d}^3r_4\mathrm{d}^3r_5 e^{i\frac{\vec{k}}{2}\left(\vec{r}_3-\vec{r}_4\right)}e^{i\frac{\vec{q}}{2}\left(\vec{r}_4-\vec{r}_5+\vec{r}_2-\vec{r}_1\right)}\frac{1}{V^3} \\
& \cdot\sum_{\vec{k}_1,\vec{k}_2,\vec{k}_3}F_m^*\left(\vec{k},\vec{k}_1\right)F_{m_2''}\left(\vec{k}-\vec{q},\vec{k}_2\right)F_{m_3'}\left(\vec{q},\vec{k}_3\right)\cdot \\
& \cdot\left(\vec{k}_1+\frac{\vec{k}}{2}\right)\cdot\left(\vec{k}_2+\frac{\vec{k}-\vec{q}}{2}\right)\; e^{-i\vec{k}_1\left(\vec{r}_3-\vec{r}_2\right)}e^{i\vec{k}_2\left(\vec{r}_4-\vec{r}_2\right)}e^{i\vec{k}_3\left(\vec{r}_5-\vec{r}_1\right)} \\
& \cdot\left\langle\rho\left(\vec{r}_1\right)\rho\left(\vec{r}_2\right)\rho\left(\vec{r}_3\right)\rho\left(\vec{r}_4\right)\rho\left(\vec{r}_5\right)\right\rangle \\
& + \left\{m_2''\leftrightarrow m_3', \vec{q}\leftrightarrow\vec{k}-\vec{q}\right\} \\
= \;& \frac{4k_BT}{m}\int \mathrm{d}^3r_1\mathrm{d}^3r_2\mathrm{d}^3r_3\mathrm{d}^3r_4\mathrm{d}^3r_5\; e^{i\frac{\vec{q}}{2}\left(\vec{r}_2+\vec{r}_3-\vec{r}_5-\vec{r}_1\right)}e^{i\frac{\vec{k}-\vec{q}}{2}\left(\vec{r}_3-\vec{r}_4\right)}F_{m_3'}\left(\vec{q},\vec{r}_5-\vec{r}_1\right)\cdot \\
& \cdot\left(i\vec{\nabla}_r+\frac{\vec{k}}{2}\right)F_m^*\left(\vec{k},\vec{r}\right)\Big|_{\vec{r}=\vec{r}_3-\vec{r}_2}\left(-i\vec{\nabla}_{r'}+\frac{\vec{k}-\vec{q}}{2}\right)F_{m_2''}\left(\vec{k}-\vec{q},\vec{r}'\right)\Big|_{\vec{r}'=\vec{r}_4-\vec{r}_2} \\
& \cdot\left\langle\rho\left(\vec{r}_1\right)\rho\left(\vec{r}_2\right)\rho\left(\vec{r}_3\right)\rho\left(\vec{r}_4\right)\rho\left(\vec{r}_5\right)\right\rangle \\
& + \left\{m_2''\leftrightarrow m_3', \vec{q}\leftrightarrow\vec{k}-\vec{q}\right\}
\end{aligned}
\tag{A.4}
$$

and from Eq. (5.53) we obtain

$$
\begin{aligned}
&\left\langle \sigma_m\left(\vec{k}\right) | \sigma_{m_2''}\left(\vec{k}-\vec{q}\right) \sigma_{m_3'}\left(\vec{q}\right)\right\rangle = \\
= \;& \frac{1}{V^3} \sum_{\vec{k}_1,\vec{k}_2,\vec{k}_3} F_m^*\left(\vec{k},\vec{k}_1-\frac{\vec{k}}{2}\right) F_{m_2''}\left(\vec{k}-\vec{q},\vec{k}_2-\frac{\vec{k}-\vec{q}}{2}\right) F_{m_3'}\left(\vec{q},\vec{k}_3-\frac{\vec{q}}{2}\right) \cdot \\
& \cdot \left\langle \rho\left(\vec{k}_1-\vec{k}\right)\rho\left(-\vec{k}_1\right)\rho\left(\vec{k}-\vec{q}-\vec{k}_2\right)\rho\left(\vec{k}_2\right)\rho\left(\vec{q}-\vec{k}_3\right)\rho\left(\vec{k}_3\right)\right\rangle \\
= \;& \frac{1}{V^3} \sum_{\vec{k}_1,\vec{k}_2,\vec{k}_3} F_m^*\left(\vec{k},\vec{k}_1\right) F_{m_2''}\left(\vec{k}-\vec{q},\vec{k}_2\right) F_{m_3'}\left(\vec{q},\vec{k}_3\right) \cdot \\
& \cdot \left\langle \rho\left(\vec{k}_1-\frac{\vec{k}}{2}\right)\rho\left(-\vec{k}_1-\frac{\vec{k}}{2}\right)\rho\left(\frac{\vec{k}-\vec{q}}{2}-\vec{k}_2\right)\rho\left(\frac{\vec{k}-\vec{q}}{2}+\vec{k}_2\right)\right. \\
& \left.\rho\left(\frac{\vec{q}}{2}-\vec{k}_3\right)\rho\left(\frac{\vec{q}}{2}+\vec{k}_3\right)\right\rangle \\
= \;& \frac{1}{V^3}\int \mathrm{d}^3r_1\mathrm{d}^3r_2\mathrm{d}^3r_3\mathrm{d}^3r_4\mathrm{d}^3r_5\mathrm{d}^3r_6 \sum_{\vec{k}_1,\vec{k}_2,\vec{k}_3} F_m^*\left(\vec{k},\vec{k}_1\right) F_{m_2''}\left(\vec{k}-\vec{q},\vec{k}_2\right) F_{m_3'}\left(\vec{q},\vec{k}_3\right) \cdot \\
& \cdot e^{-i\left(\vec{k}_1-\frac{\vec{k}}{2}\right)\vec{r}_1} e^{i\left(\vec{k}_1+\frac{\vec{k}}{2}\right)\vec{r}_2} e^{-i\left(\frac{\vec{k}-\vec{q}}{2}-\vec{k}_2\right)\vec{r}_3} e^{-i\left(\frac{\vec{k}-\vec{q}}{2}+\vec{k}_2\right)\vec{r}_4} e^{-i\left(\frac{\vec{q}}{2}-\vec{k}_3\right)\vec{r}_5} e^{-i\left(\frac{\vec{q}}{2}+\vec{k}_3\right)\vec{r}_6} \\
& \cdot \left\langle \rho\left(\vec{r}_1\right)\rho\left(\vec{r}_2\right)\rho\left(\vec{r}_3\right)\rho\left(\vec{r}_4\right)\rho\left(\vec{r}_5\right)\rho\left(\vec{r}_6\right)\right\rangle \\
= \;& \frac{1}{V^3}\int \mathrm{d}^3r_1\mathrm{d}^3r_2\mathrm{d}^3r_3\mathrm{d}^3r_4\mathrm{d}^3r_5\mathrm{d}^3r_6 \; e^{i\frac{\vec{q}}{2}\left(\vec{r}_1+\vec{r}_2-\vec{r}_5-\vec{r}_6\right)} e^{i\frac{\vec{k}-\vec{q}}{2}\left(\vec{r}_1+\vec{r}_2-\vec{r}_3-\vec{r}_4\right)} \cdot \\
& \cdot \sum_{\vec{k}_1} F_m^*\left(\vec{k},\vec{k}_1\right) e^{-i\vec{k}_1\left(\vec{r}_1-\vec{r}_2\right)} \sum_{\vec{k}_2} F_{m_2''}\left(\vec{k}-\vec{q},\vec{k}_2\right) e^{i\vec{k}_2\left(\vec{r}_3-\vec{r}_4\right)} \sum_{\vec{k}_3} F_{m_3'}\left(\vec{q},\vec{k}_3\right) \cdot \\
& \cdot e^{i\vec{k}_3\left(\vec{r}_5-\vec{r}_6\right)} \left\langle \rho\left(\vec{r}_1\right)\rho\left(\vec{r}_2\right)\rho\left(\vec{r}_3\right)\rho\left(\vec{r}_4\right)\rho\left(\vec{r}_5\right)\rho\left(\vec{r}_6\right)\right\rangle \\
= \;& \int \mathrm{d}^3r_1\mathrm{d}^3r_2\mathrm{d}^3r_3\mathrm{d}^3r_4\mathrm{d}^3r_5\mathrm{d}^3r_6 \; e^{i\frac{\vec{q}}{2}\left(\vec{r}_1+\vec{r}_2-\vec{r}_5-\vec{r}_6\right)} e^{i\frac{\vec{k}-\vec{q}}{2}\left(\vec{r}_1+\vec{r}_2-\vec{r}_3-\vec{r}_4\right)} \\
& \cdot F_m^*\left(\vec{k},\vec{r}_1-\vec{r}_2\right) F_{m_2''}\left(\vec{k}-\vec{q},\vec{r}_3-\vec{r}_4\right) F_{m_3'}\left(\vec{q},\vec{r}_5-\vec{r}_6\right) \\
& \cdot \left\langle \rho\left(\vec{r}_1\right)\rho\left(\vec{r}_2\right)\rho\left(\vec{r}_3\right)\rho\left(\vec{r}_4\right)\rho\left(\vec{r}_5\right)\rho\left(\vec{r}_6\right)\right\rangle . \qquad \text{(A.5)}
\end{aligned}
$$

A.3 Transformation of the distribution function

In this section we want to give a derivation of Eqs. (5.62) and (5.64). From Eq. (5.57) we obtain

$$
\begin{aligned}
&\left\langle \sigma_m\left(\vec{k}\right)\right| \mathcal{L}^2 \left|\sigma_m\left(\vec{k}\right)\right\rangle = \\
= \;& 4\frac{k_B T}{m}\int \mathrm{d}^3r_1\mathrm{d}^3r_2\mathrm{d}^3r_3\; e^{i\frac{\vec{k}}{2}(\vec{r}_1-\vec{r}_2)}\left(i\vec{\nabla}_r+\frac{\vec{k}}{2}\right)F_m^*\left(\vec{k},\vec{r}\right)\Big|_{\vec{r}=\vec{r}_1-\vec{r}_3} \\
& \cdot\left(-i\vec{\nabla}_{r'}+\frac{\vec{k}}{2}\right)F_m\left(\vec{k},\vec{r}'\right)\Big|_{\vec{r}'=\vec{r}_2-\vec{r}_3}\left\langle\rho\left(\vec{r}_1\right)\rho\left(\vec{r}_2\right)\rho\left(\vec{r}_3\right)\right\rangle \\
= \;& 4\frac{k_B T}{m}\int \mathrm{d}^3r_1\mathrm{d}^3r_2\mathrm{d}^3r_3\; e^{i\frac{\vec{k}}{2}(\vec{r}_1-\vec{r}_2)}\,\vec{\nabla}_r F_m^*\left(\vec{k},\vec{r}\right)\Big|_{\vec{r}=\vec{r}_1-\vec{r}_3}\,\vec{\nabla}_{r'}F_m\left(\vec{k},\vec{r}'\right)\Big|_{\vec{r}'=\vec{r}_2-\vec{r}_3} \\
& \cdot\left\langle\rho\left(\vec{r}_1\right)\rho\left(\vec{r}_2\right)\rho\left(\vec{r}_3\right)\right\rangle \\
& +4\frac{k_B T}{m}\frac{k^2}{4}\int \mathrm{d}^3r_1\mathrm{d}^3r_2\mathrm{d}^3r_3\; e^{i\frac{\vec{k}}{2}(\vec{r}_1-\vec{r}_2)}\,F_m^*\left(\vec{k},\vec{r}\right)\Big|_{\vec{r}=\vec{r}_1-\vec{r}_3}\,F_m\left(\vec{k},\vec{r}'\right)\Big|_{\vec{r}'=\vec{r}_2-\vec{r}_3} \\
& \cdot\left\langle\rho\left(\vec{r}_1\right)\rho\left(\vec{r}_2\right)\rho\left(\vec{r}_3\right)\right\rangle \\
& +4\frac{k_B T}{m}i\int \mathrm{d}^3r_1\mathrm{d}^3r_2\mathrm{d}^3r_3\; e^{i\frac{\vec{k}}{2}(\vec{r}_1-\vec{r}_2)}\,\frac{\vec{k}}{2}\cdot\vec{\nabla}_r F_m^*\left(\vec{k},\vec{r}\right)\Big|_{\vec{r}=\vec{r}_1-\vec{r}_3} \\
& \cdot F_m\left(\vec{k},\vec{r}'\right)\Big|_{\vec{r}'=\vec{r}_2-\vec{r}_3}\left\langle\rho\left(\vec{r}_1\right)\rho\left(\vec{r}_2\right)\rho\left(\vec{r}_3\right)\right\rangle \\
& -4\frac{k_B T}{m}i\int \mathrm{d}^3r_1\mathrm{d}^3r_2\mathrm{d}^3r_3\; e^{i\frac{\vec{k}}{2}(\vec{r}_1-\vec{r}_2)}\,F_m^*\left(\vec{k},\vec{r}\right)\Big|_{\vec{r}=\vec{r}_1-\vec{r}_3} \\
& \cdot\frac{\vec{k}}{2}\cdot\vec{\nabla}_{r'}F_m\left(\vec{k},\vec{r}'\right)\Big|_{\vec{r}'=\vec{r}_2-\vec{r}_3}\left\langle\rho\left(\vec{r}_1\right)\rho\left(\vec{r}_2\right)\rho\left(\vec{r}_3\right)\right\rangle \\
= \;& 4\frac{k_B T}{m}\int \mathrm{d}^3r_1\mathrm{d}^3r_2\mathrm{d}^3r_3\;\cos\left(\frac{\vec{k}}{2}\left(\vec{r}_1-\vec{r}_2\right)\right)\vec{\nabla}_r F_m^*\left(\vec{k},\vec{r}\right)\Big|_{\vec{r}=\vec{r}_1-\vec{r}_3} \\
& \cdot\vec{\nabla}_{r'}F_m\left(\vec{k},\vec{r}'\right)\Big|_{\vec{r}'=\vec{r}_2-\vec{r}_3}\left\langle\rho\left(\vec{r}_1\right)\rho\left(\vec{r}_2\right)\rho\left(\vec{r}_3\right)\right\rangle \\
& +4\frac{k_B T}{m}\frac{k^2}{4}\int \mathrm{d}^3r_1\mathrm{d}^3r_2\mathrm{d}^3r_3\;\cos\left(\frac{\vec{k}}{2}\left(\vec{r}_1-\vec{r}_2\right)\right)F_m^*\left(\vec{k},\vec{r}\right)\Big|_{\vec{r}=\vec{r}_1-\vec{r}_3} \\
& \cdot F_m\left(\vec{k},\vec{r}'\right)\Big|_{\vec{r}'=\vec{r}_2-\vec{r}_3}\left\langle\rho\left(\vec{r}_1\right)\rho\left(\vec{r}_2\right)\rho\left(\vec{r}_3\right)\right\rangle \\
& -4\frac{k_B T}{m}\int \mathrm{d}^3r_1\mathrm{d}^3r_2\mathrm{d}^3r_3\;\sin\left(\frac{\vec{k}}{2}\left(\vec{r}_1-\vec{r}_2\right)\right)\frac{\vec{k}}{2}\cdot\vec{\nabla}_r F_m^*\left(\vec{k},\vec{r}\right)\Big|_{\vec{r}=\vec{r}_1-\vec{r}_3} \\
& \cdot F_m\left(\vec{k},\vec{r}'\right)\Big|_{\vec{r}'=\vec{r}_2-\vec{r}_3}\left\langle\rho\left(\vec{r}_1\right)\rho\left(\vec{r}_2\right)\rho\left(\vec{r}_3\right)\right\rangle \\
& +4\frac{k_B T}{m}\int \mathrm{d}^3r_1\mathrm{d}^3r_2\mathrm{d}^3r_3\;\sin\left(\frac{\vec{k}}{2}\left(\vec{r}_1-\vec{r}_2\right)\right)F_m^*\left(\vec{k},\vec{r}\right)\Big|_{\vec{r}=\vec{r}_1-\vec{r}_3} \\
& \cdot\frac{\vec{k}}{2}\cdot\vec{\nabla}_{r'}F_m\left(\vec{k},\vec{r}'\right)\Big|_{\vec{r}'=\vec{r}_2-\vec{r}_3}\left\langle\rho\left(\vec{r}_1\right)\rho\left(\vec{r}_2\right)\rho\left(\vec{r}_3\right)\right\rangle
\end{aligned}
$$

$$
\begin{aligned}
&= 4\frac{k_B T}{m}\int \mathrm{d}^3 r_1 \mathrm{d}^3 r_2 \mathrm{d}^3 r_3 \; Y\left(\vec{k},\vec{r}_1,\vec{r}_2,\vec{r}_3\right)\left\langle \rho\left(\vec{r}_1\right)\rho\left(\vec{r}_2\right)\rho\left(\vec{r}_3\right)\right\rangle \\
&= 4\frac{k_B T}{m}\int \mathrm{d}^3 r_1 \mathrm{d}^3 r_2 \mathrm{d}^3 r_3 \; Y\left(\vec{k},\vec{r}_1,\vec{r}_2,\vec{r}_3\right)\rho^3 g^{(3)}\left(\vec{r}_1,\vec{r}_2,\vec{r}_3\right) + \\
&\quad +4\frac{k_B T}{m}\int \mathrm{d}^3 r_1 \mathrm{d}^3 r_3 \; Y\left(\vec{k},\vec{r}_1,\vec{r}_1,\vec{r}_3\right)\rho^2 g^{(2)}\left(\vec{r}_1,\vec{r}_3\right) \qquad \text{(A.6)}
\end{aligned}
$$

with

$$
\begin{aligned}
&Y\left(\vec{k},\vec{r}_1,\vec{r}_2,\vec{r}_3\right) = \\
= \;& \cos\left(\frac{\vec{k}}{2}\left(\vec{r}_1-\vec{r}_2\right)\right)\vec{\nabla}_r F_m^*\left(\vec{k},\vec{r}\right)\Big|_{\vec{r}=\vec{r}_1-\vec{r}_3}\vec{\nabla}_{r'} F_m\left(\vec{k},\vec{r}'\right)\Big|_{\vec{r}'=\vec{r}_2-\vec{r}_3} \\
&+\cos\left(\frac{\vec{k}}{2}\left(\vec{r}_1-\vec{r}_2\right)\right)\frac{k^2}{4}\,F_m^*\left(\vec{k},\vec{r}\right)\Big|_{\vec{r}=\vec{r}_1-\vec{r}_3} F_m\left(\vec{k},\vec{r}'\right)\Big|_{\vec{r}'=\vec{r}_2-\vec{r}_3} \\
&-\sin\left(\frac{\vec{k}}{2}\left(\vec{r}_1-\vec{r}_2\right)\right)\frac{\vec{k}}{2}\cdot\vec{\nabla}_r F_m^*\left(\vec{k},\vec{r}\right)\Big|_{\vec{r}=\vec{r}_1-\vec{r}_3} F_m\left(\vec{k},\vec{r}'\right)\Big|_{\vec{r}'=\vec{r}_2-\vec{r}_3} \\
&+\sin\left(\frac{\vec{k}}{2}\left(\vec{r}_1-\vec{r}_2\right)\right)F_m^*\left(\vec{k},\vec{r}\right)\Big|_{\vec{r}=\vec{r}_1-\vec{r}_3}\frac{\vec{k}}{2}\cdot\vec{\nabla}_{r'} F_m\left(\vec{k},\vec{r}'\right)\Big|_{\vec{r}'=\vec{r}_2-\vec{r}_3}. \qquad \text{(A.7)}
\end{aligned}
$$

$V^1_{m,m_2'',m_3'}\left(\vec{k},\vec{q}\right)$ can be obtained by rewriting the term in Eq. (5.58)

$$
\begin{aligned}
&F_{m_3'}\left(\vec{q},\vec{r}_5-\vec{r}_1\right)\vec{H}_m^*\left(\vec{k},\vec{r}_3-\vec{r}_2\right)\cdot\vec{H}_{m_2''}\left(\vec{k}-\vec{q},\vec{r}_4-\vec{r}_2\right) = \\
= \;& F_{m_3'}\left(\vec{q},\vec{r}_5-\vec{r}_1\right)\left(i\vec{\nabla}_r+\frac{\vec{k}}{2}\right)F_m^*\left(\vec{k},\vec{r}\right)\Big|_{\vec{r}=\vec{r}_3-\vec{r}_2} \\
&\cdot\left(-i\vec{\nabla}_{r'}+\frac{\vec{k}}{2}\right)F_{m_2''}\left(\vec{k}-\vec{q},\vec{r}'\right)\Big|_{\vec{r}'=\vec{r}_4-\vec{r}_2} \\
= \;& \frac{k^2}{4}F_{m_3'}\left(\vec{q},\vec{r}_5-\vec{r}_1\right)F_m^*\left(\vec{k},\vec{r}_3-\vec{r}_2\right)F_{m_2''}\left(\vec{k}-\vec{q},\vec{r}_4-\vec{r}_2\right)+ \\
&+F_{m_3'}\left(\vec{q},\vec{r}_5-\vec{r}_1\right)\vec{\nabla}_r F_m^*\left(\vec{k},\vec{r}\right)\Big|_{\vec{r}=\vec{r}_3-\vec{r}_2}\cdot\vec{\nabla}_{r'}F_{m_2''}\left(\vec{k}-\vec{q},\vec{r}'\right)\Big|_{\vec{r}'=\vec{r}_4-\vec{r}_2} \\
&+iF_{m_3'}\left(\vec{q},\vec{r}_5-\vec{r}_1\right)\frac{\vec{k}}{2}\cdot\vec{\nabla}_r F_m^*\left(\vec{k},\vec{r}\right)\Big|_{\vec{r}=\vec{r}_3-\vec{r}_2}\cdot F_{m_2''}\left(\vec{k}-\vec{q},\vec{r}'\right)\Big|_{\vec{r}'=\vec{r}_4-\vec{r}_2} \\
&-iF_{m_3'}\left(\vec{q},\vec{r}_5-\vec{r}_1\right)F_m^*\left(\vec{k},\vec{r}\right)\Big|_{\vec{r}=\vec{r}_3-\vec{r}_2}\cdot\vec{\nabla}_{r'}\frac{\vec{k}}{2}F_{m_2''}\left(\vec{k}-\vec{q},\vec{r}'\right)\Big|_{\vec{r}'=\vec{r}_4-\vec{r}_2} \\
= \;& \tilde{X}_{m_1 m_2'' m_3'}\left(\vec{k},\vec{q},\vec{r}_1,\vec{r}_2,\vec{r}_3,\vec{r}_4,\vec{r}_5\right)-i\tilde{Y}_{m_1 m_2'' m_3'}\left(\vec{k},\vec{q},\vec{r}_1,\vec{r}_2,\vec{r}_3,\vec{r}_4,\vec{r}_5\right) \qquad \text{(A.8)}
\end{aligned}
$$

with

$$\begin{aligned}
&\tilde{X}_{m,m_2'',m_3'}\left(\vec{k},\vec{q},\vec{r}_1,\vec{r}_2,\vec{r}_3,\vec{r}_4,\vec{r}_5\right) = \\
= \;& \frac{k^2}{4} F_{m_3'}\left(\vec{q},\vec{r}_5-\vec{r}_1\right) F_m^*\left(\vec{k},\vec{r}_3-\vec{r}_2\right) F_{m_2''}\left(\vec{k}-\vec{q},\vec{r}_4-\vec{r}_2\right) + \\
& + F_{m_3'}\left(\vec{q},\vec{r}_5-\vec{r}_1\right) \vec{\nabla}_r F_m^*\left(\vec{k},\vec{r}\right)\Big|_{\vec{r}=\vec{r}_3-\vec{r}_2} \cdot \vec{\nabla}_{r'} F_{m_2''}\left(\vec{k}-\vec{q},\vec{r}'\right)\Big|_{\vec{r}'=\vec{r}_4-\vec{r}_2}
\end{aligned} \tag{A.9}$$

and

$$\begin{aligned}
&\tilde{Y}_{m,m_2'',m_3'}\left(\vec{k},\vec{q},\vec{r}_1,\vec{r}_2,\vec{r}_3,\vec{r}_4,\vec{r}_5\right) = \\
= \;& -F_{m_3'}\left(\vec{q},\vec{r}_5-\vec{r}_1\right) \frac{\vec{k}}{2} \cdot \vec{\nabla}_r F_m^*\left(\vec{k},\vec{r}\right)\Big|_{\vec{r}=\vec{r}_3-\vec{r}_2} \cdot F_{m_2''}\left(\vec{k}-\vec{q},\vec{r}'\right)\Big|_{\vec{r}'=\vec{r}_4-\vec{r}_2} \\
& + F_{m_3'}\left(\vec{q},\vec{r}_5-\vec{r}_1\right) F_m^*\left(\vec{k},\vec{r}\right)\Big|_{\vec{r}=\vec{r}_3-\vec{r}_2} \cdot \frac{\vec{k}}{2} \cdot \vec{\nabla}_{r'} F_{m_2''}\left(\vec{k}-\vec{q},\vec{r}'\right)\Big|_{\vec{r}'=\vec{r}_4-\vec{r}_2}
\end{aligned} \tag{A.10}$$

where $\tilde{X}$ and $\tilde{Y}$ have the symmetry

$$\begin{aligned}
\tilde{X}_{m,m_2'',m_3'}\left(\vec{k},\vec{q},\vec{r}_1,\vec{r}_2,\vec{r}_3,\vec{r}_4,\vec{r}_5\right) &= \tilde{X}_{m,m_2'',m_3'}\left(\vec{k},\vec{q},-\vec{r}_1,-\vec{r}_2,-\vec{r}_3,-\vec{r}_4,-\vec{r}_5\right) \\
\tilde{Y}_{m,m_2'',m_3'}\left(\vec{k},\vec{q},\vec{r}_1,\vec{r}_2,\vec{r}_3,\vec{r}_4,\vec{r}_5\right) &= -\tilde{Y}_{m,m_2'',m_3'}\left(\vec{k},\vec{q},-\vec{r}_1,-\vec{r}_2,-\vec{r}_3,-\vec{r}_4,-\vec{r}_5\right).
\end{aligned}$$

This can be used to rewrite Eq. (5.58) as

$$\begin{aligned}
&V^1_{m,m_2'',m_3'}\left(\vec{k},\vec{q}\right) = \\
= \;& 4\frac{k_B T}{m}\frac{1}{V}\int \mathrm{d}^3r_1\mathrm{d}^3r_2\mathrm{d}^3r_3\mathrm{d}^3r_4\mathrm{d}^3r_5 \; \cos\left(\frac{\vec{q}}{2}\left(\vec{r}_2+\vec{r}_3-\vec{r}_5-\vec{r}_1\right)+\frac{\vec{k}-\vec{q}}{2}\left(\vec{r}_3-\vec{r}_4\right)\right)\cdot \\
& \cdot\tilde{X}_{m,m_2'',m_3'}\left(\vec{k},\vec{q},\vec{r}_1,\vec{r}_2,\vec{r}_3,\vec{r}_4,\vec{r}_5\right)\left\langle\rho\left(\vec{r}_1\right)\rho\left(\vec{r}_2\right)\rho\left(\vec{r}_3\right)\rho\left(\vec{r}_4\right)\rho\left(\vec{r}_5\right)\right\rangle \\
& -4\frac{k_B T}{m}\frac{1}{V}\int \mathrm{d}^3r_1\mathrm{d}^3r_2\mathrm{d}^3r_3\mathrm{d}^3r_4\mathrm{d}^3r_5 \; \sin\left(\frac{\vec{q}}{2}\left(\vec{r}_2+\vec{r}_3-\vec{r}_5-\vec{r}_1\right)+\frac{\vec{k}-\vec{q}}{2}\left(\vec{r}_3-\vec{r}_4\right)\right)\cdot \\
& \cdot\tilde{Y}_{m,m_2'',m_3'}\left(\vec{k},\vec{q},\vec{r}_1,\vec{r}_2,\vec{r}_3,\vec{r}_4,\vec{r}_5\right)\left\langle\rho\left(\vec{r}_1\right)\rho\left(\vec{r}_2\right)\rho\left(\vec{r}_3\right)\rho\left(\vec{r}_4\right)\rho\left(\vec{r}_5\right)\right\rangle \\
= \;& \frac{1}{V}\int \mathrm{d}^3r_1\mathrm{d}^3r_2\mathrm{d}^3r_3\mathrm{d}^3r_4\mathrm{d}^3r_5 \; X_{m,m_2'',m_3'}\left(\vec{k},\vec{q},\vec{r}_1,\vec{r}_2,\vec{r}_3,\vec{r}_4,\vec{r}_5\right) \\
& \cdot\left\langle\rho\left(\vec{r}_1\right)\rho\left(\vec{r}_2\right)\rho\left(\vec{r}_3\right)\rho\left(\vec{r}_4\right)\rho\left(\vec{r}_5\right)\right\rangle
\end{aligned} \tag{A.11}$$

with

$$
\begin{aligned}
& X_{m,m_2'',m_3'}\left(\vec{k},\vec{q},\vec{r}_1,\vec{r}_2,\vec{r}_3,\vec{r}_4,\vec{r}_5\right) = \\
= \; & 4\frac{k_BT}{m}\cos\left(\frac{\vec{q}}{2}\left(\vec{r}_2+\vec{r}_3-\vec{r}_5-\vec{r}_1\right)+\frac{\vec{k}-\vec{q}}{2}\left(\vec{r}_3-\vec{r}_4\right)\right) \\
& \cdot\tilde{X}_{m,m_2'',m_3'}\left(\vec{k},\vec{q},\vec{r}_1,\vec{r}_2,\vec{r}_3,\vec{r}_4,\vec{r}_5\right)+ \\
& -4\frac{k_BT}{m}\sin\left(\frac{\vec{q}}{2}\left(\vec{r}_2+\vec{r}_3-\vec{r}_5-\vec{r}_1\right)+\frac{\vec{k}-\vec{q}}{2}\left(\vec{r}_3-\vec{r}_4\right)\right) \\
& \cdot\tilde{Y}_{m,m_2'',m_3'}\left(\vec{k},\vec{q},\vec{r}_1,\vec{r}_2,\vec{r}_3,\vec{r}_4,\vec{r}_5\right) \qquad \text{(A.12)}
\end{aligned}
$$

so that Eq. (5.58) can finally be rewritten as

$$
\begin{aligned}
& V^1_{m,m_2'',m_3'}\left(\vec{k},\vec{q}\right) = \\
= \; & \frac{1}{V}\int \mathrm{d}^3r_1\mathrm{d}^3r_2\mathrm{d}^3r_3\mathrm{d}^3r_4\mathrm{d}^3r_5\; X_{m,m_2'',m_3'}\left(\vec{k},\vec{q},\vec{r}_1,\vec{r}_2,\vec{r}_3,\vec{r}_4,\vec{r}_5\right)\cdot\rho^5 g^{(5)}\left(\vec{r}_1,\vec{r}_2,\vec{r}_3,\vec{r}_4,\vec{r}_5\right) \\
& +2\frac{1}{V}\int \mathrm{d}^3r_1\mathrm{d}^3r_3\mathrm{d}^3r_4\mathrm{d}^3r_5\; X_{m,m_2'',m_3'}\left(\vec{k},\vec{q},\vec{r}_1,\vec{r}_1,\vec{r}_3,\vec{r}_4,\vec{r}_5\right)\cdot\rho^4 g^{(4)}\left(\vec{r}_1,\vec{r}_3,\vec{r}_4,\vec{r}_5\right)+ \\
& +2\frac{1}{V}\int \mathrm{d}^3r_1\mathrm{d}^3r_2\mathrm{d}^3r_4\mathrm{d}^3r_5\; X_{m,m_2'',m_3'}\left(\vec{k},\vec{q},\vec{r}_1,\vec{r}_2,\vec{r}_1,\vec{r}_4,\vec{r}_5\right)\cdot\rho^4 g^{(4)}\left(\vec{r}_1,\vec{r}_2,\vec{r}_4,\vec{r}_5\right)+ \\
& +2\frac{1}{V}\int \mathrm{d}^3r_1\mathrm{d}^3r_2\mathrm{d}^3r_3\mathrm{d}^3r_5\; X_{m,m_2'',m_3'}\left(\vec{k},\vec{q},\vec{r}_1,\vec{r}_2,\vec{r}_3,\vec{r}_1,\vec{r}_5\right)\cdot\rho^4 g^{(4)}\left(\vec{r}_1,\vec{r}_2,\vec{r}_3,\vec{r}_5\right)+ \\
& +\frac{1}{V}\int \mathrm{d}^3r_1\mathrm{d}^3r_2\mathrm{d}^3r_3\mathrm{d}^3r_5\; X_{m,m_2'',m_3'}\left(\vec{k},\vec{q},\vec{r}_1,\vec{r}_2,\vec{r}_3,\vec{r}_3,\vec{r}_5\right)\cdot\rho^4 g^{(4)}\left(\vec{r}_1,\vec{r}_2,\vec{r}_3,\vec{r}_5\right)+ \\
& +2\frac{1}{V}\int \mathrm{d}^3r_1\mathrm{d}^3r_2\mathrm{d}^3r_5\; X_{m,m_2'',m_3'}\left(\vec{k},\vec{q},\vec{r}_1,\vec{r}_2,\vec{r}_1,\vec{r}_1,\vec{r}_5\right)\cdot\rho^3 g^{(3)}\left(\vec{r}_1,\vec{r}_2,\vec{r}_5\right)+ \\
& +2\frac{1}{V}\int \mathrm{d}^3r_1\mathrm{d}^3r_3\mathrm{d}^3r_5\; X_{m,m_2'',m_3'}\left(\vec{k},\vec{q},\vec{r}_1,\vec{r}_1,\vec{r}_3,\vec{r}_3,\vec{r}_5\right)\cdot\rho^3 g^{(3)}\left(\vec{r}_1,\vec{r}_3,\vec{r}_5\right)+ \\
& +2\frac{1}{V}\int \mathrm{d}^3r_1\mathrm{d}^3r_3\mathrm{d}^3r_4\; X_{m,m_2'',m_3'}\left(\vec{k},\vec{q},\vec{r}_1,\vec{r}_1,\vec{r}_3,\vec{r}_4,\vec{r}_3\right)\cdot\rho^3 g^{(3)}\left(\vec{r}_1,\vec{r}_3,\vec{r}_4\right)+ \\
& +2\frac{1}{V}\int \mathrm{d}^3r_1\mathrm{d}^3r_3\mathrm{d}^3r_4\; X_{m,m_2'',m_3'}\left(\vec{k},\vec{q},\vec{r}_1,\vec{r}_1,\vec{r}_3,\vec{r}_4,\vec{r}_4\right)\cdot\rho^3 g^{(3)}\left(\vec{r}_1,\vec{r}_3,\vec{r}_4\right)+ \\
& +2\frac{1}{V}\int \mathrm{d}^3r_1\mathrm{d}^3r_2\mathrm{d}^3r_4\; X_{m,m_2'',m_3'}\left(\vec{k},\vec{q},\vec{r}_1,\vec{r}_2,\vec{r}_1,\vec{r}_4,\vec{r}_4\right)\cdot\rho^3 g^{(3)}\left(\vec{r}_1,\vec{r}_2,\vec{r}_4\right)+ \\
& +2\frac{1}{V}\int \mathrm{d}^3r_1\mathrm{d}^3r_2 X_{m,m_2'',m_3'}\left(\vec{k},\vec{q},\vec{r}_1,\vec{r}_2,\vec{r}_1,\vec{r}_1,\vec{r}_2\right)\cdot\rho^2 g^{(2)}\left(\vec{r}_1,\vec{r}_2\right). \qquad \text{(A.13)}
\end{aligned}
$$

Bibliography

[1] W. Götze, *Complex dynamics of glass-forming liquids: A mode-coupling theory* (Oxford University Press, USA, 2009).

[2] G. Parisi and F. Zamponi, *Amorphous packings of hard spheres for large space dimension*, Journal of Statistical Mechanics: Theory and Experiment **2006**, P03017 (2006).

[3] T. R. Kirkpatrick and P. G. Wolynes, *Connections between some kinetic and equilibrium theories of the glass transition*, Phys. Rev. A **35**, 3072 (1987).

[4] D. Levesque, L. Verlet, and J. Kurkijärvi, *Computer "Experiments" on Classical Fluids. IV. Transport Properties and Time-Correlation Functions of the Lennard-Jones Liquid near Its Triple Point*, Phys. Rev. A **7**, 1690 (1973).

[5] L. Sjögren, *Kinetic theory of current fluctuations in simple classical liquids*, Phys. Rev. A **22**, 2866 (1980).

[6] U. Bengtzelius, W. Götze, and A. Sjölander, *Dynamics of supercooled liquids and the glass transition*, Journal of Physics C: solid state Physics **17**, 5915 (1984).

[7] W. Götze, *Aspects of structural glass transitions*, in *Liquids, Freezing and the Glass Transition*, edited by J. P. Hansen, D. Levesque, and J. Zinn-Justin, North-Holland, Amsterdam, 1991.

[8] W. Götze and L. Sjögren, *Relaxation processes in supercooled liquids*, Reports on Progress in Physics **55**, 241 (1992).

[9] W. Götze and M. R. Mayr, *Evolution of vibrational excitations in glassy systems*, Phys. Rev. E **61**, 587 (2000).

[10] K. Dawson, G. Foffi, M. Fuchs, W. Götze, F. Sciortino, M. Sperl, P. Tartaglia, T. Voigtmann, and E. Zaccarelli, *Higher-order glass-transition singularities in colloidal systems with attractive interactions*, Phys. Rev. E **63**, 011401 (2000).

[11] F. Sciortino and W. Kob, *Debye-Waller Factor of Liquid Silica: Theory and Simulation*, Phys. Rev. Lett. **86**, 648 (2001).

[12] R. Schilling and T. Scheidsteger, *Mode coupling approach to the ideal glass transition of molecular liquids: Linear molecules*, Phys. Rev. E **56**, 2932 (1997).

[13] T. Franosch, M. Fuchs, W. Götze, M. R. Mayr, and A. P. Singh, *Asymptotic laws and preasymptotic correction formulas for the relaxation near glass-transition singularities*, Phys. Rev. E **55**, 7153 (1997).

[14] J. Barrat and A. Latz, *Mode coupling theory for the glass transition in a simple binary mixture*, Journal of Physics Condensed Matter **2**, 4289 (1990).

[15] W. Götze and T. Voigtmann, *Effect of composition changes on the structural relaxation of a binary mixture*, Phys. Rev. E **67**, 021502 (2003).

[16] S. Lang, V. Boţan, M. Oettel, D. Hajnal, T. Franosch, and R. Schilling, *Glass Transition in Confined Geometry*, Phys. Rev. Lett. **105**, 125701 (2010).

[17] M. Bayer, J. M. Brader, F. Ebert, M. Fuchs, E. Lange, G. Maret, R. Schilling, M. Sperl, and J. P. Wittmer, *Dynamic glass transition in two dimensions*, Phys. Rev. E **76**, 011508 (2007).

[18] D. Hajnal, J. M. Brader, and R. Schilling, *Effect of mixing and spatial dimension on the glass transition*, Phys. Rev. E **80**, 021503 (2009).

[19] H. L. Frisch, N. Rivier, and D. Wyler, *Classical Hard-Sphere Fluid in Infinitely Many Dimensions*, Phys. Rev. Lett. **54**, 2061 (1985).

[20] D. Wyler, N. Rivier, and H. L. Frisch, *Hard-sphere fluid in infinite dimensions*, Phys. Rev. A **36**, 2422 (1987).

[21] S. Torquato and F. H. Stillinger, *Jammed hard-particle packings: From Kepler to Bernal and beyond*, Rev. Mod. Phys. **82**, 2633 (2010).

[22] G. Parisi and F. Zamponi, *Mean-field theory of hard sphere glasses and jamming*, Rev. Mod. Phys. **82**, 789 (2010).

[23] G. Szamel, *Dynamic glass transition: Bridging the gap between mode-coupling theory and the replica approach*, EPL (Europhysics Letters) **91**, 56004 (2010).

[24] W. Schirmacher and H. Sinn, *Collective dynamics of simple liquids: A mode-coupling description*, Condens. Matter Phys. **11**, 127 (2008).

[25] A. H. Said, H. Sinn, A. Alatas, C. A. Burns, D. L. Price, M. L. Saboungi, and W. Schirmacher, *Collective excitations in an early molten transition metal*, Phys. Rev. B **74**, 172202 (2006).

[26] L. Berthier and G. Tarjus, *Critical test of the mode-coupling theory of the glass transition*, Phys. Rev. E **82**, 031502 (2010).

[27] R. Schilling and G. Szamel, *Microscopic theory for the glass transition in a system without static correlations*, EPL (Europhysics Letters) **61**, 207 (2003).

[28] R. Schilling and G. Szamel, *Glass transition in systems without static correlations: a microscopic theory*, Journal of Physics: Condensed Matter **15**, S967 (2003).

[29] J.-P. Hansen and I. R. McDonald, *Theory of Simple Liquids* (Academic Press, Amsterdam, 2006).

[30] D. Forster, *Hydrodynamic Fluctuations, Broken Symmetry, and Correlation Functions* (Benjamin, Reading, 1975).

[31] J. L. Barrat, J. P. Hansen, and G. Pastore, *On the equilibrium structure of dense fluids*, Molecular Physics **63**, 747 (1988).

[32] V. Arnol'd, *Catastrophe theory* (Springer, Berlin, 1992).

[33] W. Götze and L. Sjögren, *The mode coupling theory of structural relaxations*, Transport theory and statistical physics **24**, 801 (1995).

[34] W. Kauzmann, *The Nature of the Glassy State and the Behavior of Liquids at Low Temperatures.*, Chemical Reviews **43**, 219 (1948).

[35] C. A. Angell, *Perspective on the glass transition*, Journal of Physics and Chemistry of Solids **49**, 863 (1988).

[36] G. Biroli and J. Bouchaud, *Diverging length scale and upper critical dimension in the Mode-Coupling Theory of the glass transition*, EPL (Europhysics Letters) **67**, 21 (2004).

[37] G. Biroli and J. Bouchaud, *Critical fluctuations and breakdown of the Stokes–Einstein relation in the mode-coupling theory of glasses*, Journal of Physics: Condensed Matter **19**, 205101 (2007).

[38] P. Charbonneau, A. Ikeda, J. A. van Meel, and K. Miyazaki, *Numerical and theoretical study of a monodisperse hard-sphere glass former*, Phys. Rev. E **81**, 040501 (2010).

[39] I. S. Gradshteyn and I. M. Ryzhik, *Table of Integrals, Series, and Products* (Academic, New York, 1980).

[40] M. Abramowitz and I. A. Stegun, *Handbook of Mathematical Functions* (Dover Publications, New York, 1970).

[41] H. L. Frisch and J. K. Percus, *Nonuniform classical fluid at high dimensionality*, Phys. Rev. A **35**, 4696 (1987).

[42] B. Bagchi and S. Rice, *On the stability of the infinite dimensional fluid of hard hyperspheres: A statistical mechanical estimate of the density of closest packing of simple hypercubic lattices in spaces of large dimensionality*, The Journal of chemical physics **88**, 1177 (1988).

[43] H. L. Frisch and J. K. Percus, *High dimensionality as an organizing device for classical fluids*, Phys. Rev. E **60**, 2942 (1999).

[44] A. Winkler, A. Latz, R. Schilling, and C. Theis, *Molecular mode-coupling theory applied to a liquid of diatomic molecules*, Phys. Rev. E **62**, 8004 (2000).

[45] J. Bergenholtz and M. Fuchs, *Nonergodicity transitions in colloidal suspensions with attractive interactions*, Phys. Rev. E **59**, 5706 (1999).

[46] A. Ikeda and K. Miyazaki, *Mode-Coupling Theory as a Mean-Field Description of the Glass Transition*, Phys. Rev. Lett. **104**, 255704 (2010).

[47] J. Boon and S. Yip, *Molecular Hydrodynamics* (McGraw-Hill, New York, 1980).

[48] J. Bergenholtz and M. Fuchs, *Gel transitions in colloidal suspensions*, Journal of Physics: Condensed Matter **11**, 10171 (1999).

[49] J. Bergenholtz, M. Fuchs, and T. Voigtmann, *Colloidal gelation and non-ergodicity transitions*, Journal of Physics: Condensed Matter **12**, 6575 (2000).

[50] T. Scopigno, G. Ruocco, and F. Sette, *Microscopic dynamics in liquid metals: The experimental point of view*, Rev. Mod. Phys. **77**, 881 (2005).

[51] T. Scopigno, U. Balucani, G. Ruocco, and F. Sette, *Evidence of Two Viscous Relaxation Processes in the Collective Dynamics of Liquid Lithium*, Phys. Rev. Lett. **85**, 4076 (2000).

[52] T. Scopigno, U. Balucani, G. Ruocco, and F. Sette, *Collective dynamics of liquid aluminum probed by inelastic x-ray scattering*, Phys. Rev. E **63**, 011210 (2000).

[53] T. Scopigno, G. Ruocco, F. Sette, and G. Viliani, *Evidence of short-time dynamical correlations in simple liquids*, Phys. Rev. E **66**, 031205 (2002).

[54] T. Scopigno, R. Di Leonardo, L. Comez, A. Q. R. Baron, D. Fioretto, and G. Ruocco, *Hard-Sphere-like Dynamics in a Non-Hard-Sphere Liquid*, Phys. Rev. Lett. **94**, 155301 (2005).

[55] W. Götze and M. Lücke, *Dynamical current correlation functions of simple classical liquids for intermediate wave numbers*, Phys. Rev. A **11**, 2173 (1975).

[56] J. Bosse, W. Götze, and M. Lücke, *Mode-coupling theory of simple classical liquids*, Phys. Rev. A **17**, 434 (1978).

[57] J. Bosse, W. Götze, and M. Lücke, *Current fluctuation spectra of liquid argon near its triple point*, Phys. Rev. A **17**, 447 (1978).

[58] S. Wiebel and J. Wuttke, *Structural relaxation and mode coupling in a non-glassforming liquid: depolarized light scattering in benzene*, New Journal of Physics **4**, 56 (2002).

[59] L. Verlet, *Computer "Experiments" on Classical Fluids. II. Equilibrium Correlation Functions*, Phys. Rev. **165**, 201 (1968).

[60] M. Fuchs, W. Gotze, I. Hofacker, and A. Latz, *Comments on the alpha-peak shapes for relaxation in supercooled liquids*, Journal of Physics: Condensed Matter **3**, 5047 (1991).

[61] D. G. Naugle, J. H. Lunsford, and J. R. Singer, *Volume viscosity in liquid argon at high pressures*, The Journal of Chemical Physics **45**, 4669 (1966).

[62] R. D. Mountain, *Spectral Distribution of Scattered Light in a Simple Fluid*, Rev. Mod. Phys. **38**, 205 (1966).

[63] A. Rahman, *Current fluctuations in classical liquids*, in *Neutron Inelastic Scattering*, Int. Atomic Energy Agency, Vienna, 1968.

[64] I. M. de Schepper, P. Verkerk, A. A. van Well, and L. A. de Graaf, *Short-Wavelength Sound Modes in Liquid Argon*, Phys. Rev. Lett. **50**, 974 (1983).

[65] P. Verkerk, *Dynamics in liquids*, Journal of Physics: Condensed Matter **13**, 7775 (2001).

[66] A. Rahman, *Density fluctuations in liquid rubidium. II. Molecular-dynamics calculations*, Phys. Rev. A **9**, 1667 (1974).

[67] L. Sjögren, *Numerical results on the density fluctuations in liquid rubidium*, Phys. Rev. A **22**, 2883 (1980).

[68] W. Götze and L. Sjögren, *The glass transition singularity*, Zeitschrift für Physik B Condensed Matter **65**, 415 (1987).

[69] J. D. Copley and S. W. Lovesey, *The dynamic properties of monatomic liquids*, Reports on Progress in Physics **38**, 461 (1975).

[70] J. Hubbard and J. L. Beeby, *Collective motion in liquids*, Journal of Physics C: Solid State Physics **2**, 556 (1969).

[71] L. Fabbian, F. Sciortino, F. Thiery, and P. Tartaglia, *Semischematic model for the center-of-mass dynamics in supercooled molecular liquids*, Phys. Rev. E **57**, 1485 (1998).

[72] L. Fabbian, R. Schilling, F. Sciortino, P. Tartaglia, and C. Theis, *Test of the semischematic model for a liquid of linear molecules*, Phys. Rev. E **58**, 7272 (1998).

[73] J. Bosse, W. Götze, and M. Lücke, *Current-fluctuation spectra of liquid rubidium*, Phys. Rev. A **18**, 1176 (1978).

[74] P. A. Egelstaff, *An Introduction to the Liquid State* (Clarendon Press, Oxford, 1994).

[75] J. A. Schouten, *Tensor analysis for physicists* (Oxford, Clarendon, 1951).

[76] P. B. Visscher and W. T. Logan, *Stress as an order parameter for the glass transition*, Phys. Rev. B **42**, 4779 (1990).

[77] U. Balucani, R. Vallauri, and T. Gaskell, *Stress autocorrelation function in liquid rubidium*, Phys. Rev. A **37**, 3386 (1988).

Acknowledgements